LBL-3143
c.2

SEMICLASSICAL METHODS AND THEIR APPLICATION TO PROBLEMS IN COLLISION THEORY

Stuart Dudley Augustin
(Ph. D. thesis)

September, 1974

Prepared for the U. S. Atomic Energy Commission
under Contract W-7405-ENG-48

TWO-WEEK LOAN COPY

This is a Library Circulating Copy which may be borrowed for two weeks. For a personal retention copy, call Tech. Info. Division, Ext. 5545

LAWRENCE BERKELEY LABORATORY
UNIVERSITY OF CALIFORNIA
BERKELEY

LBL-3143
c.2

DISCLAIMER

This document was prepared as an account of work sponsored by the United States Government. While this document is believed to contain correct information, neither the United States Government nor any agency thereof, nor the Regents of the University of California, nor any of their employees, makes any warranty, express or implied, or assumes any legal responsibility for the accuracy, completeness, or usefulness of any information, apparatus, product, or process disclosed, or represents that its use would not infringe privately owned rights. Reference herein to any specific commercial product, process, or service by its trade name, trademark, manufacturer, or otherwise, does not necessarily constitute or imply its endorsement, recommendation, or favoring by the United States Government or any agency thereof, or the Regents of the University of California. The views and opinions of authors expressed herein do not necessarily state or reflect those of the United States Government or any agency thereof or the Regents of the University of California.

SEMICLASSICAL METHODS AND THEIR APPLICATION TO PROBLEMS IN COLLISION THEORY

Contents

Abstract v

I. Theory of Electronic Transitions 1

A. Introduction 1

B. The Curve Crossing Problem 5

C. Summary of LZS Theory 10

D. Extensions and Improvements of LZS Theory 18

E. Uniform Approximation for the Wave Function 22

F. Solution of the Model System 25

II. Electronic Transitions in Collisions of He and O^+ 31

A. Introduction 31

B. Estimation of the Spin-Orbit Coupling 33

C. Calculation of the Cross Sections 37

D. Oscillatory Structure of the Cross Sections 41

III. Semiclassical Treatment of Atom-Asymmetric Rotor Collisions; Rotational Excitation of Formaldehyde at Low Energies . . . 51

A. Introduction 51

B. Semiclassical Description of the Isolated Asymmetric Rotor 53

C. Semiclassical Theory of Atom-Asymmetric Rotor Collisions; Methodology 56

D. Results and Discussion 70

Appendix 1. Semiclassical Treatment of the Asymmetric Rotor 77

Appendix 2. Action-Angle Variables for Atom-Asymmetric Rotor Collisions 85

Appendix 3. Monte-Carlo Technique for Asymmetric Rotor Transitions 90

IV. Semiclassical Theory of Non-Reactive Diatom-Diatom Collisions 93

V. The Use of Action Angle Variables for Collision Dynamics . . .116

VI. Classical Trajectory Study of Rotational Excitation in Low Energy He-CO Collisions 130

VII. Additional Topics 137

A. Alternate Calculation of Jacobians 137

B. Three-Dimensional Generalization of the Wall-Porter Potential 140

Acknowledgements 145

References 146

SEMICLASSICAL METHODS AND THEIR APPLICATION TO PROBLEMS IN COLLISION THEORY

Stuart Dudley Augustin

Inorganic Materials Research Division, Lawrence Berkeley Laboratory and Department of Chemistry; University of California, Berkeley, California 94720

ABSTRACT

With the recent development of classical S-matrix theory, semiclassical methods have been applied to an increasing range of problems in collision dynamics. This work involves the application and improvement of older methods as well as the extension of classical S-matrix methods to systems more complex than those previously considered.

The first chapter includes a review of previous methods for treating electronic transitions in the collision of two atoms. Special emphasis is given to Stueckelberg's method and how it can be extended to give improved results for the transition probability. Approaches are also presented by which more of the quantum behavior may be taken into account.

The second chapter describes the application of semiclassical methods to the calculation of the cross section for the $^4S \rightarrow {}^2D$ excitation of O^+ during collisions with ground state He. The transition arises from a spin-orbit interaction at a crossing of the lowest $^4\Sigma$ and $^2\Pi$ states of HeO^+. There is a residual oscillatory structure in the energy dependence of the cross section, and it is shown how experimental observation of this could be used to obtain precise information concerning the relevant potential curves.

In the next section, the formalism necessary for the application of classical S-matrix theory to collisions of an atom with a rigid asymmetric rotor is derived. This is applied to rotational excitation of formaldehyde by H_2 (taken to be spherically symmetric) at energies from 10°K to 15°K. Classical Monte-Carlo trajectory calculations were also carried out for the same system in the energy range 10°K to 40°K. The results support the proposal of Townes and Cheung that a collisional mechanism is responsible for the $1_{11} \rightarrow 1_{10}$ anomalous absorption of formaldehyde in cool interstellar dust clouds.

The asymmetric rotor work is the first application of classical S-matrix methods to a collision involving a polyatomic molecule. The formalism necessary for the extension of the theory to the simplest two center problem, the diatom-diatom system, is derived in the following chapter. Indications are also given as to how this may be generalized to include more complex molecules as collision partners.

Chapter V considers the advantages and disadvantages of using action-angle variable for computing classical trajectories. Consideration is given to the computation of complex-valued trajectories and to apparent singularities in the action-angle variable formalism for a model system.

Classical trajectory calculations for the rotational excitation of CO by collisions with He at low energies are presented in the next chapter. The results are compared with accurate quantum mechanical calculations by other workers.

The last chapter considers a procedure by which the Jacobian factors necessary for the use of classical S-matrix theory can be calculated from perturbed classical trajectories. A three-dimensional generalization of

the Wall-Porter potential for collinear diatom-atom reactions is also presented.

I. THEORY OF ELECTRONIC TRANSITIONS

A. Introduction

In the collision of two atoms in which an electronic transition can occur, it is clear that the electronic degrees of freedom must be handled quantum mechanically. However, classical dynamics is usually adequate to describe the translational degree of freedom. A satisfactory semiclassical theory of such a process then requires the explicit blending of classical and quantum dynamics. The obvious way to proceed is to expand the total wave function in a complete set of functions which give partial separation of the electronic and nuclear degrees of freedom.

If $\vec{R}$ is the relative internuclear coordinate and $\vec{r}$ is shorthand for all the electron coordinates, the complete Hamiltonian for a diatomic system is

$$H = T_R + T_r + V(\vec{R},\vec{r}) \tag{1}$$

where T_R and T_r are the nuclear and electronic kinetic energies, respectively, and $V(\vec{R},\vec{r})$ is the total potential energy. The last two terms of Eq. (1) (often called the electronic Hamiltonian) may be further divided if the electrons are assigned to either nucleus a or nucleus b. Let $\vec{R}_a$ and $\vec{R}_b$ be the position vectors of the two nuclei and $\vec{r}_a$, $\vec{r}_b$ be the position vectors of the electrons assigned to nucleus a, b; then

$$H_{el} = T_r + V(\vec{R},\vec{r}) = T_{r_a} + T_{r_b} + \frac{Z_a Z_b e^2}{R} + V_a(|\vec{R}_a - \vec{r}_a|,\vec{r}_a) \tag{2}$$

$$+ V_b(|\vec{R}_b - \vec{r}_b|,\vec{r}_b) + V_{ab}(\vec{R},\vec{r}_a,\vec{r}_b) \quad .$$

If the total wave function $\Psi(\vec{R},\vec{r})$ is expanded in eigenfunctions of the electronic Hamiltonian, the adiabatic representation for the scattering problem is obtained. That is we let $\psi_i(\vec{R},\vec{r})$ be the ith solution of the equation

$$[T_r + V(\vec{R},\vec{r})]\ \psi_i(\vec{R},\vec{r}) = \varepsilon_i(\vec{R})\ \psi_i(\vec{R},\vec{r}) \tag{3}$$

where $\psi_i(\vec{R},\vec{r})$ and $\varepsilon_i(\vec{R})$ have only a parametric dependence on $\vec{R}$. The total wave function is then given by

$$\Psi(\vec{R},\vec{r}) = \sum_{i=1}^{\infty} \phi_i(\vec{R})\ \psi_i(\vec{R},\vec{r}) \tag{4}$$

if a complete set of ϕ_i's is included. The full Schrödinger equation is now

$$(T_R + H_{el}) \sum_{i=1}^{\infty} \phi_i(\vec{R})\ \psi_i(\vec{R},\vec{r}) \tag{5}$$

$$= E \sum_{i=1}^{\infty} \phi_i(\vec{R})\ \psi_i(\vec{R},\vec{r}) \quad .$$

Equation (5) is then multiplied on the left by $\psi_j^*(\vec{R},\vec{r})$ and integrated over $\vec{r}$ to give the matrix equation

$$(\underset{\sim}{T}_R - \underset{\sim}{W}(\vec{R}))\ \vec{\phi}(\vec{R}) = \underset{\sim}{0} \tag{6}$$

where $\vec{\phi}(\vec{R})$ is the column matrix of nuclear wave functions,

$$[\underset{\sim}{W}(R)]_{ij} = [\varepsilon_i(\vec{R}) - E]\ \delta_{ij} \quad ,$$

and

$$[T_R]_{ij} = \langle\psi_i|T_R|\psi_j\rangle \quad .$$

It may be noted that $\underset{\sim}{W}(\vec{R})$ is a diagonal matrix while $\underset{\sim}{T}_R$ is not diagonal. In the limit that the nuclear mass is infinitely greater than the electron mass, the off-diagonal elements of $\underset{\sim}{T}_R$ go to zero (neglecting relativistic effects) and the familiar Born-Oppenheimer approximation[1] is obtained. If this were the case, the $\phi_i(\vec{R})$'s would be uncoupled and no transitions would occur.

Of course there are many more possible choices for the electronic basis set since any two bases that are related by a unitary transformation are equally valid. For the purpose of studying electronic transitions, it is desirable to have a basis in which the transitions are explicitly allowed to occur. In addition, for the scattering problem, it is important that the electronic basis functions go to a product of separated atom wave functions in the asymptotic region, a property that the adiabatic basis does posess. The electronic basis set formed by a complete set of products of atomic functions obviously satisfies this requirement and is unique[2] in that it diagonalizes the kinetic energy matrix for all values of R.

In keeping with Smith[2], the above basis will henceforth be referred to in this work as the diabatic basis. Other workers have also defined bases that may be called locally diabatic bases. In these, the adiabatic representation is followed except in the neighborhood of an avoided crossing. A linear combination of the adiabatic functions is defined in that region such that the off-diagonal couplings are locally transferred from the kinetic energy matrix to the potential matrix. These locally diabatic representations depend on the specific system for which they are defined, and it is thus desirable to retain

the designation "diabatic representation" for the unique representation that diagonalizes the kinetic energy matrix everywhere.

The diabatic electronic basis set consists of a complete set of products of eigenfunctions of the separated atoms. These functions are the solutions $\xi_i(\vec{r})$ of the equation

$$[T_{r_a} + T_{r_b} + V_a(|\vec{R}_a - \vec{r}_a|,\vec{r}_a) + V_b(|\vec{R}_b - \vec{r}_b|),\vec{r}_b)]\ \xi_i(\vec{r}) = e_i\xi_i(\vec{r}) \quad . \tag{7}$$

The total wave function can now be expanded as

$$\Psi(\vec{R},\vec{r}) = \sum_{i=1}^{\infty} \chi_i(R)\ \xi_i(r) \tag{8}$$

so that the χ_i's obey the matrix equation

$$[\underset{\sim}{I}T_R + \underset{\sim}{V}(\vec{R}) - \underset{\sim}{E}]\ \vec{\chi}(\vec{R}) = \underset{\sim}{0} \tag{9}$$

where

$$[\underset{\sim}{V}(\vec{R})]_{ij} = \langle\xi_i\left|\left[\frac{Z_aZ_be^2}{R} + V_{ab}(\vec{R},\vec{r}_a,\vec{r}_b)\right]\right|\ \xi_j\rangle \quad ,$$

$$\underset{\sim}{E}_{ij} = (E - e_i)\ \delta_{ij} \quad ,$$

and $\underset{\sim}{I}$ is the idenity matrix. It can be seen from Eq. (9) that in this representation electronic transitions arise from the off-diagonal elements of the matrix $\underset{\sim}{V}(\vec{R})$.

If $\underset{\sim}{A}(\vec{R})$ is the unitary transformation that diagonalizes $[\underset{\sim}{V}(\vec{R}) - \underset{\sim}{E}]$, the relationship between the nuclear functions χ and ϕ can be readily obtained. Equation (9) can be written as

$$\{\underset{\sim}{A}(\vec{R})\ T_R \underset{\sim}{A}^{-1}(\vec{R}) + \underset{\sim}{A}(\vec{R})[\underset{\sim}{V}(\vec{R}) - \underset{\sim}{E}]\ \underset{\sim}{A}^{-1}(\vec{R})\} \tag{9'}$$

$$\underset{\sim}{A}(\vec{R})\ \vec{\chi}(\vec{R}) = 0 \quad .$$

Since

$$\underset{\sim}{A}(\vec{R})[\underset{\sim}{V}(\vec{R}) - \underset{\sim}{E}]\ \underset{\sim}{A}^{-1}(\vec{R})$$

must be equal to $\underset{\sim}{W}(\vec{R})$, it is clear by comparison with Eq. (6) that

$$\underset{\sim}{T}_R = \underset{\sim}{A}(\vec{R})\ T_R \underset{\sim}{A}^{-1}(\vec{R}) \tag{10a}$$

$$\vec{\phi}(\vec{R}) = \underset{\sim}{A}(\vec{R})\ \vec{\chi}(\vec{R}) \quad . \tag{10b}$$

Although knowledge of $\underset{\sim}{V}(\vec{R})$ is enough to define the relationship of the adiabatic and diabatic representations, to go the other way requires a knowledge of the off-diagonal matrix elements of $\underset{\sim}{T}_R$. Virtually all calculations of potential energy surfaces are done within the Born-Oppenheimer approximation so that information about the off-diagonal elements of $\underset{\sim}{T}_R$ is difficult to obtain. The great difficulty with the diabatic representation then is that relatively little can be determined about the matrix $\underset{\sim}{V}(\vec{R})$ from a knowledge of the Born-Oppenheimer potential curves.

B. The Curve Crossing Problem

The primary rationale for the application of semiclassical methods to the electronic transition problem is the relatively classical behavior of the nuclear motion for most of the collision. Ideally then, the region in which quantum effects are important should be relatively small and localized. One case in which this ideal is often well realized is that of the crossing of two potential curves. According to the Franck-Condon

principle, a radiationless transition between two crossing potential curves will occur only at the place where the curves cross since this is the only place where the transition can take place with the nuclei remaining fixed. It would seem then that the curve crossing problem is the most propitious case for the use of semiclassical methods.

The non-crossing rule[3] for molecular states is an important consideration for the curve crossing problem. Since the born-Oppenheimer approximation is generally very good for molecular systems, it would be expected that the motion of the nuclei during a collision would follow the adiabatic potential curves. An exception to this is when two curves of the same symmetry approach each other and the non Born-Oppenheimer terms become large compared to the energy separation of the two states. In this case the adiabatic potential curves will have an avoided crossing; they approach each other and then move apart without intersecting. At such an avoided crossing the diabatic potential curves will actually cross and they intersect at about the same R value where the adiabatic curves approach each other most closely (see Fig. 1). The locally diabatic representations mentioned earlier are basically a linear combination of adiabatic states needed to give a potential matrix whose diagonal elements do cross.

If the transitions occur only in the near vicinity of the crossing point, the effect of the presence of other electronic states on the transition should be minimal. Therefore, it is a good approximation that only the two states that cross need be considered in determining the likelihood of an electronic transition (provided that all such crossings are well separated). The relationship between the adiabatic

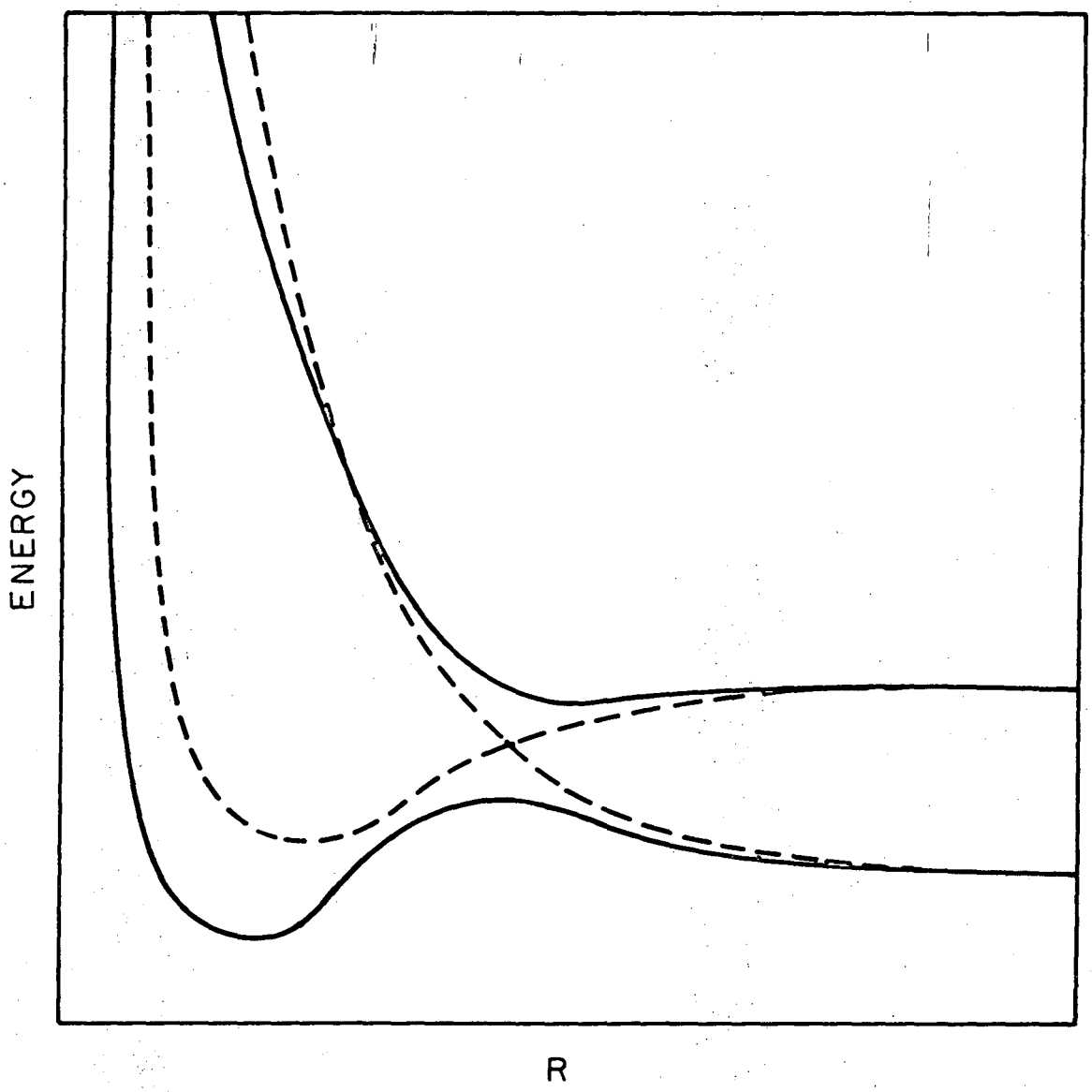

XBL749-7128

Fig. 1. A hypothetical case of the avoided crossing of two curves, illustrating the typical behavior. The solid lines are the adiabatic potential curves while the dashed lines are the diabatic curves.

diabatic potential curves can be simply expressed when the electronic basis is truncated to the two states under consideration.

In the two state approximation, Eq. (9) can be written as

$$\left[\begin{pmatrix} T_R & 0 \\ 0 & T_R \end{pmatrix} + \begin{pmatrix} V_{11}(R) & V_{12}(R) \\ V_{12}(R) & V_{22}(R) \end{pmatrix} - \begin{pmatrix} E-e_1 & 0 \\ 0 & E-e_1 \end{pmatrix}\right] \begin{pmatrix} \chi_1(R) \\ \chi_2(R) \end{pmatrix} = \begin{pmatrix} 0 \\ 0 \end{pmatrix} \tag{11}$$

A partial wave expansion of the functions $\chi_i(R)$ can now be performed to eliminate the spatial dependence of the operator T_R. This expansion will add

$$\frac{\hbar^2 \ell(\ell + 1)}{2\mu R^2}$$

to the diagonal elements of $\underset{\sim}{V}$ and may add other terms to $\underset{\sim}{V}$ from the coupling of orbital and electronic angular momentum.[4] The coupled channel equations for the radial functions are now

$$\left[-\frac{\hbar^2}{2\mu}\begin{pmatrix} \frac{d^2}{dR^2} & 0 \\ 0 & \frac{d^2}{dR^2} \end{pmatrix} + \begin{pmatrix} U_{11}(R) & U_{12}(R) \\ U_{12}(R) & U_{22}(R) \end{pmatrix}\right] \begin{pmatrix} u_1(R) \\ u_2(R) \end{pmatrix} = \begin{pmatrix} 0 \\ 0 \end{pmatrix} \tag{12}$$

where $U_{ij}(R) = V_{ij}(R) + (e_i - E)\,\delta_{ij}$ plus angular momentum terms. The $\underset{\sim}{U}(R)$ matrix is diagonalized by the transformation

$$\begin{pmatrix} \sqrt{\frac{\gamma+\beta}{2\gamma}} & \sqrt{\frac{\gamma-\beta}{2\gamma}} \\ -\sqrt{\frac{\gamma-\beta}{2\gamma}} & \sqrt{\frac{\gamma+\beta}{2\gamma}} \end{pmatrix} \begin{pmatrix} U_{11} & U_{12} \\ U_{12} & U_{22} \end{pmatrix} \begin{pmatrix} \sqrt{\frac{\gamma+\beta}{2\gamma}} & -\sqrt{\frac{\gamma-\beta}{2\gamma}} \\ \sqrt{\frac{\gamma-\beta}{2\gamma}} & \sqrt{\frac{\gamma+\beta}{2\gamma}} \end{pmatrix} \tag{13}$$

$$= \underset{\sim}{A}\underset{\sim}{U}\underset{\sim}{A}^{-1} = \begin{pmatrix} \alpha+\gamma & 0 \\ 0 & \alpha-\gamma \end{pmatrix}$$

where

$$\alpha = \frac{1}{2}[U_{11} + U_{22}] \ , \ \beta = \frac{1}{2}[U_{11} - U_{22}] \ , \ \gamma = \sqrt{\beta^2 + U_{12}^2} \quad .$$

The functions

$$\begin{pmatrix} v_1(R) \\ v_2(R) \end{pmatrix} = \underset{\sim}{A} \begin{pmatrix} u_1(R) \\ u_2(R) \end{pmatrix}$$

are then the solutions of the coupled channel equations in the adiabatic representation

$$-\frac{\hbar^2}{2\mu} \underset{\sim}{A}(R) \frac{d^2}{dR^2} [\underset{\sim}{A}^{-1}(R) \vec{v}(R)] + \begin{pmatrix} \alpha+\gamma & 0 \\ 0 & \alpha-\gamma \end{pmatrix} \vec{v}(R) = \vec{0} \tag{14}$$

The coupled channel equations in the diabatic representation (Eq. (12)) are thus a simple second order system with no first derivative terms. The adiabatic representation (Eq. (14)), on the other hand, gives a significantly less mathematically tractable system of equations. It would seem then that the system Eq. (12) would be much more amenable to approximate methods of solution and to the formulation of model problems than is Eq. (14). Indeed the classical treatments of this problem by Landau,[5] Zener,[6] and Stueckelberg[7] all begin with the coupled equations in the diabatic representation.

The great advantage of the adiabatic representation lies in the availability of the adiabatic potential curves. Virtually all methods for the determination of potential curves are carried out within the Born-Oppenheimer approximation so that usually only the adiabatic curves are known. The diabatic curves are very difficult to obtain by any ab-initio or empirical procedure and a theory based on these curves would seem to be of little utility.

A major exception to the unavailability of diabatic potential curves is when the coupling of states of different symmetry is responsible for the transition at a curve crossing. In these situations the Born-Oppenheimer curves actually do cross although the two Born-Oppenheimer states are connected by off diagonal matrix elements. Under such circumstances the adiabatic potential curves may be considered as the diagonal elements of a diabatic potential matrix, and the problem of finding the diabatic matrix for such a system thus reduces to the calculation of the off-diagonal matrix elements of the coupling operator between the Born-Oppenheimer electronic wave functions. Spin orbit coupling and the coupling of electronic and orbital angular momenta[4,8] are two important examples of the interaction between electronic states of different symmetry.

C. Summary of LZS Theory

The earliest theoretical work on the curve-crossing problem is that of Landau,[5] Zener,[6] and Stueckelberg;[7] all of whom derived the well-known Landau-Zener formula for the transition probability. In each derivation, it was assumed that the transition takes place only in the immediate vicinity of the crossing point. Bates[9] and Coulson

and Zalewski[10] have found that this argument breaks down for high energies and that the width of the transition region actually becomes unbounded in the limit of infinite energy. Landau, Zener and Stueckelberg also made the assumption that the diabatic curves are approximately linear near the crossing point and that the off-diagonal matrix element is approximately constant. Stueckelberg's derivation by means of a connection formula may also be used, however, with the exact adiabatic potential curves, and it also includes the interference effects from the two classical trajectories contributing to the transition. Stueckelbert's results are, therefore, capable of much wider validity than the simple Landau-Zener formula.

The Stueckelberg derivation begins by dividing the R domain for each diabatic curve into three regions as in Fig. 2. Region I is for R between 0 and the classical turning point (R_o) for energy E, Region II lies between the turning point and the crossing point (R_x), and Region III includes all R values outside the crossing point. WKB wave functions can be written down for each of the three regions, but they are invalid at the classical turning point and at the crossing point. It must then be determined what linear combination of the WKB functions is a regular solution with the proper asymptotic behavior, a process that requires that the solutions be joined over the entire R domain. The well known derivation of the WKB phase shift[11] for simple elastic scattering proceeds by obtaining the quantum mechanical solution for the wave function in the immediate vicinity of the turning point, with the assumption that the potential curve is linear. The asymptotic behavior of the quantum mechanical solution is then matched to WKB wave functions in Regions I

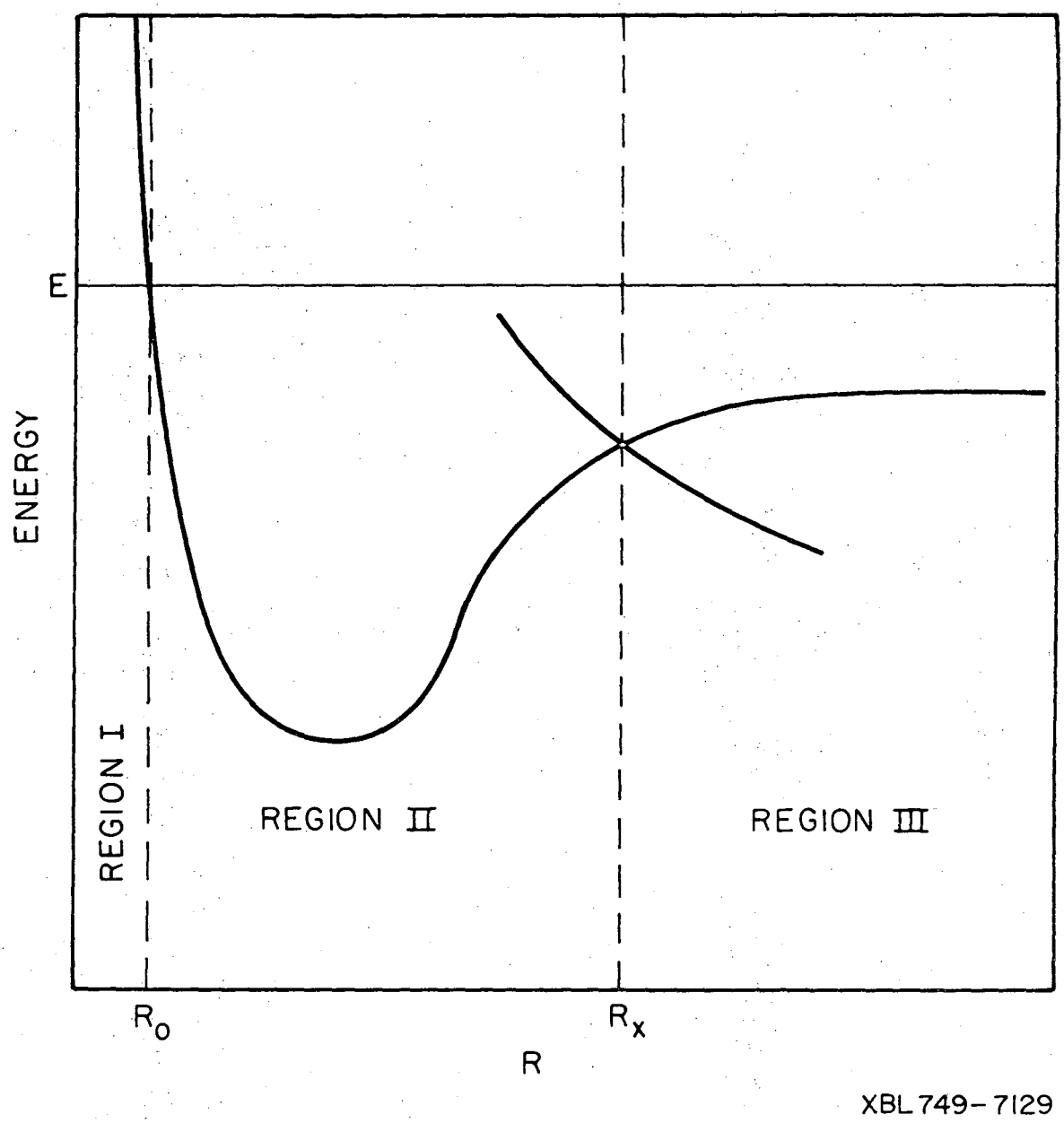

Fig. 2. Partition of the R domain for diabatic potential curves with a crossing.

and II in order to "connect" the WKB solutions in these two domains. Stueckelberg's procedure finds a "connection formula" for joining the solutions in Regions II and III as well.

His procedure for connecting the solutions is analagous to that used by Zwaan[12] and Kemble[13] for the WKB turning point problem. The WKB wave functions are analytically continued into the complex R plane, and solutions in Regions II and III are connected by following a complex R path that stays far enough away from the corssing point so that the WKB functions are still valid. The mathematical validity of Stueckelbert's procedure has been examined in more detail by Rice[14] and Thorson, et al.[15]

Stueckelberg's result for the S-matrix elements can be interpreted by realizing that there are two classical trajectories contributing to each transition (Fig. 3). Trajectory I follows the adiabatic curve to the turning point and crosses over to the other curve on the way out. Trajectory II, however, crosses curves on the way in and does not cross on the way out (the picture must be altered somewhat in the diabatic representation since a diabatic crossing is an adiabatic non-crossing and vice versa). If the transition takes place only at R_x, then the magnitude squared of the two off-diagonal S-matrix elements must be expressed as $P_x(1 - P_x)$ where P_x is the probability of a trajectory changing curves when it passes the crossing point (and of course $1 - P_x$ is the probability of staying on the same curve). The two trajectories will, however, contribute terms with different phases to the S-matrix element since the WKB phases over the trajectories will be unequal in general.

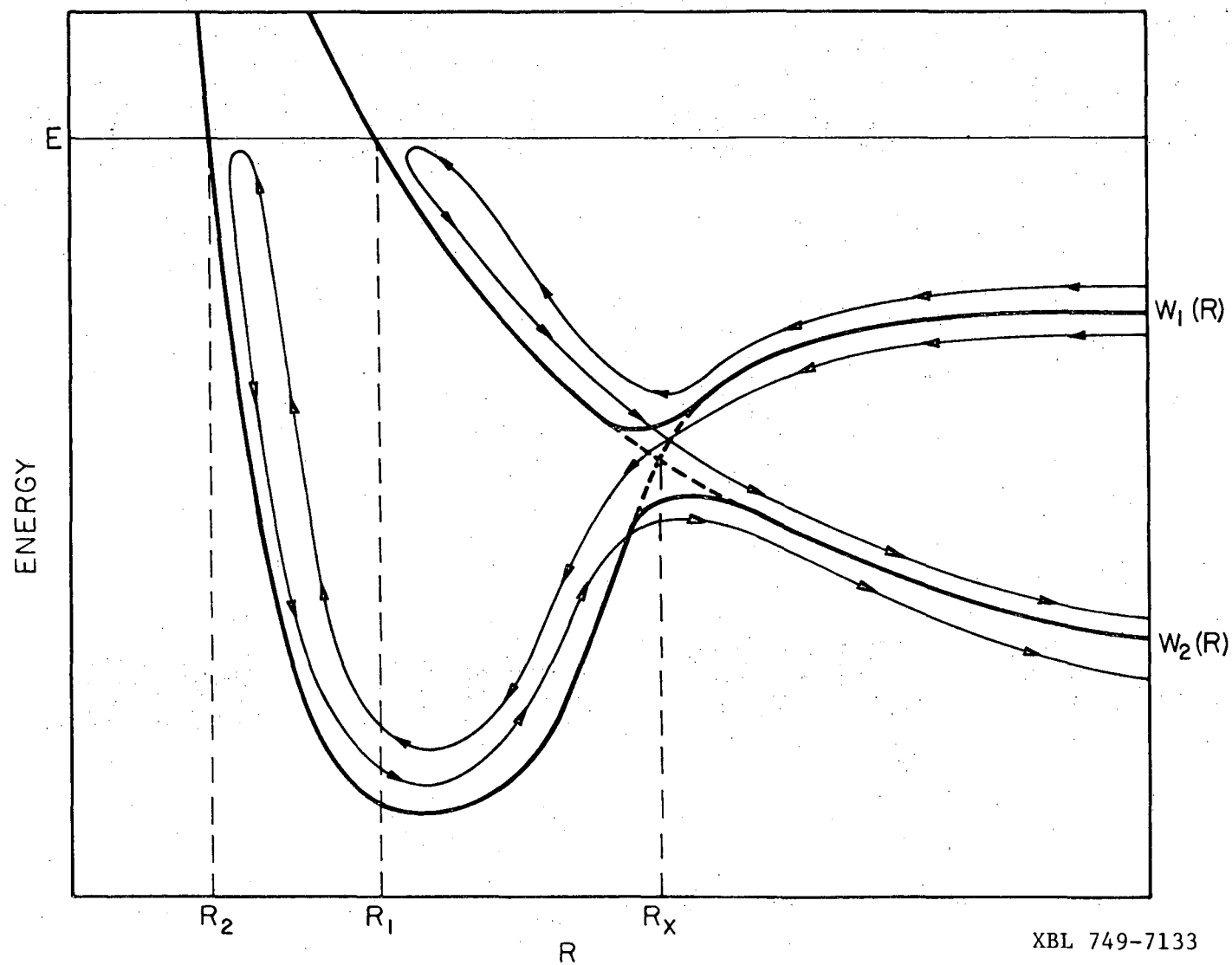

Fig. 3. Two possible classical trajectories for the transition between the upper and lower states on hypothetical adiabatic curves.

Let R_c and R_c^* be the two complex values of R at which the adiabatic curves cross. From Eq. (13) it can be seen that R_c is defined by

$$1/4[U_{11}(R_c) - U_{22}(R_c)]^2 + U_{12}^2(R_c) = 0 \quad . \tag{15}$$

Adopting the convention that $W_1(R)$ is the adiabatic curve for the upper state and $W_2(R)$ that for the lower state; let

$$k_i(R) = \frac{1}{\hbar}\{2\mu[E - W_1(R)]\}^{1/2}$$

and $k_i = k_i(\infty)$. Stueckelberg obtained the result that

$$P_x = e^{-2\delta} \ , \quad \delta = i \int_{R_c^*}^{R_c} [k_2(R) - k_1(R)]\, dR \tag{16}$$

It may be noted that δ has the appearance of a WKB barrier penetration integral. The S matrix element is given by

$$S_{2\leftarrow 1} = \sqrt{P_x(1 - P_x)}\left[e^{i\phi^I} + e^{i\phi^{II}}\right] \tag{17}$$

where ϕ^I, ϕ^{II} are the WKB phases along the two possible trajectories

$$\phi^I = \lim_{R\to\infty}\left[-\pi/4 - k_1R - k_2R + \int_{R_x}^{R} k_1(R')\, dR' + \int_{R_x}^{R} k_2(R')\, dR' + 2\int_{R_1}^{R_x} k_1(R')\, dR'\right] \tag{18a}$$

$$\phi^{II} = \lim_{R\to\infty}\left[\pi/4 - k_1R - k_2R + \int_{R_x}^{R} k_1(R')\, dR' + \int_{R_x}^{R} k_2(R')\, dR' + 2\int_{R_2}^{R_x} k_2(R')\, dR'\right] \tag{18b}$$

The transition probability $P_{2\leftarrow 1} = |S_{2\leftarrow 1}|^2$ is now given by

$$P_{2\leftarrow 1} = 4e^{-2\delta}(1 - e^{-2\delta}) \sin^2(\tau + \pi/4) \tag{19a}$$

where

$$\tau = 1/2(\phi^{I} - \phi^{II}) = \int_{R_1}^{R_x} k_1(R')\, dR' - \int_{R_2}^{R_x} k_2(R')\, dR' \tag{19b}$$

It may be seen that an extra constant of $\pi/4$ has been inserted in Eqs. (18a,b) as compared to Stueckelberg's derived results. Recent work[15] indicates that there is an undetermined constant phase in the derivation, but by analogy with the Distorted Wave Born Approximation it ought to be $\pi/4$.

It is important to note that all of the quantities in Eqs. (17) through (19) refer to the exact adiabatic curves. As was argued earlier this is desirable since, in general, only the adiabatic potential curves are available.

The Landau-Zener formula for the transition probability may be obtained from Eq. (19a) if certain approximations are made to δ and the phase difference τ is assumed to be large. To follow the Stueckelberg derivation, the integrand in the expression for δ is expanded in a power series in the variable

$$t(R) = \frac{\beta(R)}{U_{12}(R)}$$

If only the first order term in t is kept[16] and the assumptions are made that $U_{11}(R)$, $U_{22}(R)$ are linear and $U_{12}(R)$ is constant near R_x, then the Landau-Zener expression is obtained for δ

$$\delta = \frac{\pi}{\hbar V(R_x)} \frac{|U_{12}(R_x)|^2}{|U'_{11}(R_x) - U'_{22}(R_x)|} \tag{20}$$

where $V(R_x)$ is the local velocity at the crossing point. If it is assumed that τ is large, $\sin^2(\tau + \pi/4)$ may be replaced by its average value, 1/2, and

$$P_{2\leftarrow 1} = 2e^{-2\delta}(1 - e^{-2\delta}) \tag{21}$$

which is Zener's[6] result for the transition probability. Finally, if δ is assumed to be small, the exponentials in Eq. (21) may be expanded to give Landau's result

$$P_{2\leftarrow 1} = 4\delta \tag{22}$$

Examination of Eq. (20) reveals that in this approximation δ becomes infinite at threshold where $V(R_x)$ is equal to zero. This well known failure of the Landau-Zener formula is a consequence of the approximate method of evaluating the phase integral in Eq. (16) and is not a breakdown of the basic theory. Equation (16) may have some deficiencies near threshold but at least it is well behaved and continuous.

A modification to Eqs. (19a,b) must be made for energies below the crossing energy. In this case, both of the phases in Eq. (19b) are imaginary and the sin of Eq. (19a) must go over to an exponential. It would seem that it is also necessary to make the further change

$$\tau = \int_{R_1}^{R_x} k_1(R')\, dR' + \int_{R_2}^{R_x} k_2(R')\, dR' \quad . \tag{19b'}$$

This may be looked upon as forcing the atoms to "tunnel in" to the crossing point, where the transition occurs, and then "tunnel" back out.[21]

D. Extensions and Improvements of LZS Theory

Two very important assumptions are made in the derivation of the connection formula for the curve crossing problem. The first is that the breakdowns in the WKB approximation are localized. This is not true, as was mentioned earlier, for the breakdown at the crossing point in the high energy limit. The other major assumption is that the points of breakdown are isolated. This fails when there are two nearby crossing points or when the crossing point is close to a turning point. Unfortunately, the nearness of the crossing point to one or both turning points is unavoidable near threshold or when the orbital angular momentum is large enough to move the corssing energy up to the translational energy.

O. K. Rice[14] attempted to handle the low energy difficulty by taking a complex R path that circumvents the crossing point and the turning points simultaneously. However, he was unable to determine the transition probability for that case. More recently Nikitin et al.[17] have attempted to find the transition probability by solving a model problem in the vicinity of the crossing point. This has some analogy with solving the linearized potential problem for the WKB connection formula at the turning point.

In the diabatic representation, the coupled channel equations for the radial functions of the two state problem are (see Eq. (12))

$$\left[-\frac{\hbar^2}{2\mu} \begin{pmatrix} \frac{d^2}{dR^2} & 0 \\ 0 & \frac{d^2}{dR^2} \end{pmatrix} + \begin{pmatrix} U_{11}(R) & U_{12}(R) \\ U_{12}(R) & U_{22}(R) \end{pmatrix} \right] \begin{pmatrix} u_1(R) \\ u_2(R) \end{pmatrix} = \begin{pmatrix} 0 \\ 0 \end{pmatrix} \tag{23}$$

Nikitin's model problem assumes $U_{12}(R)$ is a constant and $U_{11}(R)$, $U_{22}(R)$ are linear functions of R. That is, let

$$\begin{aligned} U_{12}(R) &= a \\ U_{11}(R) &= (E - E_x) + c_1(R - R_x) \\ U_{22}(R) &= (E - E_x) + c_2(R - R_x) \end{aligned} \tag{24}$$

where E_x is the energy of the crossing point (see Fig. 4). Defining $b = E - E_x$ and $x = R - R_x$,[18] Eq. (23) becomes

$$\left[-\frac{\hbar^2}{2\mu} \begin{pmatrix} \frac{d^2}{dx^2} & 0 \\ 0 & \frac{d^2}{dx^2} \end{pmatrix} + \begin{pmatrix} b + c_1 x & a \\ a & b + c_2 x \end{pmatrix} \right] \begin{pmatrix} u_1(x) \\ U_2(x) \end{pmatrix} = \begin{pmatrix} 0 \\ 0 \end{pmatrix} \tag{25}$$

Nikitin could not find a solution of Eq. (25) valid for all values of the parameters and could only get solutions for certain limiting cases.

One of Nikitin's limiting solutions is for the situation that

$$\frac{4a^{3/2}\mu^{1/2}}{\hbar\sqrt{|c_2 - c_1|}\,(c_1c_2)^{1/4}} \gg 1$$

(basically the strong coupling limit). For this case, his solution turns out to be a subcase of Eq. (17) with δ given as in Eq. (16). The solution in the weak coupling limit is the distorted wave Born

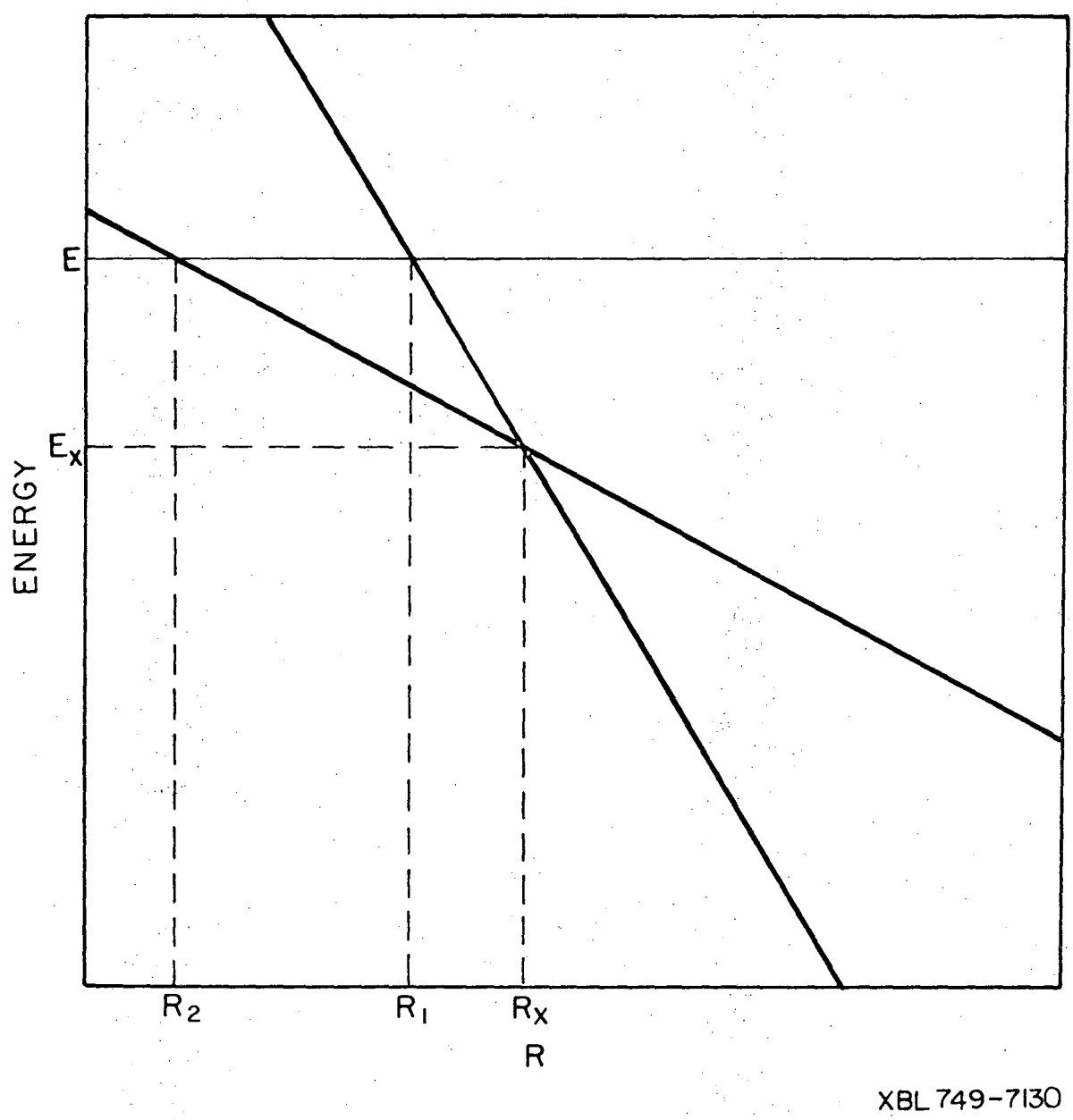

Fig. 4. Nikitin's model problem for curve-crossing.

approximation result for Eq. (25),[20] and it is of value to compare this result with that of Eq. (19a).

The distorted wave result for the transition probability is

$$P_{2\leftarrow 1}(\mathrm{DWBA}) = 4\pi^2 a^2 \left[\left(\frac{2\mu}{\hbar^2}\right)^2 \frac{1}{c_1 c_2 (c_2 - c_1)^2}\right]^{1/3} \left\{ \mathrm{Ai}^2\left[-b\,\frac{2\mu}{\hbar^2}\left(\frac{c_2 - c_1}{c_1 c_2}\right)^2\right]^{1/3}\right\} \tag{26}$$

where Ai is the Airy function. In the limit of small a, the expression for δ in Eq. (16) becomes the same as that of Eq. (20), and for this system it is

$$\delta = \frac{\pi a^2}{2|c_1 - c_2|\, b^{1/2}} \sqrt{\frac{2\mu}{\hbar^2}} \tag{27}$$

It is found from Eq. (19b) that

$$\tau = \frac{2^{3/2}\mu^{1/2} b^{3/2}}{3\hbar} \left(\frac{c_2 - c_1}{c_1 c_2}\right) \tag{28}$$

so that Eq. (26) can be written in terms of τ and δ as

$$P_{2\leftarrow 1}(\mathrm{DWBA}) = 8\pi\delta \left(\frac{3}{2}\,\tau\right)^{1/3} \mathrm{Ai}^2\left[-\left(\frac{3}{2}\,\tau\right)^{2/3}\right] \tag{29}$$

Since δ is presumed to be small in the weak coupling limit, the exponentials in Eq. (19a) can be expanded to give

$$P_{2\leftarrow 1}(\mathrm{LZS}) = 8\delta \sin^2(\tau + \pi/4) \quad . \tag{19a'}$$

For large τ, the Airy function in Eq. (29) can be replaced by its asymptotic expression[19]

$$\mathrm{Ai}(-z) \sim \frac{1}{\sqrt{\pi}}\, z^{-1/4} \sin\left(\frac{2}{3}\, z^{3/2} + \pi/4\right) \quad , \tag{30}$$

and when this is done Eq. (29) becomes identical to Eq. (20a).

Equation (26) is the quantum mechanical result for the model system in the limit of weak coupling so that the insertion of $\pi/4$ in Eqs. (18a,b) would seem to be justified. It would also be expected that if Eq. (19a) is modified to replace the sin by the appropriate Airy function, then the low energy behavior will be improved. With this modification Eq. (19a) becomes

$$P_{2\leftarrow 1} = 4\pi \left(\frac{3}{2}\,\tau\right)^{1/3} e^{-2\delta}(1 - e^{-2\delta})\mathrm{Ai}^2\left[-\left(\frac{3}{2}\,\tau\right)^{2/3}\right] \tag{31}$$

where δ is defined as in Eq. (16) and τ is as in Eq. (19b) or Eq. (19b'). Equation (26) is now just a limiting case of Eq. (31) for the model system.

E. Uniform Approximation for the Wave Function

There is an interesting procedure for handling the WKB turning point problem due to Langer.[22] Rather than using elementary functions of different types (exponential and trigonometric) on the two sides of a turning point, this method uses a single functional form over the entire domain. Such an approximation is then uniformly good over the entire region in the sense that the error of the approximation depends very little upon the position.

Consider a hypothetical problem of a potential V(x) defined on the domain from $-\infty$ to $+\infty$, with a classical turning point x_o at energy E (Fig. 5). WKB wave functions can be written down for Regions I and II away from the turning point

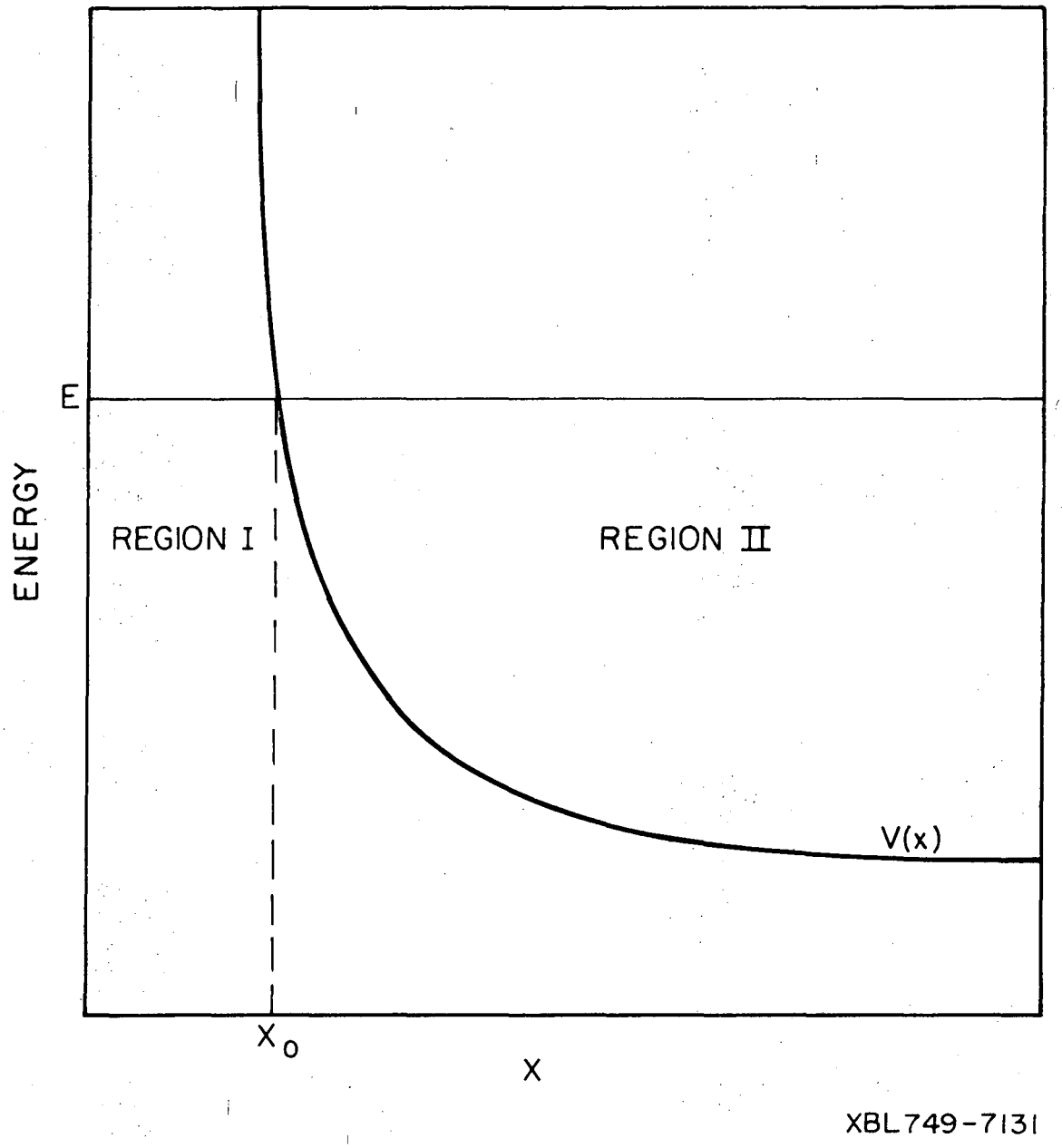

Fig. 5. A hypothetical problem to illustrate a uniform approximate for the WKB wavefunction.

$$\psi^{I}(x) \simeq \frac{1}{\sqrt{k(x)}} \exp\left[-\int_{x}^{x_o} k(x')\,dx'\right] \qquad (x < x_o)$$

$$\psi^{II}(x) \simeq \frac{1}{\sqrt{k(x)}} \sin\left[\pi/4 + \int_{x_o}^{x} k(x')\,dx'\right] \qquad (x > x_o) \tag{32}$$

where

$$k(x) = \frac{\sqrt{2\mu}}{\hbar} \sqrt{E - V(x)} \quad .$$

If the WKB approximation is reasonably good for the hypothetical system, the difference between Eq. (32) and the exact wave function will be relatively small over most of the domain of x but will be infinite at the turning point. The potential can be approximated by a straight line in the near vicinity of x_o in which case the quantum solution will be

$$\psi(x) = \mathrm{Ai}\left\{\left(\frac{2mF}{\hbar^2}\right)^{1/3}\left[\frac{2mEF}{\hbar^2} - x\right]\right\} \tag{33}$$

where F is the force at x_o. This solution (which can be used to get a "connection formula" by matching it to the WKB functions) is quite close to the true wave function near x_o, but is a very poor approximation away from this point.

The basis of the uniformized WKB wave function comes from the recognition that the asymptotic behavior of the Airy function[19] has the right nature in Regions I and II. Thus the wave function may be written

$$\psi_u(x) = \sqrt{\frac{\pi}{d\phi/dx}} \left(\frac{3}{2}\phi\right)^{1/6} \mathrm{Ai}\left[-\left(\frac{3}{2}\phi\right)^{2/3}\right] \tag{34}$$

where

$$\phi(x) = \int_{x_o}^{x} k(x')\, dx' \quad .$$

When $\phi(x)$ is large, as it will be when Eq. (32) is suitable, Eq. (34) is practically the same as the WKB solution. For the near vicinity of x_o, $\psi_u(x)$ is still a very good approximation to the exact wave function so that $\psi_u(x)$ meets the requirement for a uniform approximation to the wave function.

It would seem to be straightforward now to extend this method of the two state curve crossing problem. The model system of Eq. (25) would seem to be the analogue for this case of the linearized potential of the one-dimensional WKB approximation. If the solution of the model system were known, it should be possible to get a connection formula for the WKB wave functions on the two sides of the crossing point. It might then be possible to replace the constants of Eq. (25) by functions in a manner similar to that for the one-dimensional WKB wave function. This would yield a uniform approximation for the wave function and would presumably lead to improved results for the transition probability.

F. Solution of the Model System

For the purpose of constructing a uniform approximation, the system Eq. (25) can be generalized a bit to

$$\left[\begin{pmatrix} \frac{d^2}{dx^2} & 0 \\ 0 & \frac{d^2}{dx^2} \end{pmatrix} - \begin{pmatrix} b_1 + c_1 x & a \\ a & b_2 + c_2 x \end{pmatrix}\right] \begin{pmatrix} u_1(x) \\ u_2(x) \end{pmatrix} = \begin{pmatrix} 0 \\ 0 \end{pmatrix} \tag{35}$$

The changes here are the inclusion of the factor $\frac{2\mu}{\hbar^2}$ in the various constants and the constant terms of the diagonal elements of the "potential" matrix being allowed to be unequal. In matrix notation Eq. (35) becomes

$$\frac{d^2\vec{u}(x)}{dx^2} - [\underset{\sim}{B} + \underset{\sim}{C}x]\,\vec{u}(x) = \vec{0} \tag{36}$$

where

$$\vec{u}(x) = \begin{pmatrix} u_1(x) \\ u_2(x) \end{pmatrix}, \quad \underset{\sim}{B} = \begin{pmatrix} b_1 & a \\ a & b_2 \end{pmatrix}, \quad \underset{\sim}{C} = \begin{pmatrix} c_1 & 0 \\ 0 & c_2 \end{pmatrix}.$$

If Eq. (36) is solved in matrix form there is no reason why the dimensions of the matrices in the equation cannot be increased.

It is possible to get a formal solution to Eq. (36) by expanding $\vec{u}$ in a power series in x with matrix coefficients. Thus let

$$\vec{u}(x) = \sum_{n=0}^{\infty} \underset{\sim}{A}_n x^n \tag{37}$$

which substituted in Eq. (36) gives

$$\sum_{n=2}^{\infty} \underset{\sim}{A}_n n(n-1)\, x^{n-2} - \sum_{n=0}^{\infty} \underset{\sim}{B}\underset{\sim}{A}_n x^n - \sum_{n=0}^{\infty} \underset{\sim}{C}\underset{\sim}{A}_n x^{n+1} = 0$$

so that the $\underset{\sim}{A}_n$'s are determined by the recurrence relation

$$\underset{\sim}{A}_n = \frac{1}{n(n-1)}\,[\underset{\sim}{B}\underset{\sim}{A}_{n-2} + \underset{\sim}{C}\underset{\sim}{A}_{n-3}] \tag{38}$$

with the proviso that $\underset{\sim}{A}_n = \underset{\sim}{0}$ for negative n. The first two coefficient matrices are not determined by Eq. (38) and must be adjusted to fit the boundary conditions. It may again be noted that there is no restriction on the dimensionality of the matrices; the only requirement is that all the elements of $\underset{\sim}{B}$ and $\underset{\sim}{C}$ are constants.

Because Eq. (38) is a two term recurrence relation, it is quite difficult to establish that the formal series Eq. (37) is convergent for all $\underset{\sim}{B}$ and $\underset{\sim}{C}$ and for all values of x. For this problem, however, we first want to use the solution to obtain a connection formula for WKB approximats on the two sides of the crossing point. This would require knowing the behavior of the solution of Eq. (36) for large positive and negative x, in which case the formal solution is slowly convergent (if at all) and of little use. Suffice it to say that for a = 0 Eq. (37) is diagonal and the power series for u_1 and u_2 is that for the well known Airy function[19] (choosing appropriate values for $\underset{\sim}{A}_o$ and $\underset{\sim}{A}_1$).

Unfortunately no method could be found to determine the asymptotic behavior of the solutions of Eq. (36) so that a connection could be effected. The methods that work for one-dimensional systems apparently fail in this case because the $\underset{\sim}{B}$ and $\underset{\sim}{C}$ matrices do not commute in general. For instance, if the Laplace transform is applied to Eq. (36)

$$\int_o^\infty e^{-xt}\vec{u}''(x)\,dx - \int_o^\infty [\underset{\sim}{B} + \underset{\sim}{C}x]\,\vec{u}(x)\,e^{-xt}dx = \underset{\sim}{0}$$

or

$$t^2\vec{v}(t) - t\vec{u}(o) - \vec{u}'(o) - \underset{\sim}{B}\vec{v} + \underset{\sim}{C}\,\frac{d\vec{v}}{dt} = \underset{\sim}{0} \tag{39}$$

where

$$\vec{v}(t) = \int_o^\infty e^{-xt}\vec{u}(x)\,dx \quad .$$

Assuming that things can be arranged so that the $\vec{u}(o)$ and $\vec{u}'(o)$ terms can be eliminated, the equation for $\vec{v}(t)$ is

$$\frac{d\vec{v}}{dt} + \underset{\sim}{C}^{-1}[\underset{\sim}{I}t^2 - \underset{\sim}{B}]\,\vec{v} = 0 \tag{40}$$

If $\underset{\sim}{C}^{-1}$ commuted with $\underset{\sim}{C}^{-1}\underset{\sim}{B}$, the solution to Eq. (40) would be

$$\vec{v}(t) = \exp\left[\underset{\sim}{C}^{-1}\underset{\sim}{B}t - \underset{\sim}{C}^{-1}\frac{t^3}{3}\right] \tag{41}$$

The inverse transform could then be applied to Eq. (41) to give an integral representation of $\vec{u}(x)$. This integral representation could then be evaluated by the method of steepest descent[23] to give the asymptotic behavior of the solutions of Eq. (36). Unfortunately, the appropriate matrices only compute for the special cases a = 0 ($\underset{\sim}{B}$ a diagonal matrix) or $c_1 = c_2$ ($\underset{\sim}{C}$ a scalar matrix). Of course a formal power series solution can be written down for Eq. (40) but it apparently is of no help in determining the desired asymptotic properties of the solutions of Eq. (36).

Therefore, unless better methods can be found to devine the character of the solutions of Eq. (36), the construction of the desired uniform approximation would seem to be impossible. Without knowing the form of the solutions, it is also impossible to say whether a further goal could also be attained. This goal is the expression of all the quantities in the solution in terms of the adiabatic potential curves; a highly desirable objective because of the aforementioned greater availability of the adiabatic curves.

Before leaving the model problem, it is interesting to consider the one case in which there is a simple solution to Eq. (36); the situation in which the diabatic potential curves are parallel ($c_1 = c_2$ of Eq. (35)). This model has some physical significance since the repulsive walls of two potential curves are often near parallel for high energies (Fig. 6);

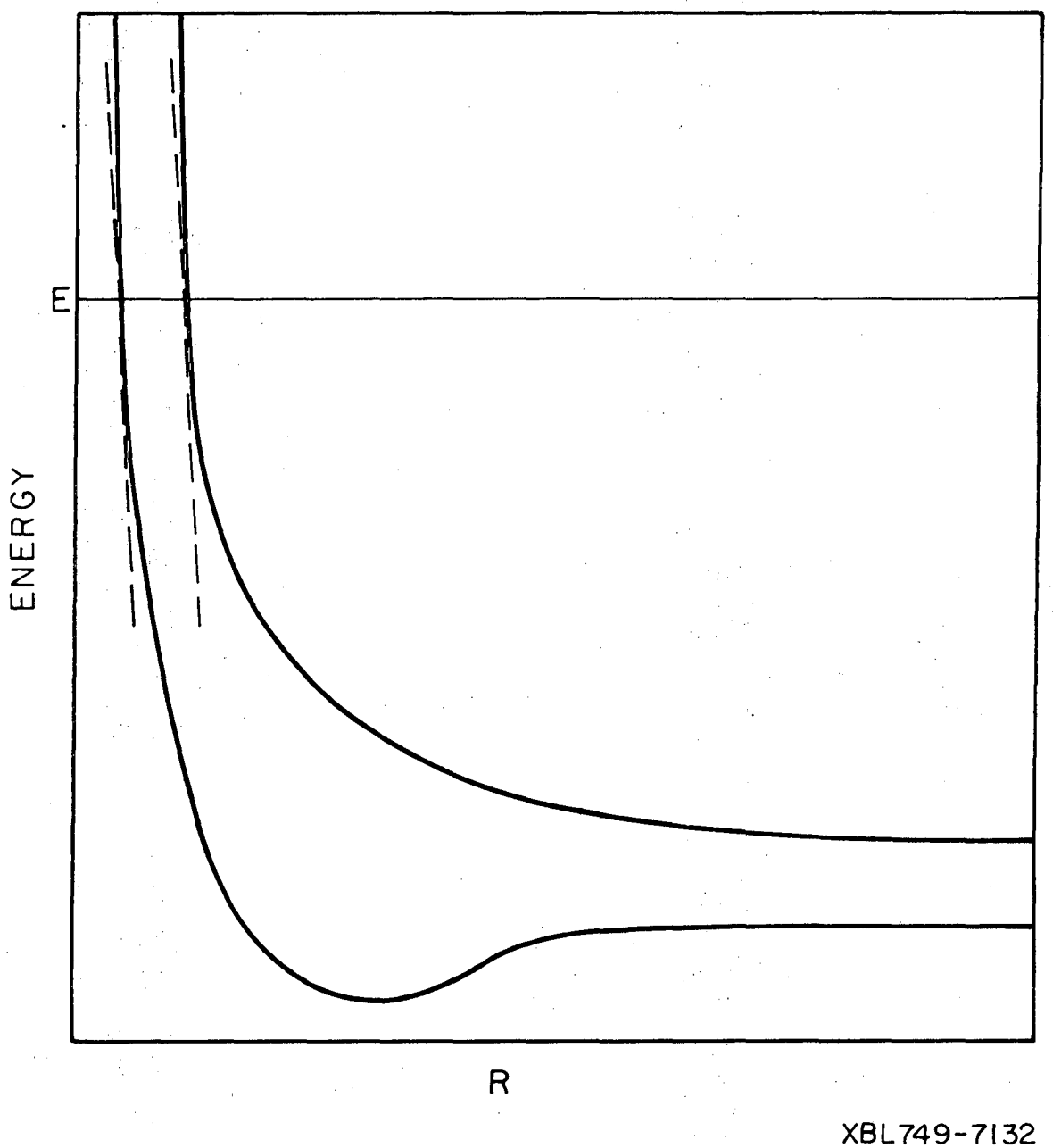

Fig. 6. A physical situation that may be approximated by the parallel curves model.

although in the actual case it would be expected that the diabatic coupling is large and rapidly varying. Since the diabatic curves have no real crossing point and the adiabatic complex crossing point has moved off to infinity, this would be a case where any transitions would be nonlocal.

The solution for the parallel curves model is obtained quite simply if it is realized that the unitary transformation (Eq. (13)) that diagonalizes the potential matrix has no x dependence. It can then be seen from Eq. (14) that the coupled channel equations in the adiabatic representation are completely uncoupled so that the transition probability is zero. It is interesting to note that transition probability predicted by the Stueckelberg theory is also zero since δ as defined by Eq. (16) is zero for this case. If some x dependence (such as a linear term) is added to the diabatic coupling, the transformation matrix is no longer x independent and transitions occur. The prediction of this model problem then is that for the parallel curves situation, transitions are caused by the variation of the diabatic coupling.

Although the discussion has been limited to the model system Eq. (35) for the electronic transition problem, the solution of this equation may be useful in other situations as well. An arbitrary set of coupled channel equations ought to be representable locally by Eq. (36). For these other kinds of inelastic processes though, no assumption of localized transitions is likely to be valid, and the solution would have to be varied point by point. In this context, the solutions of Eq. (36) can be looked upon as a coupled channel extension of the one-dimensional Airy function and may perhaps be useable in a similar fashion.

II. ELECTRONIC TRANSITIONS IN COLLISIONS OF He AND O^+

A. Introduction

It was decided to do a calculation of the cross sections for electronic excitation of O^+ during collisions with He. Preliminary analysis indicated that molecular potential curves corresponding to the ^4S_u and ^2D_u atomic states of O^+ would probably cross. Estimation of the spin-orbit coupling between the two molecular states along with an accurate calculation of the potential curves for the states then permitted a detailed calculation of the inelastic collision processes. The calculated cross sections had oscillations as a function of energy which can be related to the properties of the potential curves.

Peter K. Pearson[24] performed a minimum basis full CI calculation of all the diatomic potential curves arising from the ground states of He and He^+, the ^4S_u, ^2D_u and ^2P_u states of O^+, and the ^3P_g, ^1D_g and ^1S_g states of O. He also carried out more accurate calculations of the curves for the $^2\Pi$ and $^4\Sigma^-$ states since these were believed to be the most interesting for the dynamics. The potential curves obtained are shown in Fig. 7 (suitably shifted vertically so that the dissociation limits correspond to the experimental atomic energy levels).

The lowest $^2\Pi$ and $^4\Sigma$ potential curves from this calculation cross at about 2.3 a_o. Although these curves are of different symmetry, they are coupled by spin-orbit terms so that transitions may occur between the ^4S and ^2D states of O^+ (with ground state He). Since the calculation of the Born-Oppenheimer potential curves ignores all the relativistic terms in the Hamiltonian, these Born-Oppenheimer curves are actually the diagonal "diabatic" curves for the crossing. The adiabatic potentials

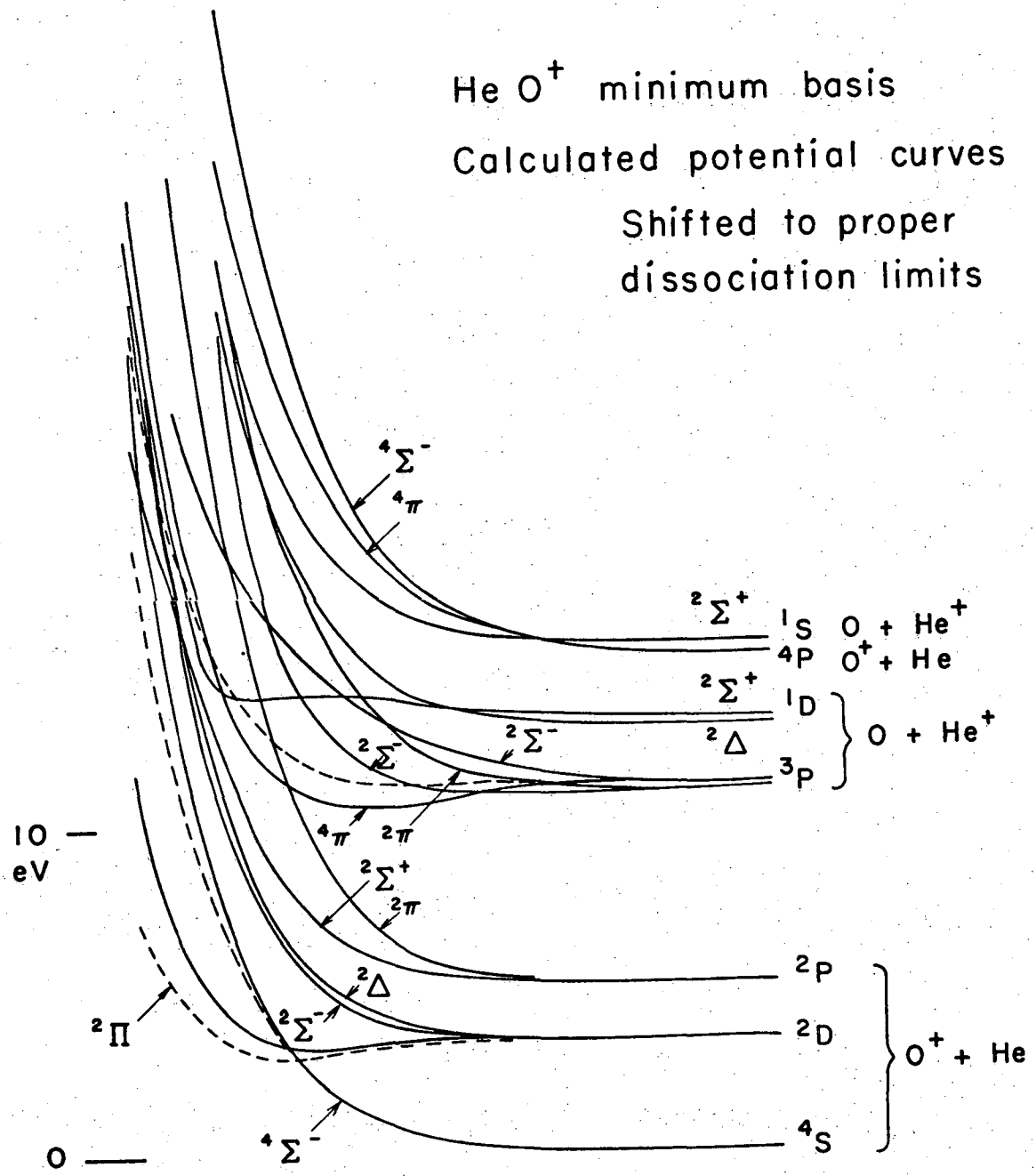

XBL 7410-4234

Fig. 7. Potential curves arising from the valence states of He and O^+, and He^+ and O, shifted vertically so as to match the known atomic energy levels at infinite separation. The dashed curves are the results of the more accurate calculations.

$W_i(r)$ are then the eigenvalues of the 2×2 matrix

$$\begin{pmatrix} V_{11}(r) & V_{12}(r) \\ V_{12}(r) & V_{22}(r) \end{pmatrix} \tag{1}$$

where $V_{11}(r)$ and $V_{22}(r)$ are the calculated $^4\Sigma$ and $^2\Pi$ potential curves and $V_{12}(r)$ is the spin-orbit coupling between these two states.

B. Estimation of the Spin-Orbit Coupling

A rigorous calculation of the spin-orbit coupling between the two molecular states would be a substantial project in itself,[23] but a reasonable estimate can be made quite easily[26] by using information from atomic spin-orbit calculations.

In brief, one assumes the molecular spin-orbit Hamiltonian to be a sum of terms related to each of the nuclei separately.

$$H_{so} = \sum_{i,N} \xi(r_{iN})\ \vec{\ell}_i \cdot \vec{S}_i \tag{2}$$

where r_{iN} is the distance from electron i to nucleus N, and for purposes of estimating the matrix elements of this operator one writes the wave functions in terms of individual atomic states. At the crossing point, the minimum basis wave function for the $^4\Sigma$ state from the aforementioned calculation by P. Pearson has a single dominant configuration, corresponding to the ground state of He and the ^4S state of O^+

$$|^4\Sigma\rangle_{HeO^+} \simeq |^1S\rangle_{He}|\ ^4S_{3/2}\rangle_{O^+} \quad . \tag{3}$$

The $^2\Pi$ state, on the other hand, involves three significant atomic components at the crossing point.

$$|^2\pi\rangle_{HeO^+} \simeq 0.631|^1S\rangle_{He}|^2P_{3/2}\rangle_{O^+} + 0.668|^1S\rangle_{He}|^2D_{3/2}\rangle_{O^+} - 0.338|^1S\rangle_{He}|^2D_{3/2}\rangle_{O^+} \tag{4}$$

In constructing the matrix element of the spin-orbit operator between these two wave functions one furthermore neglects overlap between orbitals centered on different nuclei. Since all the wave functions contain only the ^1S state of He, there is no contribution to the spin-orbit coupling related to this center, and one thus obtains

$$V_{12} = \langle^2\pi|H_{so}|^4\Sigma\rangle \simeq 0.631\langle^2P_{3/2}|H_{so}^{O^+}|^4S_{3/2}\rangle + 0.668\langle^2D_{5/2}|H_{so}^{O^+}|^4S_{3/2}\rangle - 0.338\langle^2D_{3/2}|H_{so}^{O^+}|^4S_{3/2}\rangle \tag{5}$$

where $H_{so}^{O^+}$ is the atomic spin-orbit operator for O^+ alone. The atomic spin-orbit interaction between ^4S and ^2D states of O^+ is zero, however, so that this becomes

$$V_{12} \simeq 0.631\langle^2P_{3/2}|H_{so}^{O^+}|^4S_{3/2}\rangle \tag{6}$$

The spin-orbit matrix element connecting $^2P_{3/2}$ and $^4S_{3/2}$ states of the $2p^3$ configuration is equal to ζ, the 2p radial integral of the effective central force interaction,[27]

$$\zeta = \int_0^\infty dr r^2 2p(r)^2 \; \xi_{O^+}(r) \quad .$$

The problem of calculating V_{12} thus reduces to the problem of determining ζ for O^+. The matrix of the spin-orbit operator for the $2p^3$ configuration is[27]

	$^2P_{1/2}$	$^2P_{3/2}$	$^4S_{3/2}$	$^2D_{3/2}$	$^2D_{5/2}$
$^2P_{1/2}$	0	0	0	0	0
$^2P_{3/2}$	0	0	ζ	$\frac{\zeta}{2}\sqrt{5}$	0
$^4S_{3/2}$	0	ζ	0	0	0
$^2D_{3/2}$	0	$\frac{\zeta}{2}\sqrt{5}$	0	0	0
$^2D_{5/2}$	0	0	0	0	0

(7)

If we let $E'(^SL)$ be the energy of state ^SL ignoring relativistic terms in the Hamiltonian, the energy levels including spin orbit coupling are the eigenvalues of the matrix

$$\begin{pmatrix} E'(^2P) & 0 & 0 & 0 & 0 \\ 0 & E'(^2P) & \zeta & \frac{\zeta}{2}\sqrt{5} & 0 \\ 0 & \zeta & E'(^4S) & 0 & 0 \\ 0 & \frac{\zeta}{2}\sqrt{5} & 0 & E'(^2D) & 0 \\ 0 & 0 & 0 & 0 & E'(^2D) \end{pmatrix}$$

The observed values of the energies of the relevant states are[28]

$$E\left(^4S_{3/2}\right) = 0 \text{ cm}^{-1}$$

$$E\left(^2D_{5/2}\right) = 26808.4 \text{ cm}^{-1}$$

$$E\left(^2D_{3/2}\right) = 26829.4 \text{ cm}^{-1}$$

$$E\left(^2P_{3/2}\right) = 40466.9 \text{ cm}^{-1}$$

$$E\left(^2P_{1/2}\right) = 40468.4 \text{ cm}^{-1}$$

Unfortunately, the matrix above predicts that the $^2P_{3/2}$ state is higher in energy than that of the $^2P_{1/2}$ state. This is a clear indication that more than simple spin-orbit coupling is responsible for the splittings of the observed levels. An attempt was made to see if the proper orderings could be obtained if small perturbations were made to all the off-diagonal elements of the central block of the matrix, but this effort was unsuccessful.

For the p^3 configuration of O^+ it is, therefore, impossible to estimate ζ directly from the spectroscopic data. This problem is in large part because ζ enters quadratically into the eigenvalue equation for the energy levels. Although they are probably much smaller than the spin-orbit coupling, spin-spin and other interactions may enter into the eigenvalues linearly and thus obscure the effects of the spin orbit coupling. This problem does not arise for $O^{+3}(2p')$, $O^{+2}(2p^2)$, and $O(2p^4)$ so that the ζ values for these species can be determined from spectroscopic data to be 256,202, and 253 cm^{-1}, respectively. Assuming that the shielding is approximately constant for these configurations, the value of 168 cm^{-1} for O^+ can be obtained by interpolation. The spin-orbit interaction connecting the $^4\Sigma$ and $^2\Pi$ states at the crossing point is thus estimated to be

$$V_{12} \simeq (0.631)(168\ cm^{-1}) = 106\ cm^{-1} \tag{8}$$

which should be reliable to within 20%.

C. Calculation of the Cross Sections

The cross sections were calculated for the transition between the ^4S and ^2D states of O^+ for collisions with the ^1S ground state of He. Letting 1 denote the ^4S state and 2 denote the ^2D state of O^+, the cross section is given by

$$\sigma_{2\leftarrow 1}(E_1) = 2\pi \int_0^\infty dbbP_{2\leftarrow 1}(b,E_1) \tag{9}$$

where $P_{2\leftarrow 1}(b,E_1)$ is the transition probability as a function of impact parameter b and initial translational energy E_1. The ^4S to ^2D transition is dominated by the single isolated curve crossing so that the transition probability can be approximated by the LZS formula

$$P_{2\leftarrow 1} = 4\pi e^{-2\delta}(1 - e^{-2\delta}) \left(\frac{3}{2}\tau\right)^{1/3} Ai^2\left[\left(\frac{3}{2}\tau\right)^{3/2}\right] \tag{10}$$

It may be recalled that δ and τ are given by

$$2\delta = \mathrm{Im} \int_{r_-}^{r_+} dr[k_2(r) - k_1(r)] \tag{11}$$

and

$$\tau = \int_{r_1}^{r_o} drk_1(r) - \int_{r_2}^{r_o} drk_2(r) \tag{12}$$

where $k_i(r)$ is the local momentum on the appropriate diagonalized potential curve

$$k_i(r) = \frac{1}{\hbar}\{2\mu[E - W_i(r) - Eb^2/r^2]\}^{1/2} \quad , \tag{13}$$

r_1, r_2 are the classical turning points, $r_\pm$ are the roots of $W_1(r) = W_2(r)$, and r_o is the point where the "diabatic" curves cross.

For the claculation of τ, the Born-Oppenheimer curves were used instead of the diagonalized curves $W_i(r)$ in Eq. (12). The off-diagonal matrix element is so small that these curves are practically the same, and, therefore, no significant inaccuracy results from the approximation. The integrations in Eq. (12) were done by a five-point Gauss quadrature after the integrand was transformed somewhat. Letting r(x) be

$$r(x) = r_o - x(r_o - r_i) \tag{14}$$

then

$$\frac{\sqrt{2\mu}}{\hbar} \int_{r_i}^{r_o} dr \sqrt{E - V_i(r) - \frac{Eb^2}{r^2}} = \frac{\sqrt{2\mu E}}{\hbar} \int_o^1 dx\sqrt{1 - x} \left\{ \frac{\sqrt{1 - V_i[r(x)] - \frac{b^2}{r^2(x)}}}{\sqrt{1 - x}} \right\} \tag{15}$$

If f(x) is defined as

$$\frac{\sqrt{1 - V_i[r(x)] - \frac{b^2}{r^2(x)}}}{\sqrt{1 - x}} ,$$

Eq. 15 can be approximated by[29]

$$\frac{\sqrt{2\mu E}}{\hbar} \int_o^1 dx\sqrt{1 - x}\, f(x) \simeq \frac{\sqrt{2\mu E}}{\hbar} \sum_{i=1}^{5} W_i f(x_i) \tag{16}$$

where $x_i = 1 - \xi_i^2$ and $w_i = 2\xi_i^2 w_i$ (ξ_i, w_i are the ith points and weight factors for 9th order Gauss - Legendre guadrature). This method of calculating the integrals was found to be accurate to ten significant figures for typical values of the constants and $V_i(r) = 0$.

For the assumption of linear diabatic curves and constant coupling at the crossing point, the integral for δ in Eq. (11) can be done explicitly. The result is[30]

$$2\delta = \left\{ \frac{2\pi}{\hbar V_x} \frac{V_{12}^2}{|V_n' - V_{22}'|} \right\} \frac{16}{3\pi} \varepsilon^{1/2}(1 + \varepsilon^2)^{1/4} \left[\frac{\sqrt{1 + \varepsilon^2} + \varepsilon}{2} K(k) - \varepsilon E(k) \right] \tag{17}$$

where

$$k^2 = \frac{\sqrt{1 + \varepsilon^2} - \varepsilon}{2\sqrt{1 + \varepsilon^2}} ,$$

and

$$\varepsilon = \frac{mV_x^2}{4V_{12}} \frac{|V_{22}' - V_{11}'|}{\sqrt{|V_{11}'V_{22}'|}}$$

and K(k), E(k) are the complete elliptic integrals of the first and second kinds. The term in braces may be recognized as the Landau-Zener approximation to 2δ while the rest is a function of ε that goes to unity for large ε. Since ε may be rewritten as

$$\varepsilon = \frac{E - E_x}{E_c} \tag{18}$$

where E_x is the energy of the crossing and E_c is a characteristic energy

$$E_c = \frac{2V_{12}\sqrt{V'_{11}V'_{22}}}{|V'_{22} - V'_{11}|} \quad , \tag{19}$$

the parameter ε may be seen to be the energy above the crossing point weighted by the strength of the coupling and the properties of the diagonal curves. For large ε there is a good deal of cancellation between the two terms in the square brackets so that δ is better represented by a series in k

$$2\delta = \left\{\frac{2\pi}{\hbar V_x} \frac{V_{12}^2}{|V'_{11} - V'_{22}|}\right\} \frac{\sqrt{1 - 2k^2}}{1 - k^2} \left[1 - \sum_{n=1}^{\infty} A_n k^{2n}\right] \tag{20}$$

where $A_1 = 3/8$ and

$$A_{n+1} = \frac{(2n + 1)(2n - 3)}{4n(n + 1)} A_n \quad .$$

For the particular case of He and O^+, the smallness of V_{12} led to the result that the calculated cross sections were almost unaffected by using the Landau-Zener result for δ

$$2\delta \simeq \left(\frac{2\pi}{\hbar V_x}\right) \frac{V_{12}^2(r_x)}{|V'_1(r_x) - V'_2(r_x)|} \tag{21}$$

However, the replacement of the Airy function in Eq. (10) by its asymptotic value

$$\left\{\pi \left(\frac{3}{2}\tau\right)^{1/3} Ai^2\left[\left(\frac{3}{2}\tau\right)^{2/3}\right] \to \sin^2(\tau + \pi/4)\right\}$$

causes a large shift in the magnitude of the calculated cross section. The reason for this is that the weakness of the spin-orbit interaction causes the most significant impact parameters to be those for which the crossing point is close to the turning points, precisely the situation

where the substitution of the sin for the Airy function is poorest.

Figure 8 shows the cross section for the $^4S \rightarrow {}^2D$ transition of O^+ as a function of initial collision energy, as calculated from Eqs. (9) and (10) with τ calculated from Eq. (12) by the method of Eq. (16) and δ calculated from Eq. (17) or Eq. (20) (for ε greater than 2). The oscillatory structure of the cross section in Fig. 8 is a remnant of the oscillatory nature of $P_{2\leftarrow 1}(b,E_1)$. Thus if the Airy function is replaced by the sin and the average value of 1/2 is substituted for $\sin^2(\tau + \pi/4)$, i.e.,

$$4\pi \left(\frac{3}{2}\tau\right)^{1/3} \mathrm{Ai}^2 \left[\left(\frac{3}{2}\tau\right)^{2/3}\right] \rightarrow 2$$

the oscillations in $\sigma_{2\leftarrow 1}$ vs E_1 disappear.

D. Oscillatory Structure of the Cross Sections

As was previously mentioned, the oscillations in the cross sections as a function of energy disappeared when the τ dependence of the transition probabilities was removed. It was, therefore, decided to analyze the oscillatory structure to see what information could be gained about τ and the potential curves from the oscillations.

To do this the transition probability was approximated by

$$P_{2\leftarrow 1} = \bar{P}_{2\leftarrow 1} 2\sin^2[\tau(b,E) + \pi/4] \tag{22}$$

where

$$\bar{P}_{2\leftarrow 1} = 2e^{-2\delta}(1 - e^{-2\delta})$$

is the phase averaged transition probability. As was noted, the replacement of the Airy function by its asymptotic value shifted the

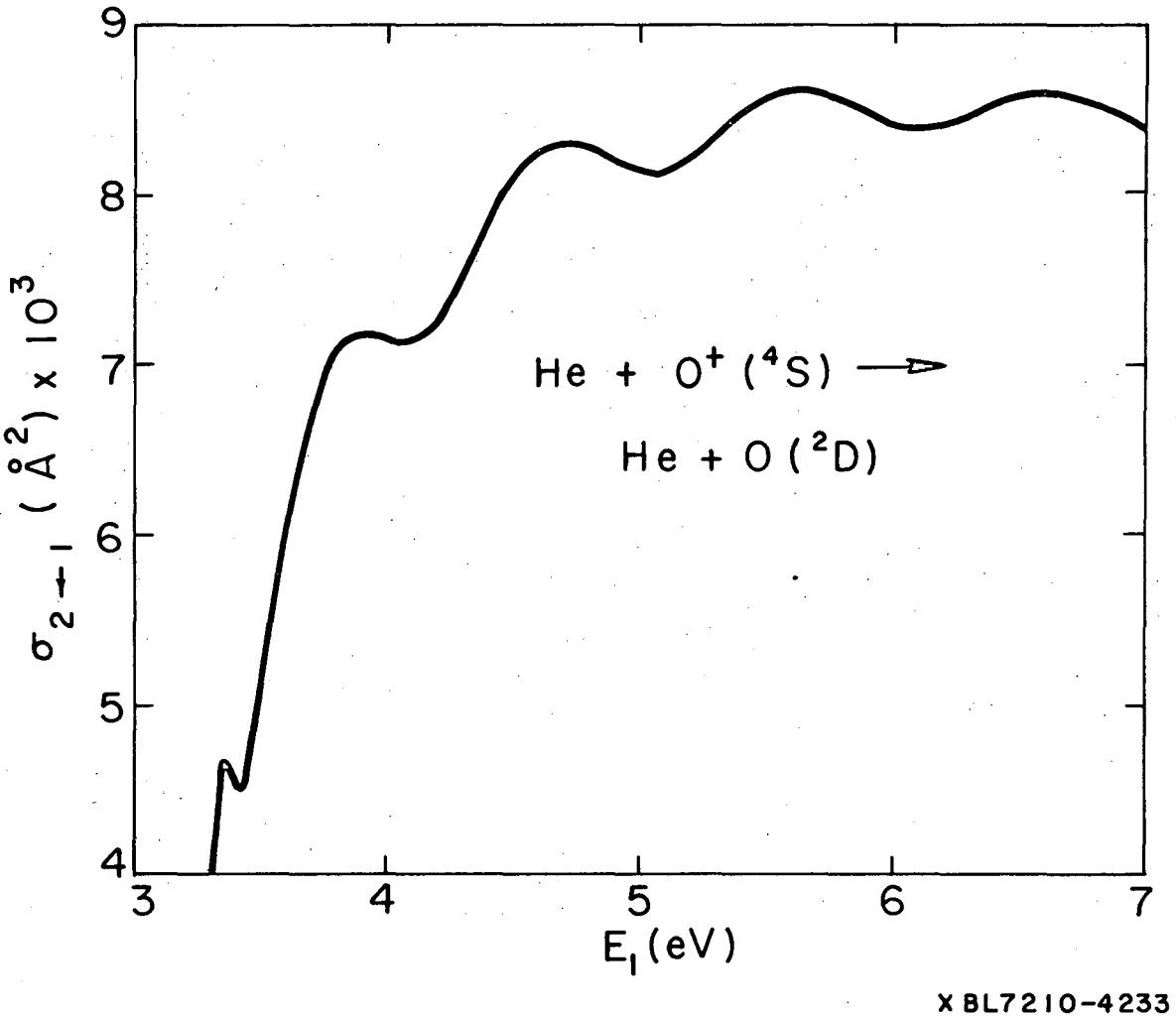

Fig. 8. The inelastic cross section for He + $O^+(^4S) \rightarrow$ He + $O^+(^2D)$ as a function of initial collision energy.

cross section vs energy curve significantly, but the curve was shifted uniformly without a significant change in the amplitude of the oscillations.

The cross section can then be approximated by

$$\sigma_{2\leftarrow 1}(E_1) = 2\pi \int_0^\infty dbb\bar{P}_{2\leftarrow 1}(b,E_1)\ 2\sin^2[\pi/4 + \tau(b,E_1)] \tag{23}$$

Since

$$2\sin^2[\pi/4 + \tau(b,E_1)] = 1 + \sin[2\tau(b,E_1)] \quad ,$$

Eq. (23) becomes

$$\sigma_{2\leftarrow 1} = \bar{\sigma}(E_1) + \Delta\sigma(E_1) \tag{24}$$

where the nonoscillatory part of the cross section is the usual Landau-Zener result

$$\bar{\sigma}(E_1) = 2\pi \int_0^\infty dbb\bar{P}_{2\leftarrow 1}(b,E_1)$$

and the oscillatory part is given by

$$\Delta\sigma(E_1) = 2\pi \int_0^\infty dbb\bar{P}_{2\leftarrow 1}(b,E_1)\ \sin[2\tau(b,E_1)] \quad . \tag{25}$$

Define b_c to be the value of b at which τ (and hence V_x) vanishes for energy E_1. The Landau-Zener approximation for δ can then be written as

$$2\delta \simeq \frac{\alpha}{\sqrt{b_c^2 - b^2}} \tag{26}$$

where

$$\alpha = \frac{\pi r_o V_{12}^2}{\hbar \left| V'_{11} - V'_{22} \right|} \sqrt{\frac{2\mu}{E_1}} \quad .$$

For this system, α is much less than one (typically about 10^{-3} a_o) so that $\bar{P}_{2\leftarrow 1}(b,E_1)$ has a very sharp spike for b slightly less than b_c and is small and slowly varying elsewhere. It might then be expected that the behavior of τ near b_c will be the major determinant of $\Delta\sigma$, but this is not the case because $\sin 2\tau$ is very small there.

For energies well above the crossing energy, it is expected that τ should depend mainly on $(b_c - b)$ when b is near b_c, an expectation that is born out for this system (see Fig. 9). Because of this property and the similar b dependence of δ (Eq. (26)), $P_{2\leftarrow 1}(b,E_1)$ is very nearly also a function of $b_c - b$ for large b (Fig. 10). Since the cross section is the area under the curve $[bP_{2\leftarrow 1}(b,E_1)]$ the difference in the cross sections for nearby energies will, therefore, be dominated by the behavior of τ for small b.

To verify this expectation numerically for this system, it was found that the b dependence of $\tau(b,E_1)$ for E_1 = 5.7 eV is reasonably given by

$$\tau(b,5.7\text{ eV}) \simeq \tau(0,5.7\text{ eV}) \left[1 - \left(\frac{b}{b_c}\right)^2\right] \quad . \tag{27}$$

Except for b near to b_c, δ is very small and $\bar{P}_{2\leftarrow 1}$ may be approximated as

$$\bar{P}_{2\leftarrow 1} \simeq 4\delta \simeq \frac{4\alpha}{\sqrt{b_c^2 - b^2}} \tag{28}$$

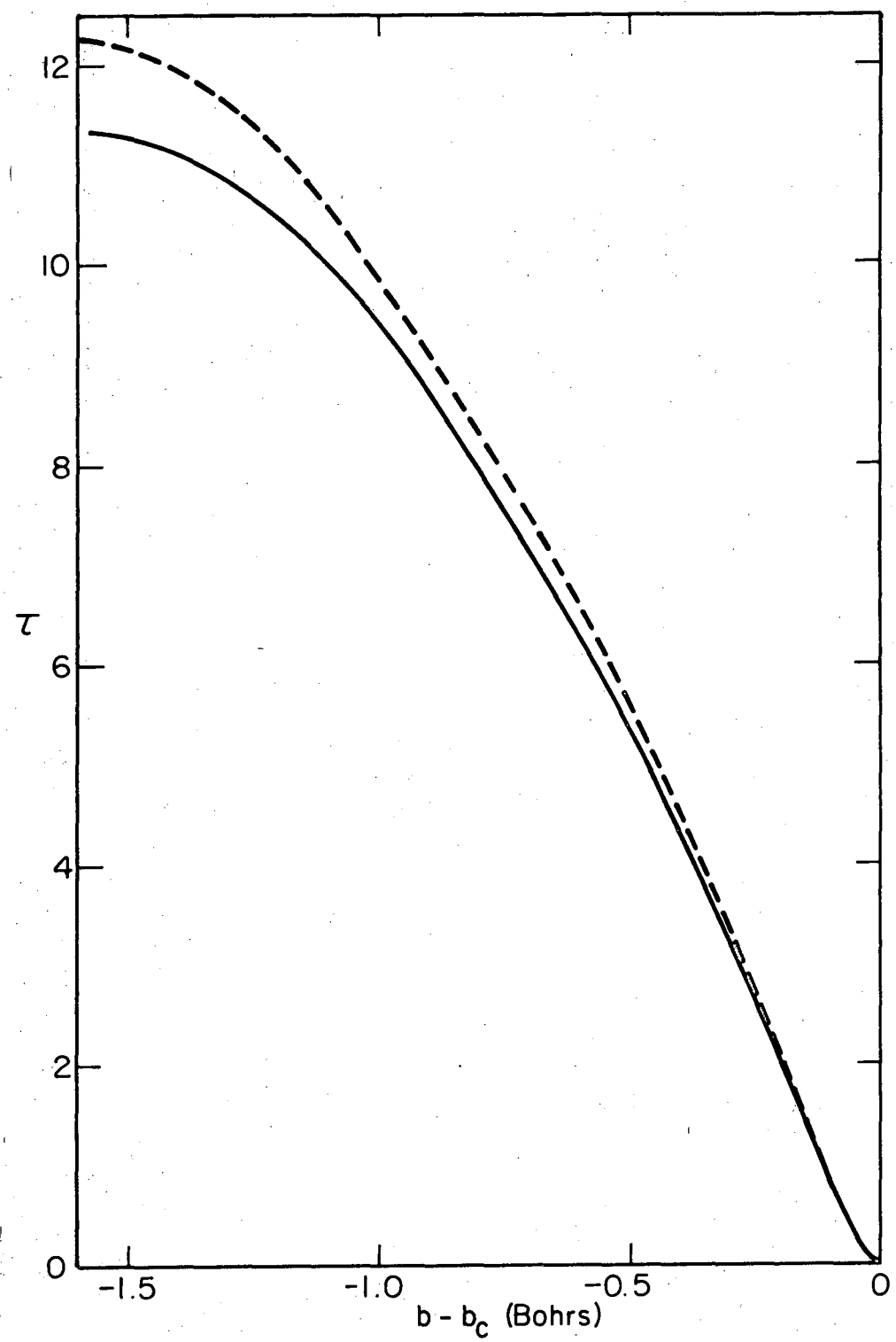

XBL 749-7135

Fig. 9. Phase difference (τ) vs $b - b_c$ for $E_1 = 5.7$ eV (solid line) as $E_1 = 6.0$ eV (dashed line).

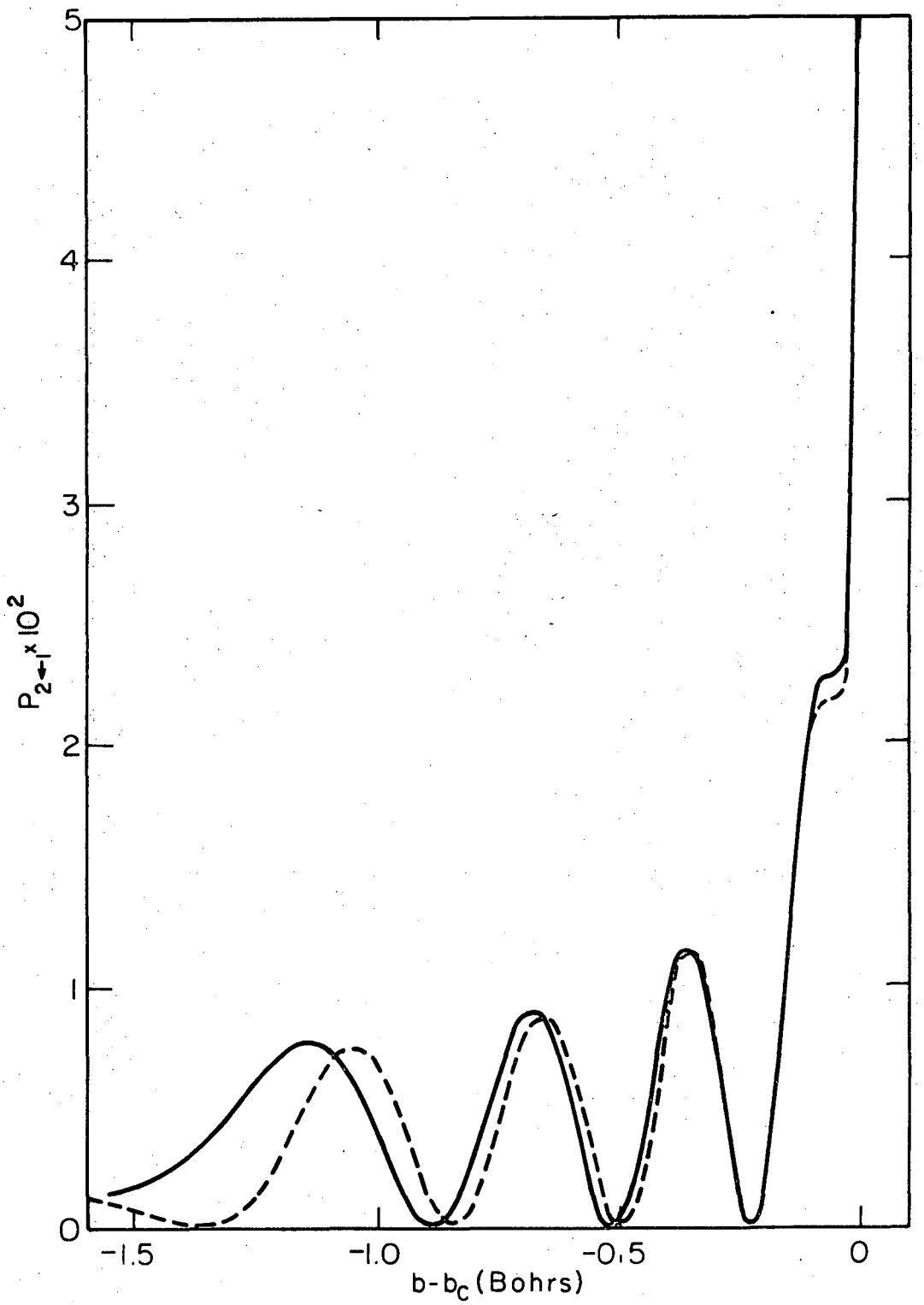

XBL749-7136

Fig. 10. $P_{2\to1}(b,E_1)$ vs $b - b_c$ for E_1 = 5.7 eV (solid line) and E_1 = 6.0 eV (dashed line).

The integral for $\Delta\sigma$ in Eq. (25) is now given by

$$\Delta\sigma(E_1) \simeq 8\pi\alpha \int_0^{b_c} db \frac{b}{\sqrt{b_c^2 - b^2}} \sin\left[2\tau_o\left(1 - \frac{b^2}{b_c^2}\right)\right] \tag{29}$$

where τ_o is shorthand for $\tau(0,E_1)$. Making the substitution

$$x = \left(1 - \frac{b^2}{b_c^2}\right)$$

Eq. (29) becomes

$$\Delta\sigma(E_1) \simeq 4\pi\alpha b_c \int_0^1 dx \frac{\sin(2\tau_o x)}{\sqrt{x}} \tag{30}$$

so that the expression for $\Delta\sigma$ is

$$\Delta\sigma(E_1) \simeq 4\rho\alpha b_c \sqrt{\frac{\pi}{\tau_o}} \; S_2(2\tau_o) \tag{31}$$

where S_2 is the Fresnel sin integral.[31]

Values of $\Delta\sigma$ calculated from Eq. (31) agree essentially exactly with the observed values in phase although the agreement in magnitude is not particularly good. For this system the values of $2\tau_o$ are relatively large for energies well above threshold ($2\tau_o \sim 5$ for $E_1 = 3.35$ eV and $2\tau_o \sim 24.5$ for $E_1 = 6.0$ eV). The cumbersome Fresnel integral in Eq. (31) can then be well represented its asymptotic behavior[31]

$$S_2(x) \sim \frac{1}{2} - \frac{1}{\sqrt{2\pi x}} \cos x + O\left(\frac{1}{x}\right) \tag{32}$$

A plot of $\cos(\pi - 2\tau_o)$ superimposed on a plot of the observed $\Delta\sigma(E_1)$ is shown in Fig. 11. It can be seen from the figure that the function

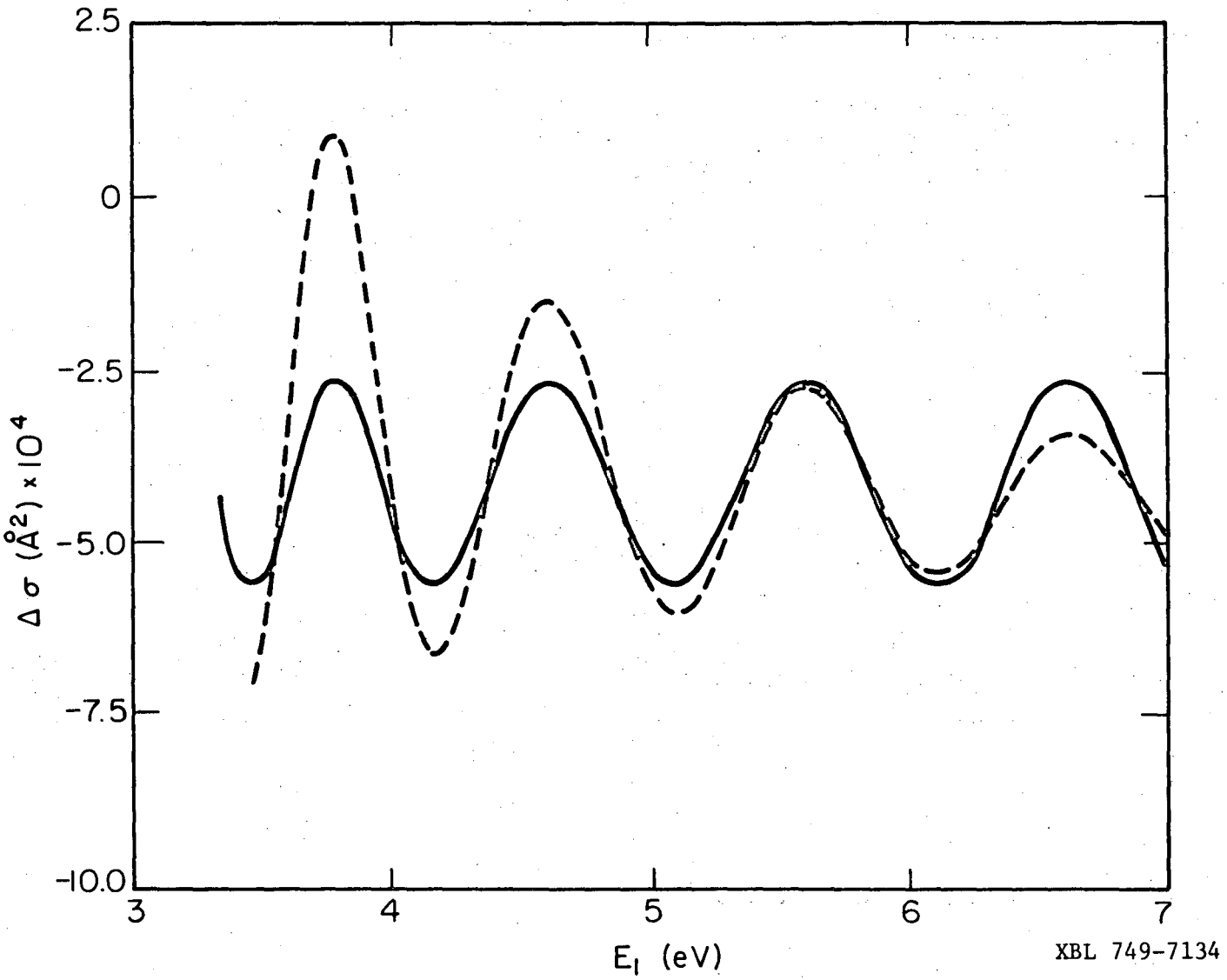

Fig. 11. Plot of $\cos(\pi - 2\tau_0)$ (the solid curve, in arbitrary units) superimposed on a plot of the observed $\Delta\sigma$ as a function of the initial translational energy E_1 (dashed curve).

$\cos(\pi - 2\tau_o)$ represents the positions of the peaks and valleys of the observed oscillatory cross section essentially exactly, so that it is safe to say that within a good approximation

$$\Delta\sigma(E_1) = A + B(E_1,\tau_o)\cos(\pi - 2\tau_o) \tag{33}$$

where A is a constant and B is a nonoscillatory function.

Observation of the oscillations in the energy dependence of the cross section would, by Eq. (33), thus determine the energy dependence of τ at zero impact parameter; i.e., $\tau_o(E)$ which is given by

$$\tau_o(E) = \int_{r_2}^{r_o} dr\left(\frac{2\mu[E - V_2(r)]}{\hbar^2}\right)^{1/2} - \int_{r_1}^{r_o} dr\left(\frac{2\mu[E - V_1(r)]}{\hbar^2}\right)^{1/2} \tag{34}$$

would be an experimentally known function. An RKR like integral transform of this function could thus be used to give definite information about the crossing potential curves. Proceeding in the usual fashion,[32] one thus obtains the following result:

$$r_1(E) - r_2(E) = r_1(o) - r_2(o) + \frac{2}{\pi}\sqrt{\frac{\hbar^2}{2\mu}} \int_o^E dE'\tau_o'(E')(E - E')^{-1/2} , \tag{35}$$

$r_1(E)$ and $r_2(E)$ being the classical turning points for b = 0 and energy E on potential curves $V_1(r)$ and $V_2(r)$, respectively. Equation (35) pertains as written to the case that the position of the crossing point

is below $V_2(\infty)$, the asymptotic value of the excited state. If the crossing point is above this value, then the result becomes

$$r_1(E) - R_2(E) = \frac{2}{\pi} \frac{\hbar^2}{2\mu} \int_{V_o}^{E} dE' \tau_o'(E')(E - E')^{-1/2} \qquad (35a)$$

V_o being the common value of V_1 and V_2 at the crossing point.

Observation of oscillatory structure in $\sigma_{2\leftarrow 1}(E_1)$ would thus be a valuable piece of information in obtaining precise knowledge about the potential curves involved in the transition. Equations (35) and (35a) show specifically what this information is, namely the lateral distance between points on the potential curves $V_1(r)$ and $V_2(r)$ that correspond to the same value of the total energy.

III. SEMICLASSICAL TREATMENT OF ATOM-ASYMMETRIC ROTOR COLLISIONS; ROTATIONAL EXCITATION OF FORMALDEHYDE AT LOW ENERGIES

A. Introduction

The $1_{11} \rightarrow 1_{10}$ transition of formaldehyde is seen in absorption against the 2.7°K cosmic background radiation in cool interstellar dust clouds, indicating that the lower state (1_{11}) has a population greater than would be expected if the system were in equilibrium with the background radiation.[33,34] Townes and Cheung[35] have noted that since the 2_{12} state spontaneously decays (via a dipole-allowed transition) to the 1_{11} state, while the 2_{11} state spontaneously decays to the 1_{10} state, collisional excitation which favors the 2_{12} over the 2_{11} state could produce the observed "cooling" (i.e., enhancement of the population of the 1_{11} state). They further argue[35] that since the 2_{12} state corresponds to the rotational angular momentum being predominantly about the axis perpendicular to the plane of the molecule, collisional excitation of formaldehyde from a $j = 1$ state to a $j = 2$ state should indeed be preferentially to the 2_{12} state. The results of the calculations presented here do show the cross sections for the $1_{10} \rightarrow 2_{12}$ and $1_{11} \rightarrow 2_{12}$ excitations to be larger than those for the $1_{10} \rightarrow 2_{11}$ and $1_{11} \rightarrow 2_{11}$ excitations, thus leading support to the Townes-Cheung mechanism.

In the present calculation the collision partner of formaldehyde is taken to be H_2, which is assumed to be spherically symmetric. A model potential is used which, although probably not an accurate representation of the actual potential, should give the essential features of the collision process correctly. All internal degrees of freedom of H_2 and all vibrational degrees of freedom of formaldehyde are ignored.

The cross sections for the rotational excitation transitions have been obtained by Monte Carlo trajectory methods[36] and by application of "classical S-matrix" theory,[37] a semiclassical approach that uses numerically computed classical trajectories in combination with essential quantum mechanical features. A number of applications[37-39] to atom-diatom collision processes have shown that this semiclassical theory is often an accurate description of the quantum effects in molecular collisions; the present work is the first application of it to collisions involving a polyatomic molecule. The classical Monte Carlo calculations are much simpler to carry out and were done for the energy range 10-40°K. The semiclassical calculations were performed at four energies in the range 10-15°K to provide a check on the reliability of the purely classical results. Apart from an interference structure in the semiclassical results, the two approaches are in reasonable agreement.

The chapter is organized as follows: Section B discusses first how an isolated asymmetric rotor is described semiclassically. Classical S-matrix theory for atom-asymmetric rotor collisions is summarized in Section C, along with specific aspects of the present applications; the way in which Monte Carlo trajectory calculations were carried out is also described here and in Appendix 3. The results of the calculations are presented and discussed in Section D.

B. Semiclassical Description of the Isolated Asymmetric Rotor

In order to apply classical S-matrix theory[37] to a bimolecular collision process it is first necessary to describe the internal quantum states (i.e., rotational-vibrational states) of the isolated collision partners. This section, therefore, considers the semiclassical description of an isolated asymmetric rotor.

Consider an asymmetric rotor[40] with principal moments of inertia I_x, I_y and I_z such that $I_z \geqslant I_y \geqslant I_x$. Letting $A = \frac{1}{2I_x}$, $B = \frac{1}{2I_y}$, $C = \frac{1}{2I_z}$; the asymmetry parameter κ is defined by

$$\kappa = \frac{2B - A - C}{A - C} \tag{1}$$

For a prolate symmetric top $I_y = I_z$ and $\kappa = -1$ while for a oblate symmetric top $I_x = I_y$ and $\kappa = +1$.

The rigid asymmetric rotor has three degrees of freedom, and its classical Hamiltonian can be written as

$$H(j,m,k;q_j,q_m,q_k) = B(j^2 - k^2)\cos^2 q_k + A(j^2 - k^2)\sin^2 q_k + Ck^2 \tag{2}$$

This gives the Hamiltonian in terms of the action-angle variables of the system: j is the magnitude of the rotational angular momentum, m is its component along a space-fixed z axis, and k is its component along a body-fixed z axis. The q's are the angle variables conjugate to the momenta j, k and m. In the oblate symmetric rotor limit, B = A, and the Hamiltonian becomes

$$H(j,m,k;q_j,q_m,q_k) = B(j^2 - k^2) - (B - C)\,k^2 \tag{3a}$$

In the prolate symmetric rotor limit (B = C) one needs to define k' to be the projection of $\vec{j}$ along the body fixed x axis, and the Hamiltonian then becomes

$$H(j,m,k';q_j,q_m,q_{k'}) = B(j^2 - k'^2) + (A - B)\, k'^2 \quad . \tag{3b}$$

Since Eq. (2) has no dependence on q_m or q_j, it can readily be seen that j and m are conserved. Likewise for a symmetric top k (or k') is also conserved.

The traditional way of quantizing the asymmetric rotor semi-classically[41] is to realize that it is essentially a system with only <u>one</u> degree of freedom, with j appearing in the Hamiltonian simply as a parameter; i.e., the one-dimensional Hamiltonian is

$$H_j(k,q_k) = (j^2 - k^2)(A\sin^2 q_k + B\cos^2 q_k) + Ck^2 \quad .$$

One then applies the Bohr-Sommerfeld quantum condition to this one dimensional system in order to quantize the k-degree of freedom:

$$2\pi\hbar(n + 1/2) = \oint dq_k k(q_k,j,E) \tag{4}$$

where $k(q_k,j,E)$ is determined from the Hamiltonian by conservation of energy:

$$k(q_k,j,E) = \pm \left[\frac{E - j^2(A\sin^2 q_k + B\cos^2 q_k)}{C - A\sin^2 q_k - B\cos^2 q_k}\right]^{1/2} \tag{5}$$

Equation (4) can now in principle be inverted to give E(j,n). This procedure, however, gives relatively poor results for the lowest quantum states which are our present concern. It would be desirable, therefore, to be able to use the correct quantum values for the energy levels within

an internally consistent semiclassical framework.

For this purpose we define a new momentum variable η by

$$\eta^2 = (1 + \kappa)\, j_z^2 - (1 - \kappa)\, j_x^2 \tag{6}$$

where j_x and j_z are the components of $\vec{j}$ along the corresponding body-fixed axes. It may be noted that in the oblate limit ($\kappa = +1$) $\eta^2 = 2k^2$ and in the prolate limit ($\kappa = -1$) $\eta^2 = -2k'^2$. The classical Hamiltonian in terms of this new variable is given by

$$H(j,\eta;q_j,q_\eta) = Bj^2 - \frac{(A - C)}{2}\, \eta^2 \tag{7a}$$

so that η^2 is a constant of the motion. If one lets $j^2 = \hbar^2 j(j + 1)$, $\nu^2 = \frac{\eta^2}{\hbar^2}$, $a = \hbar^2 A$ etc, then Eq. (7a) becomes

$$H = bj(j + 1) - \frac{(a - c)\, \nu^2}{2} \tag{7b}$$

so that ν is related to the quantum mechanical quantity $E(\kappa)$ by[40]

$$E(\kappa) = \kappa j(j + 1) - \nu^2 \quad . \tag{8}$$

The rotational state of the asymmetric rotor can now be described within the semiclassical framework by specifying the quantum number j and the quantity ν (determined from tabulated values of $E(\kappa)$). Appendix 1 carries out the canonical transformations necessary to replace k by η.

C. Semiclassical Theory of Atom-Asymmetric Rotor Collisions; Methodology

The cross section for the inelastic process

$$CH_2O(j_1,\nu_1) + H_2 \rightarrow CH_2O(j_2,\nu_2) + H_2$$

is given by

$$\sigma_{j_2\nu_2 \leftarrow j_1\nu_1}(E) = \frac{\pi\hbar^2}{(2\mu E)(2j_1 + 1)} \sum_{J=0}^{\infty} (2J + 1) \sum_{\ell_1,\ell_2} |S^J_{\ell_2 j_2 \nu_2, \ell_1 j_1 \nu_1}|^2 \qquad (9)$$

where ℓ is the orbital angular momentum quantum number for relative translation of the collision partners, j and ν are the quantities that define the rotational state of the isolated formaldehyde as in Eq. (7b), J is the total angular momentum quantum number, rotational (j) plus orbital (ℓ), of the composite system, E is the initial translational energy, and μ is the reduced mass of the collision partners. The reader will recognize that Eq. (9) is identical in form to the expression for rotational-vibrational excitation in the atom-diatom collision system,[42] except that here ν is related to the components of j about body fixed axes rather than being a vibrational quantum number. The sums over ℓ_1 and ℓ_2 in Eq. (9) result from an average and a sum over the initial and final m states of the rotor, respectively.

The semiclassical approximation to the S-matrix elements in Eq. (9) is constructed according to the general prescription that has been given.[37-42] Again, the expression is of the same form as that for the atom-diatom rotational-vibrational system:[42,38d]

$$S^J_{\ell_2 j_2 \nu_2, \ell_1 j_1 \nu_1}(E) = \sum \left[(-2\pi i\hbar)^3 \frac{\partial(\ell_2, j_2, \nu_2)}{\partial(q_{\ell_1}, q_{j_1}, q_{\nu_1})} \right]^{-1/2} \exp[i\phi(\ell_2 j_2 \nu_2, \ell_1 j_1 \nu_1)/\hbar] \quad , \tag{10}$$

where the sum indicates a sum of such terms for all trajectories which obey the correct initial and final boundary conditions; see Ref. 37 and 42 for more details.

In order to use Eqs. (9) and (10) it is necessary that J^2 be quantized everywhere and that j^2, ℓ^2 and ν^2 be quantized in the initial and final asymptotic regions. J^2 and ℓ^2 are quantized by the usual Langer prescription

$$\begin{aligned} \ell^2 &\to \hbar^2(\ell + 1/2)^2 \\ J^2 &\to \hbar^2(J + 1/2)^2 \quad , \end{aligned} \tag{11}$$

ν^2 is "quantized" by setting it equal to the value determined from Eq. (8) by j and the quantum value of $E(\kappa)$. The quantum mechanical quantization of j^2 (i.e., $j^2 \to \hbar^2 j(j + 1)$) was retained because it was felt that this would be more accurate for treating the low rotational levels which were of interest in this calculation.

The numerically integrated classical trajectories needed to evaluate Eq. (10) may be computed in any convenient set of canonical variables as long as the proper transformation to the $\ell, j, \nu, q_\ell, q_j, q_\nu$ set is performed in the initial and final asymptotic regions. Formaldehyde is almost a prolate symmetric top ($\kappa = -0.9610644$ for the adopted geometry) so that the component of angular momentum along the CO bond axis of isolated formaldehyde is almost conserved.[43] Since the relationship between k

and η is also not very tractable (see Appendix 1), it was decided to compute the trajectories[44] in the $\ell, j, k, q_\ell, q_j, q_k$ set of canonical coordinates. Appendix 2 gives the canonical transformations and necessary relations for this coordinate set.

The classical Hamiltonian is given in this set of cononical variables by

$$H(p_R, \ell, j, k; R, q_\ell, q_j, q_k) = \frac{P_R^2}{2\mu} + \frac{\ell^2}{2\mu R^2} + j^2[C\sin^2 q_k + B\cos^2 q_k] \tag{12}$$

$$+ k^2(A - B\cos^2 q_k - C\sin^2 q_k) + V(R, \gamma, \zeta)$$

where R is the distance between the centers of mass of the collision partners and μ is the reduced mass for the relative motion of the centers of mass (i.e., $\mu = \frac{m_{CH_2O} m_{H_2}}{m_{H_2} + m_{CH_2O}}$). The potential energy depends on only the three parameters (R, γ, ζ), where γ is the angle between $\vec{R}$ and the body-fixed z axis of formaldehyde, and ζ is the angle between $\vec{R}$ and the corresponding x axis.

The equations of motion are given by

$$\dot{R} = p_R/\mu \tag{13}$$

$$\dot{q}_j = 2j[B + (C - B)\sin^2 q_k] + \frac{\partial V}{\partial \cos\gamma}\frac{\partial \cos\gamma}{\partial j} + \frac{\partial V}{\partial \cos\zeta}\frac{\partial \cos\zeta}{\partial j}$$

$$\dot{q}_\ell = \ell/(\mu R^2) + \frac{\partial V}{\partial \cos\gamma}\frac{\partial \cos\gamma}{\partial \ell} + \frac{\partial V}{\partial \cos\zeta}\frac{\partial \cos\zeta}{\partial \ell}$$

$$\dot{q}_k = 2k[A - B - (C - B)\sin^2 q_k] + \frac{\partial V}{\partial \cos\gamma}\frac{\partial \cos\gamma}{\partial k} + \frac{\partial V}{\partial \cos\zeta}\frac{\partial \cos\zeta}{\partial k}$$

$$\dot{p}_R = \ell^2/(\mu R^3) - \frac{\partial V}{\partial R}$$

$$\dot{j} = -\frac{\partial V}{\partial \cos\gamma}\frac{\partial \cos\gamma}{\partial q_j} - \frac{\partial V}{\partial \cos\zeta}\frac{\partial \cos\zeta}{\partial q_j}$$

$$\dot{\ell} = -\frac{\partial V}{\partial \cos\gamma}\frac{\partial \cos\gamma}{\partial q_\ell} - \frac{\partial V}{\partial \cos\zeta}\frac{\partial \cos\zeta}{\partial q_\ell}$$

$$\dot{k} = 2(C - B)\sin q_k \cos q_k (k^2 - j^2) - \frac{\partial V}{\partial \cos\zeta}\frac{\partial \cos\zeta}{\partial q_k}$$

where the potential parameters $\cos\gamma$, $\cos\zeta$ and their partial derivatives are given by

$$\frac{\partial \cos\gamma}{\partial q_j} = \frac{\sqrt{j^2 - k^2}}{j}\left\{-\sin q_j \cos q_\ell + \frac{(J^2 - j^2 - \ell^2)}{2\ell j}\cos q_j \sin q_\ell\right\} \tag{14}$$

$$\frac{\partial \cos\gamma}{\partial q_\ell} = \frac{k\xi \cos q_\ell}{2\ell j^2} + \frac{\sqrt{j^2 - k^2}}{j}$$

$$\left\{-\cos q_j \sin q_\ell + \frac{(J^2 - j^2 - \ell^2)}{2\ell j}\sin q_j \cos q_\ell\right\}$$

$$\frac{\partial \cos\gamma}{\partial j} = \frac{k \sin q_\ell}{\ell j}\left[\frac{-\xi}{j^2} + \frac{(J^2 + \ell^2 - j^2)}{\xi}\right] + \frac{k^2}{j^2\sqrt{j^2 - k^2}}$$

$$\left\{\cos q_j \cos q_\ell + \frac{(J^2 - j^2 - \ell^2)}{2\ell j}\sin q_j \sin q_\ell\right\}$$

$$- \frac{\sqrt{j^2 - k^2}\,(J^2 + j^2 - \ell^2)}{2\ell j^3}\sin q_j \sin q_\ell$$

$$\frac{\partial \cos\gamma}{\partial \ell} = \frac{k \sin q_\ell}{j^2}\left[\frac{-\xi}{2\ell^2} + \frac{(J^2 + j^2 + \ell^2)}{\xi}\right] - \frac{\sqrt{j^2 - k^2}(J^2 + \ell^2 - j^2)\ \sin q_j\ \sin q_\ell}{2\ell^2 j^2}$$

$$\frac{\partial \cos\gamma}{\partial k} = \frac{\xi \sin q_\ell}{2\ell j^2} - \frac{k}{j\sqrt{j^2 - k^2}}\left\{\cos q_j\ \cos q_\ell + \frac{(J^2 - j^2 - \ell^2)}{2\ell j}\ \sin q_j\ \sin q_\ell\right\}$$

$$\frac{\partial \cos\zeta}{\partial q_j} = \frac{k \sin q_k}{\sqrt{j^2 - k^2}}\ \frac{\partial \cos\gamma}{\partial q_j} + \cos q_k\left\{\cos q_j\ \cos q_\ell + \frac{(J^2 - j^2 - \ell^2)}{2\ell j}\ \sin q_j\ \sin q_\ell\right\}$$

$$\frac{\partial \cos\zeta}{\partial q_\ell} = \frac{k \sin q_k}{\sqrt{j^2 - k^2}}\ \frac{\partial \cos\gamma}{\partial q_\ell} - \frac{\xi \sin q_k\ \cos q_\ell}{2\ell\sqrt{j^2 - k^2}} - \cos q_k\left\{\sin q_\ell\ \sin q_j + \frac{(J^2 - j^2 - \ell^2)}{2\ell j}\cos q_\ell\ \cos q_j\right\}$$

$$\frac{\partial \cos\zeta}{\partial q_k} = \frac{\sin q_k}{2\ell\sqrt{j^2 - k^2}}\ [2\ell k \cos\gamma - \xi \sin q_\ell] - \sin q_k\left[\cos q_\ell\ \sin q_j - \frac{(J^2 - j^2 - \ell^2)}{2\ell j}\ \sin q_\ell\ \cos q_j\right]$$

$$\frac{\partial\cos\zeta}{\partial j} = \frac{k\sin q_k}{\sqrt{j^2 - k^2}} \frac{\partial\cos\gamma}{\partial j} + \frac{j\sin q_k \sin q_\ell}{\ell}$$

$$\left[\frac{\xi}{2(j^2 - k^2)^{3/2}} - \frac{(J^2 + \ell^2 - j^2)}{\xi\sqrt{j^2 - k^2}}\right]$$

$$\frac{-2jk\cos\gamma \sin q_k}{2(j^2 - k^2)^{3/2}} + \frac{(J^2 + j^2 - \ell^2)}{2\ell j^2} \sin q_\ell \cos q_j \cos q_k$$

$$\frac{\partial\cos\zeta}{\partial \ell} = \frac{k\sin q_k}{\sqrt{j^2 - k^2}} \frac{\partial\cos\gamma}{\partial \ell} + \frac{\sin q_k \sin q_\ell}{\sqrt{j^2 - k^2}} \left[\frac{\xi}{2\ell^2} - \frac{(J^2 + j^2 - \ell^2)}{\xi}\right]$$

$$+ \frac{(J^2 + \ell^2 - j^2)}{2\ell^2 j} \sin q_\ell \cos q_j \cos q_k$$

$$\frac{\partial\cos\zeta}{\partial k} = \frac{k\sin q_k}{\sqrt{j^2 - k^2}} \frac{\partial\cos\gamma}{\partial k} + \frac{2j^2\cos\gamma \sin q_k}{(j^2 - k^2)^{3/2}} - \frac{k\xi\sin q_k \sin q_\ell}{\ell(j^2 - k^2)^{3/2}}$$

$$\cos\gamma = \frac{\sqrt{j^2 - k^2}}{j} \left[\cos q_\ell \cos q_j + \frac{(J^2 - j^2 - \ell^2)}{2\ell j} \sin q_\ell \sin q_j\right] + \frac{k\xi\sin q_\ell}{2\ell j^2} \tag{15a}$$

$$\cos\zeta = \frac{\sin q_k}{2\ell\sqrt{j^2 - k^2}} \left[2\ell k\cos\gamma - \xi\sin q_\ell\right] \tag{15b}$$

$$+ \cos q_k \left[\cos q_\ell \sin q_j - \frac{(J^2 - j^2 - \ell^2)}{2\ell j} \sin q_\ell \cos q_j\right]$$

The trajectories were begun with the initial conditions

$$R = R_{max} \tag{16}$$

$$q_j = q_{j_1}$$

$$q_\ell = q_{\ell_1}$$

$$q_k = q_{k_1}$$

$$p_R = -\sqrt{2\mu E_1 - \ell_1^2/R_{max}^2}$$

$$j = \hbar\sqrt{j_1(j_1 + 1)}$$

$$\ell = \hbar(\ell_1 + 1/2)$$

$$k = \sqrt{\frac{\eta_1^2 + (1 - \kappa)\hbar^2 j_1(j_1 + 1)\sin^2 q_{k_1}}{(1 + \kappa) + (1 - \kappa)\sin^2 q_{k_1}}} \quad ,$$

and were ended when $R_2 \geqslant R_{max}$ while P_R was positive. R_{max} is a value of R that was chosen to be the smallest value for which $\frac{\partial V}{\partial \cos\gamma}$ and $\frac{\partial V}{\partial \cos\zeta}$ are negligible ($R_{max} = 10\ a_o$ in this case). At the conclusion of the trajectories, the final quantum numbers j_2, ℓ_2, ν_2 were calculated from j_f, ℓ_f, k_f by

$$j_2 = -1/2 + 1/2\sqrt{1 + 4j_f^2/\hbar^2} \tag{17a}$$

$$\ell_2 = \ell_f/\hbar - 1/2 \tag{17b}$$

$$\nu_2^2 = \frac{1}{\hbar^2}\left[(1 + \kappa)\ k_f^2 - (1 - \kappa)(j_f^2 - k_f^2)\sin^2 q_{k_2}\right] \tag{17c}$$

The trajectories were rejected if conservation of energy as measured by

$$E_1 - B\hbar^2 j_2(j_2 + 1) + \frac{(C - A)}{4} \hbar^2 \nu_2^2 + B\hbar^2 j_1(j_1 + 1)$$

$$- \frac{(C - A)}{4} \hbar^2 \nu_1^2 - \left[P_{R_2}^2 + \ell_f^2/R_2^2\right]/(2\mu)$$

was violated by more than 0.5%.

A model potential of the form

$$V = \sum_{i=1}^{4} F_i \exp[-R_i^2/S_i] \tag{18}$$

was adopted for the hydrogen molecule-formaldehyde interaction. This type of potential was used in order to make the results comparable with quantum mechanical calculations[34] which were in progress at the time this work was begun. The sum is over the four atoms making up the formaldehyde and R_i^2 is the square of the distance between the ith atom of formaldehyde and the H_2 center of mass. Table I lists the values of the parameters that were chosen for this work. The S_i values were chosen so that the "sizes" of the atoms for the energy range considered would be comparable to the usual Van der Waals radii of these elements in organic compounds.

This model potential is admittedly quite crude in that it neglects the long range attractive forces and that the short range repulsion is not steep enough. Since the quantity of interest for the present astrophysical problem is the relative size of cross sections (see Section D), however, it may be that the detailed form of the potential beyond that which essentially determines the size and shape of the molecules will not seriously alter the major results. Work currently

Table I. Values of parameters chosen for the model potential.

Atom	F_i (Hartress)	$Si(a_o^2)$
O	1.0	0.88333
C	1.0	0.970
$H_{1,2}$	1.0	0.75667

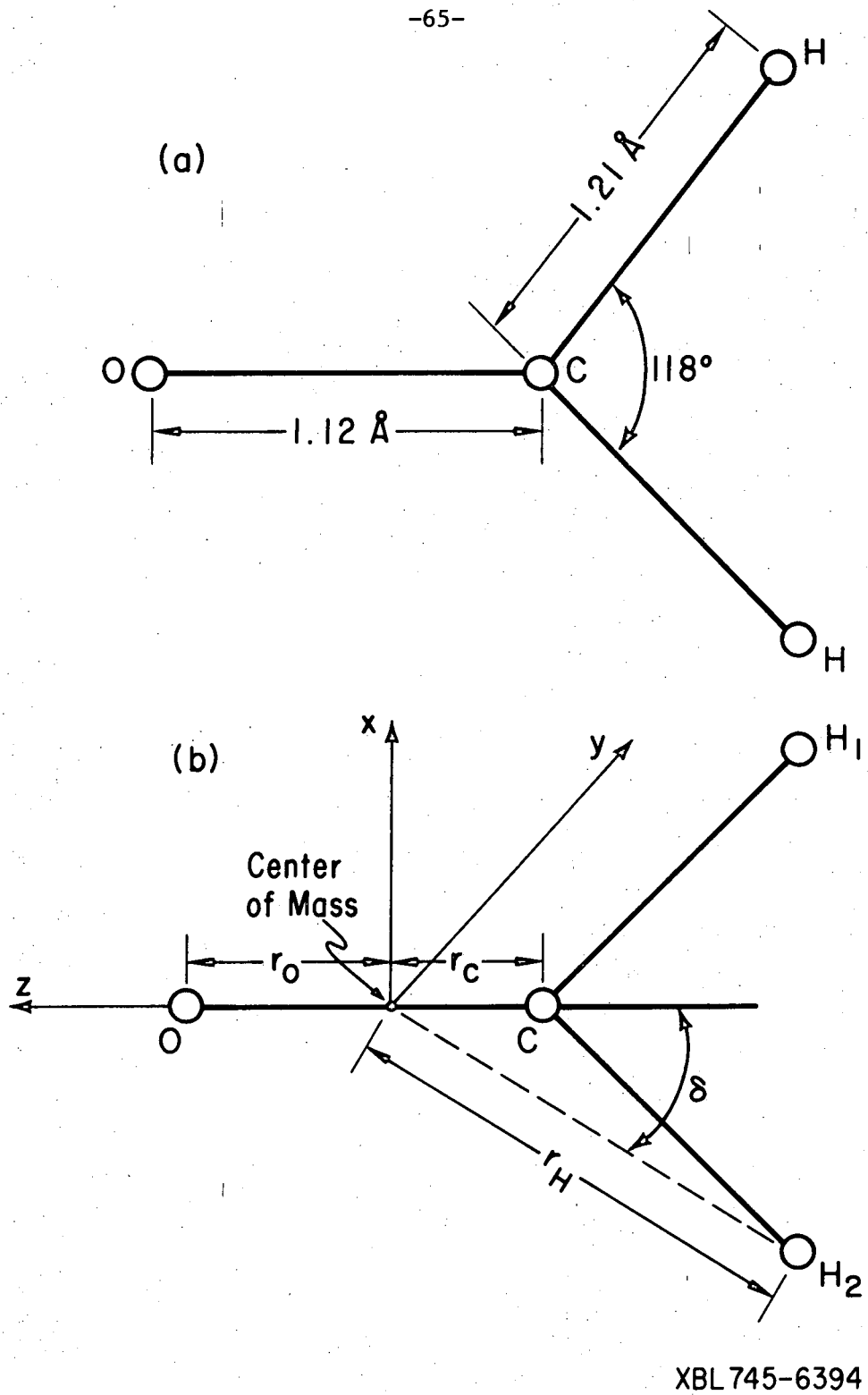

Fig. 12. (a) The geometry of formaldehyde; see Ref. 40.
(b) The coordinate system for formaldehyde.

in progress (B. J. Garrison, H. F. Schaefer, W. A. Lester and W. H. Miller) on the potential surface for helium-formaldehyde should provide a much more realistic interaction potential.

The structure of formaldehyde given in Ref. 40 was adopted for this work since it is the same as that used in Ref. 34 and 35. The values given[40] for the rotational constants are A_o = 282,106 Mc; B_o = 38,834 Mc; and C_o = 34,004 Mc which correspond to an asymmetry parameter κ of -0.9610644. The adopted structure and the coordinate system used are shown in Fig. 12. The values of the structural parameters with respect to the center of mass as shown in Fig. 12b are then: $r_o = 0.9943\ a_o$, $r_c = 1.2925\ a_o$, $r_H = 2.9948 a_o$ and $\delta = 37.29°$. The energies and values of ν for all the j = 1 and j = 2 rotational states of formaldehyde are given in Table II. The distances required in Eq. (18) are now given in terms of the structural parameters and the potential parameters (R,γ,ζ) by

$$R_o^2 = R^2 + r_o^2 - 2Rr_o\cos\gamma \tag{19}$$

$$R_c^2 = R^2 + r_c^2 + 2Rr_c\cos\gamma$$

$$R_{H_1}^2 = R^2 + r_H^2 + 2Rr_H(\sin\delta\ \cos\zeta - \cos\gamma\ \cos\delta)$$

$$R_{H_2}^2 = R^2 + r_H^2 - 2Rr_H(\sin\delta\ \cos\zeta + \cos\gamma\ \cos\delta)$$

Even at the low collision energies employed the excitation of the j = 1 states to j = 2 states is a "classically allowed"[45] process, i.e., there are real-valued classical trajectories which lead to these transitions. (There will also be some contribution from complex-valued classical trajectories, but this has been ignored in the present work.)

Table II. Formaldehyde energy levels.

State $(J_{k_-k_+})$	E (°K)	$\nu^2 = \frac{\eta^2}{\hbar^2}$
0_{00}	0	0
1_{01}	3.49579	0.03894
1_{11}	15.17141	-1.92213
1_{10}	15.40323	-1.96106
2_{02}	10.48396	0.11738
2_{12}	21.93119	-1.80532
2_{11}	22.62663	-1.92213
2_{21}	57.65349	-7.80532
2_{20}	57.65691	-7.80590

In general there are a number of different classical trajectories (up to 8 in the present application) which contribute to each specific S-matrix element; because of the small difference in the classical actions along such trajectories it is important not to use the "primitive" semiclassical expression, Eq. (10), but rather the appropriate uniform asymptotic expression.[38c,38d,46] The semiclassical results discussed in the following section have all been "uniformized" in this way.

An interesting feature of this system is the apparent mixing of classical and quantum behavior. At a translational energy of 10°K, the S matrix element for the transition $1_{11} \rightarrow 2_{12}$ with $J = 2$, $\ell_1 = 1$, $\ell_2 = 0$ gets contributions from eight classical trajectories; an apparent indication of classical-like behavior. However, this is the only S matrix element for that transition which gets any contributions, something that might be expected if the system behaved quantum mechanically. This situation is moderated at the higher energies and virtually disappears at 15°K (see Table V).

For the Monte Carlo trajectory calculations it was decided to modify the standard procedures[36] somewhat because only a few values of J, ℓ_1 and ℓ_2 contribute to the sums in Eq. (9) at these low collision energies. Proceeding along the lines of Ref. 38c, therefore, J and ℓ_1 were retained as integers and the Monte Carlo procedure used to calculate the square modulus of S-matrix elements individually. Appendix C gives the details of this as it pertains to the atom-asymmetric rotor collision system.

Table V. The distribution of the classical trajectories contributing to the S-matrix elements for the $1_{10} \rightarrow 2_{12}$ transition (the distribution is similar for the other transitions studied). Number of contributing terms for the energies and quantum states indicated.

J,ℓ_1,ℓ_2	Translational Energy			
	10°K	11°K	12°K	15°K
1,0,1	0	2	6	8
1,1,1	0	2	2	4
2,1,0	8	12	12	10
2,1,1	0	0	6	8
2,2,1	0	0	0	2
3,2,1	0	0	0	4

D. Results and Discussion

The cross sections for the rotational excitation of the 1_{11} and 1_{10} states to the 2_{12} and 2_{11} states of formaldehyde are shown in Fig. 13; the solid line is the result of the Monte Carlo classical trajectory calculation, and the points are the semiclassical values at energies of 10, 11, 12 and 15°K. Numerical values of the calculated cross sections are given in Tables III and IV. The semiclassical results show a strong interference structure which is not quenched by the sums in Eq. (9) because so few terms contribute. As expected,[47] the purely classical results do not reproduce this structure but appear to give the average result reasonably well. Since these cross sections would be averaged over a smooth distribution of translational energies in computing rate constants, the interference structure would not likely be important; if this is the case, then the classical Monte-Carlo results would be sufficient. This is quite encouraging, of course, for the classical Monte Carlo trajectory calculations are considerably earier to carry out than the semiclassical ones.

Figure 14a shows the classical Monte Carlo results for the $1_{11} \rightarrow 1_{10}$ cross section as a function of collision energy E. Since microscopic reversibility implies that

$$\sigma(1_{11} \leftarrow 1_{10}) = \frac{E}{E - \Delta\varepsilon} \; \sigma(1_{10} \leftarrow 1_{11}) \quad , \tag{20}$$

where $\Delta\varepsilon$ is the splitting of the 1_{11} and 1_{10} levels, $\Delta\varepsilon = 0.23182$°K, the cross sections for the $1_{10} \rightarrow 1_{11}$ and $1_{11} \rightarrow 1_{10}$ transitions are essentially equal at the energies E considered.

Table III. Classical S-matrix results. Cross sections (a_o^2) for the indicated transitions and energies.

Transition	Energy (°K) 10.0	11.0	12.0	15.0
(1) $1_{11} \rightarrow 2_{12}$	1.100833* (2.038357)**	4.211031 (4.552308)	2.581632 (4.981321)	1.462453 (1.850373)
(2) $1_{11} \rightarrow 2_{11}$	1.864489 (1.207066)	1.053836 (1.808262)	1.506511 (2.412053)	1.258176 (3.662941)
(3) $1_{10} \rightarrow 2_{12}$	1.044088 (1.869910)	4.712126 (5.614068)	2.259673 (5.087348)	2.390978 (3.823447)
(4) $1_{10} \rightarrow 2_{11}$	2.149583 (1.986073)	1.307034 (2.936735)	1.651284 (3.674114)	1.717957 (4.618388)
(5) Ratio of (3) to (2)	0.559986 (1.549137)	4.471404 (3.104676)	1.499938 (2.109136)	1.900353 (1.043819)
(6) Total (1) + (2) + (3) + (4)	6.158993 (7.101406)	11.284027 (14.911373)	7.999100 (16.154836)	6.829564 (13.955149)

*Uniformized results.

**Primitive classical S-matrix results given in parentheses.

Table IV. Monte-Carlo classical trajectory results. Cross sections (a_o^2) for the indicated transitions and energies.

	Transition					
Energy (°K)	(1) $1_{11} \rightarrow 2_{12}$	(2) $1_{11} \rightarrow 2_{11}$	(3) $1_{10} \rightarrow 2_{12}$	(4) $1_{10} \rightarrow 2_{11}$	(5) Ratio of (3) to (2)	(6) Total (1) + (2) + (3) + (4)
10.0	4.03274	0.94633	3.07623	1.30732	3.25070	9.36262
11.0	3.66518	1.09063	2.86338	1.48791	2.62544	9.10711
12.0	3.48989	1.19020	2.77504	1.40964	2.33157	8.86478
15.0	3.48592	1.20464	2.78741	1.56672	2.31389	9.04470
20.0	4.68262	1.67763	4.02615	1.91998	2.39991	12.30339
25.0	3.79570	1.96233	3.21320	2.29035	1.63744	11.26158
30.0	2.80932	1.94898	2.45761	2.13178	1.26097	9.34769
40.0	2.35953	1.71022	2.09424	1.81360	1.22454	7.97759

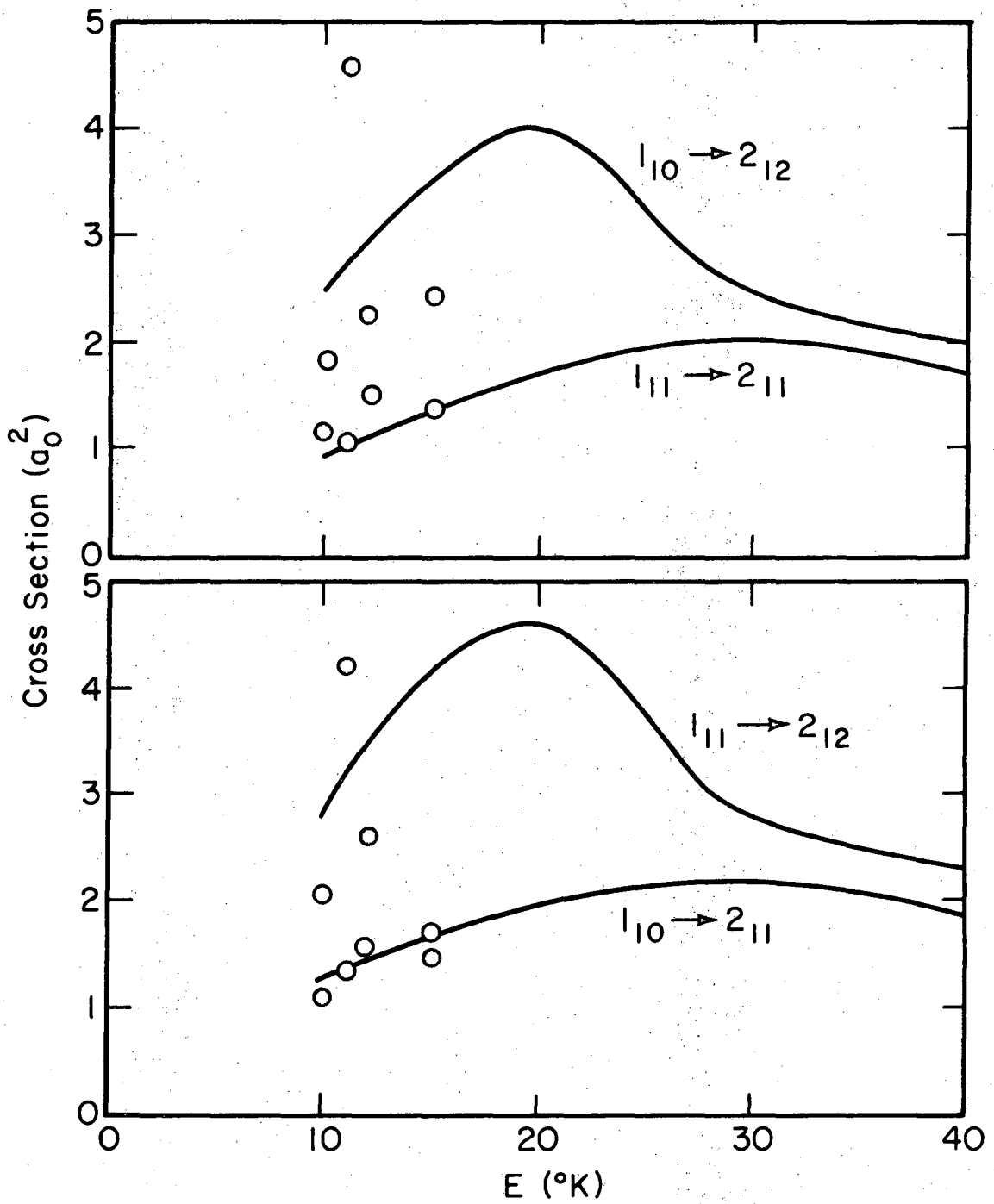

XBL 745-6395

Fig. 13. Cross sections for the indicated rotational excitations in H_2 (spherically symmetric) + H_2CO collisions as a function of initial relative translational energy. The solid lines are the results of the Monte Carlo classical trajectory calculations and the points the semiclassical values; the solid (open) points correspond to the upper (lower) curve. The energetic threshold for all four transitions is 7°K±~0.5°K (see Table II).

Although a number of additional complications[48] must be taken into account in a complete analysis of the "anomalous" absorption of formaldehyde, the following treatment may be of interest. If the rate of the dipole-allowed spontaneous decay of the j = 2 states to the j = 1 states (i.e., $2_{12} \rightarrow 1_{11}$ and $2_{11} \rightarrow 1_{10}$) were infinitely fast compared to inelastic collision rates, and if the radiative rates between the 1_{10} and 1_{11} states were neglibly slow, then simple considerations[35] imply that the steady-state ratio R of population of the 1_{11} state to that of the 1_{10} state would be

$$R = [\sigma(1_{11} \leftarrow 1_{10}) + \sigma(2_{12} \leftarrow 1_{10})] \div [\sigma(1_{10} \leftarrow 1_{11}) + \sigma(2_{11} \leftarrow 1_{11})] \quad . \qquad (21)$$

This quantity is shown as a function of collision energy in Fig. 14b, the cross sections being the Monte Carlo trajectory results from Figs. 13 and 14a. The temperature T relating the 1_{11} and 1_{10} levels is defined by

$$R \equiv \exp(\Delta\varepsilon/kT) \quad ; \qquad (22)$$

R = 1.1 and 1.2, for example, implies a temperature T = 2.4°K and 1.3°K, respectively. With the cross sections replaced by ones suitably averaged over translational energy--which would effectively smooth out the R vs E relation in Fig. 14b--this is in good qualitative agreement with the observed[1] population ratio corresponding to T ~ 1.8°K.

In summary, therefore, the results of the calculations do show that rotational excitation of formaldehyde from the 1_{11} and 1_{10} levels to the 2_{12} level is favored over that to the 2_{11} level, in accord with Townes and Cheung,[35] and the magnitude of the effect is consistent with

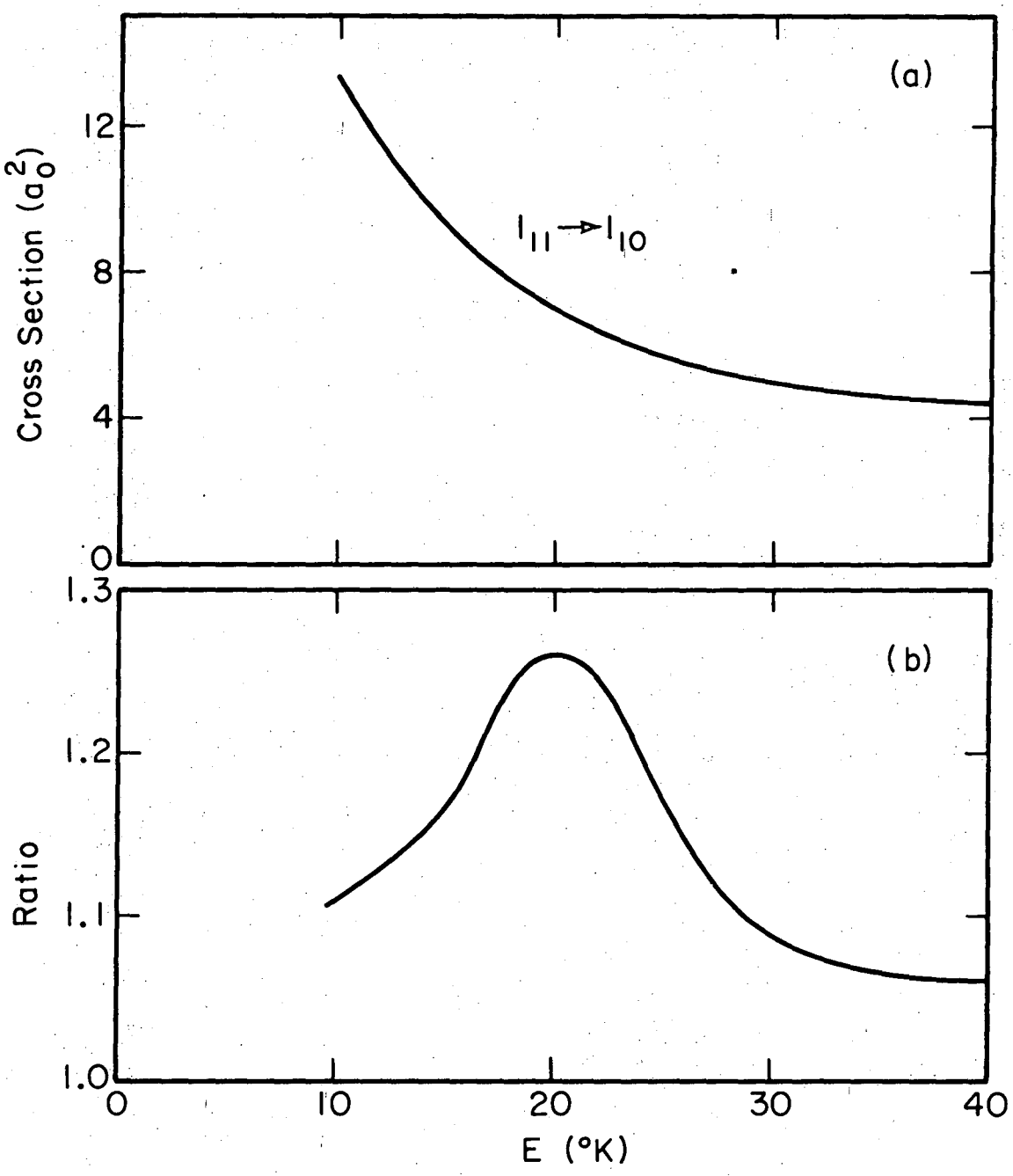

XBL 745-6396

Fig. 14. (a) Cross section for the $l_{11} \rightarrow l_{10}$ (and essentially also the $l_{10} \rightarrow l_{11}$) transition in collisions H_2 and H_2CO, as a function of initial translational energy. (b) The cross section ratio, defined by Eq. (21), as a function of initial translational energy.

this being the cooling mechanism responsible for the anamalous absorption of formaldehyde in interstellar dust clouds. The weakest aspect of the present calculations is probably the interaction potential, although it would also be useful to have completely quantum mechanical scattering calculations to check the reliability of the classical and semiclassical results.

APPENDIX 1. SEMICLASSICAL TREATMENT OF THE ASYMMETRIC ROTOR

Let x, y, z be the principal axes of the molecule with $I_z \geqslant I_y \geqslant I_x$. For a prolate symmetric top $I_y = I_z$ and for an oblate symmetric top $I_x = I_y$. The classical Hamiltonian is

$$H = \frac{I_x\omega_x^2}{2} + \frac{I_y\omega_y^2}{2} + \frac{I_z\omega_z^2}{2} \tag{1.1}$$

where the ω's are the angular velocities about the appropriate axes. Now introducing the Euler angles θ, φ, ψ of the body[49] we have

$$\omega_x = \dot{\phi}\sin\theta\ \sin\psi + \dot{\theta}\cos\psi \tag{1.2}$$

$$\omega_y = \dot{\phi}\sin\theta\ \cos\psi - \dot{\theta}\sin\psi$$

$$\omega_z = \dot{\phi}\cos\theta + \dot{\psi}$$

so that

$$p_\phi = I_x\omega_x\sin\theta\ \sin\psi + I_y\omega_y\sin\theta\ \cos\psi + I_z\omega_z\cos\theta \tag{1.3}$$

$$p_\theta = I_x\omega_x\cos\psi - I_y\omega_y\sin\psi$$

$$p_\psi = I_z\omega_z$$

are the momenta conjugate to the Euler angles. Inverting the momentum relations gives

$$j_x = I_x\omega_x = \frac{p_\phi\sin\psi}{\sin\theta} + p_\theta\cos\psi - \frac{p_\psi\cos\theta\ \sin\psi}{\sin\theta} \tag{1.4}$$

$$j_y = \frac{p_\phi\cos\psi}{\sin\theta} - p_\theta\sin\psi - p_\psi\ \frac{\cos\theta\ \cos\psi}{\sin\theta}$$

$$j_z = p_\psi$$

for the body fixed components of the rotational angular momentum. The Hamiltonian is now

$$H(\theta,\phi,\psi,p_\theta,p_\phi,p_\psi) = A\left[\frac{p_\phi \sin\psi}{\sin\theta} + p_\theta\cos\psi - \frac{p_\psi\cos\theta\ \sin\psi}{\sin\theta}\right]^2 \tag{1.5}$$

$$+ B\left[\frac{p_\phi\cos\psi}{\sin\theta} - p_\theta\sin\psi - \frac{p_\psi\cos\theta\ \cos\psi}{\sin\theta}\right]^2 + Cp_\psi^2$$

where $A = \frac{1}{2I_x}$, $B = \frac{1}{2I_y}$ and $C = \frac{1}{2I_z}$ and the square of the magnitude of the angular momentum is

$$\vec{j}^2 = j_x^2 + j_y^2 + j_z^2 = p_\theta^2 + \frac{1}{\sin^2\theta}\left[p_\phi^2 + p_\psi^2 - 2p_\phi p_\psi\cos\theta\right] \tag{1.6}$$

The asymmetry parameter κ is defined by $\kappa = \frac{2B - A - C}{A - C}$ so that $\kappa = +1$ for an oblate symmetric top and $\kappa = -1$ for a prolate symmetric top. The quantity $E(\kappa)$ which can be calculated quantum mechanically is defined by

$$2E = (a + c)\ j(j + 1) + (a - c)\ E(\kappa) \tag{1.7}$$

where $a = \hbar^2 A$ etc.

We now eliminate p_θ in favor of j, the magnitude of the rotational angular momentum by a canonical transformation using an F_2 generator.[50] This generator is

$$F_2(\theta,\phi,\psi,j,m,k) = \phi m + \psi k + j\cos^{-1}\left[\frac{j^2\cos\theta - mk}{\sqrt{(j^2 - k^2)(j^2 - m^2)}}\right] \tag{1.8}$$

$$- m\cos^{-1}\left[\frac{m\cos\theta - k}{\sin\theta\sqrt{j^2 - m^2}}\right] - k\cos^{-1}\left[\frac{k\cos\theta - m}{\sin\theta\sqrt{j^2 - k^2}}\right]$$

where $m = p_\phi$ is the component of $\vec{j}$ along the space-fixed z axis and $k = p_\psi$ is the component of $\vec{j}$ along the body-fixed z axis. Now the new coordinates (which are the coordinates canonically conjugate to j, m, k) and the transformed Hamiltonian are

$$q_j = \cos^{-1}\left[\frac{j^2\cos\theta - mk}{\sqrt{j^2 - k^2}\,\sqrt{j^2 - m^2}}\right] \tag{1.9}$$

$$q_m = \phi - \cos^{-1}\left[\frac{m\cos\theta - k}{\sin\theta\sqrt{j^2 - m^2}}\right]$$

$$q_k = \psi - \cos^{-1}\left[\frac{k\cos\theta - m}{\sin\theta\sqrt{j^2 - k^2}}\right]$$

$$\begin{aligned} H(j,k,m,q_j,q_k,q_m) &= j^2[A\sin^2 q_k + B\cos^2 q_k] \\ &\quad + k^2[C - A\sin^2 q_k - B\cos^2 q_k] \end{aligned} \tag{1.10}$$

Since q_k is the only coordinate present in the Hamiltonian, it is now obvious that j and m are conserved whereas k is not (unless A = B).

It can now be seen from Eq. (1.10) that we have an effectively one-dimensional problem and that the semiclassical energy levels might be calculated by applying the Bohr-Sommerfeld quantization rules to the k, q_k system (with j as a constant parameter). This would give

$$2\pi\hbar(n + 1/2) = \int_0^{2\pi} dq_k \left[\frac{E - j^2(A\sin^2 q_k + B\cos^2 q_k)}{C - A\sin^2 q_k - B\cos^2 q_k}\right]^{1/2} \tag{1.11}$$

with $j^2 = \hbar^2 j(j + 1)$. In the limit $A = B(\kappa = +1)$ we would get the correct quantum result that $n = k_+$ but in the limit $B = C(\kappa = -1)$ we will not get $n = k_-$. This is because the integral in Eq. (1.11) is singular for $j^2(B - A) \sin^2 q_k = k^2[(B - C) + (B - A) \sin^2 q_k]$ so that the solution in the $\kappa = +1$ limit will not go smoothly into the solution in the $\kappa = -1$ limit.

It is then desirable to seek a new momentum in which the quantization can be carried out. Define η^2 by

$$\eta^2 = (1 + \kappa)\, j_z^2 - (1 - \kappa)\, j_x^2 \tag{1.12}$$

so that the classical Hamiltonian becomes

$$H(j,m,\eta,q_j,q_m,q_\eta) = Bj^2 - \frac{(A - C)}{2}\, \eta^2 \tag{1.13}$$

It is clear now that η^2 is conserved and that if we let $j^2 = \hbar^2 j(j + 1)$ and $\nu^2 = \frac{\eta^2}{\hbar^2}$, the Hamiltonian is

$$H = bj(j + 1) - \frac{(a - c)}{2}\, \nu^2 \tag{1.14}$$

Comparing Eq. (1.14) with Eq. (1.7) it can be seen that ν is simply related to $E(\kappa)$ by

$$E(\kappa) = \kappa j(j + 1) - \nu^2 \tag{1.15}$$

In the limit of $\kappa = +1$, $j_z = \hbar k_+$, and in the limit $\kappa = -1$, $j_x = \hbar k_-$, so that η^2 has the correct behavior in the two limits. In order to transform from the k, q_k set to the η, q_η set we have that

$$\eta = (1 + \kappa)\, k^2 - (1 - \kappa)(j^2 - k^2) \sin^2 q_k \tag{1.16}$$

The F_2 generator that eliminates k in favor of η^2 is given by

$$F_2(j,\eta,q_j,q_k) = mq_m + jq_j + \int_0^{q_k} dx \sqrt{\frac{\eta^2 + (1-\kappa)\, j^2 \sin^2 x}{(1+\kappa) + (1-\kappa)\sin^2 x}} \tag{1.17}$$

Now η^2 has the dimensions of (momentum)^2, but it can be seen from Eq. (1.12) that η^2 can take on either positive or negative values. The integral in Eq. (1.17) must be worked out separately for the two signs of η^2, and it will be seen that no logical inconsistencies result from allowing η^2 to be less than zero. Indeed, the case that $\eta^2 = 0$ is exactly the point at which Eq. (1.11) becomes discontinuous.

For the case that $\eta^2 > 0$ we have that

$$F_2(j,\eta,q_j,q_k) = mq_m + jq_j + \frac{\eta^2}{\sqrt{(1+\kappa)[\eta^2 + j^2(1-\kappa)]}} \tag{1.18a}$$

$$\Pi\left(\gamma, \frac{j^2(1-\kappa)}{\eta^2 + j^2(1-\kappa)}, r\right)$$

where

$$\sin^2\gamma = \frac{\sin^2 q_k [\eta^2 + j^2(1-\kappa)]}{[\eta^2 + j^2(1-\kappa)\sin^2 q_k]} \tag{1.18b}$$

$$r^2 = \frac{(1-\kappa)}{(1+\kappa)} \frac{[j^2(1+\kappa) - \eta^2]}{[j^2(1-\kappa) + \eta^2]}$$

and $\Pi(\phi,n,k)$ is the elliptic integral of the third kind

$$\Pi(\phi,n,k) = \int_0^{\phi} \frac{d\alpha}{(1 + n\sin^2\alpha)\sqrt{1 - k^2\sin^2\alpha}}$$

The coordinate conjugate to η is given by

$$q_\eta = \frac{\eta F(\gamma,r)}{\sqrt{(1+\kappa)[j^2(1-\kappa)+\eta^2]}} \tag{1.19}$$

where

$$F(\phi,k) = \int_0^\phi \frac{d\alpha}{\sqrt{1-k^2\sin^2\alpha}}$$

is the elliptic integral of the first kind and γ, r are the same as in Eq. (1.18b).

For $\eta^2 < 0$ not all values of q_k are classically allowed. Since $k(\eta^2,q_k)$ is given by

$$k = \sqrt{\frac{\eta^2 + (1-\kappa)\, j^2\sin^2 q_k}{(1+\kappa) + (1-\kappa)\sin^2 q_k}} \tag{1.20a}$$

and k must be real, we must have

$$\eta^2 + (1-\kappa)\, j^2\sin^2 q_k \geqslant 0 \tag{1.20b}$$

If the integral in Eq. (1.17) is done considering the limits on q_k by Eq. (1.20b) we get for $\eta^2 < 0$

$$F_2(j,\eta,q_j,q_k) = mq_m + jq_j - \frac{\eta^2}{\sqrt{(1-\kappa)[(1+\kappa)\, j^2 - \eta^2]}} \tag{1.21}$$

$$\times\ \Pi\left(\gamma',\ \frac{j^2(1-\kappa)+\eta^2}{j^2(1-\kappa)},\ r'\right) - F(\gamma',r')$$

where $r' = 1/r$ and $\sin^2\gamma' = \frac{1}{\sin^2\gamma}$ [γ and r as in Eq. (1.18b)], and

$$q_\eta = \frac{\sqrt{-\eta^2}}{\sqrt{(1-\kappa)[j^2(1+\kappa)-\eta^2]}} F(\gamma',r') \tag{1.22}$$

The Eqs. (1.19) and (1.22) are all that is needed to apply classical S-matrix theory to collisions of an asymmetric rotor. The appropriate value of η^2 for a quantum state of the rotor can be obtained from the quantum mechanical values of $E(\kappa)$ by Eq. (1.15). Although there is now no need to obtain a semiclassical prediction of the energy levels, such a prediction is possible.

In order to quantize the asymmetric rotor semiclassically we use the Bohr-Sommerfeld quantization rule

$$2\pi\hbar(n+\alpha) = \oint \eta dq_\eta \tag{1.23}$$

where n is an integer and α is an arbitrary constant to be adjusted. The integral in Eq. (1.23) has parametric dependence on the energy and the magnitude of the angular momentum, which we take to be its quantum value $\hbar\sqrt{j(j+1)}$. Since η is a constant of the motion the integral is just the change in q_η over a complete cycle. Now if the left hand side of Eq. (1.23) is $2\pi\ (k_\pm + \alpha_\pm)$ for η^2 greater than or less than zero respectively, we get

$$\eta^2 > 0 : (1+\kappa)(k_+ + \alpha_+)^2 = \frac{4\nu^4 K^2(m)}{\pi^2[j(j+1)(1-\kappa)+\nu^2]} \tag{1.24a}$$

and

$$\eta^2 < 0 : (1 - \kappa)(k_- + \alpha_-)^2 = \frac{4\nu^4 K^2(1/m)}{\pi^2[j(j + 1)(1 + \kappa) - \nu^2]} \qquad (1.24b)$$

where

$$m = \frac{(1 - \kappa)[j(j + 1)(1 + \kappa) - \nu^2]}{(1 + \kappa)[j(j + 1)(1 - \kappa) + \nu^2]}$$

and K(m) is the complete elliptic integral of the first kind. By analogy with Eq. (1.12) it may be desirable to combine Eq. (1.24a) and Eq. (1.24b) by defining

$$N^2 = (1 + \kappa)(k_{+1} + \alpha_+)^2 - (1 - \kappa)(k_{-1} + \alpha_-)^2 \qquad (1.25)$$

while letting ν^2 have the same sign as N^2. It can be seen that the difficulties in Eq. (1.11) arise where $\nu^2 = 0$ and that Eq. (1.24a) and Eq. (1.24b) pass smoothly through this boundary if Eq. (1.25) is used.

The major difficulty with using the expressions in Eqs. (1.24a), (1.24b) and (1.25) for calculating the energy levels of the asymmetric rotor is the problem of determining the values of α_+ and α_-. It was found that for the lowest states ($j \leqslant 3$), the values that the alphas had to take on to reproduce the quantum levels showed considerable dependence on j, k_{+1} and k_{-1}. For some of the states the values also had a strong dependence on κ. It is possible that for large j values, where the rotor behaves more classically, the procedure outlined above may be of value in predicting the energy levels.

APPENDIX 2. ACTION-ANGLE VARIABLES FOR ATOM-ASYMMETRIC ROTOR COLLISIONS

In this section, the conventions with regard to the rotor are the same as in Appendix 1. Let $\vec{R}$ be the vector from the center of mass of the rotor to the atom, and α and β be the altitude and azimuth respectively of this vector. The Hamiltonian is

$$H = \frac{\mu}{2}(\dot{R}^2 + R^2\dot{\alpha}^2 + R^2\dot{\beta}^2\sin^2\alpha) + \frac{I_x}{2}(\dot{\phi}\sin\theta\ \sin\psi + \dot{\theta}\cos\psi)^2 \tag{2.1}$$

$$+ \frac{I_y}{2}(\dot{\phi}\sin\theta\ \cos\psi - \dot{\theta}\sin\psi)^2 + \frac{I_z}{2}(\dot{\phi}\cos\theta + \dot{\psi})^2 + V(R,\gamma,\zeta)$$

where γ is the angle between R and the body fixed z axis and is the angle between R and the body fixed x axis. Therefore,

$$\cos\gamma = \cos\theta\ \cos\alpha + \sin\theta\ \sin\alpha\ \sin(\phi - \beta) \tag{2.2}$$

$$\cos\zeta = \sin\psi[\cos\alpha\ \sin\theta - \cos\theta\ \sin\alpha\ \sin(\phi - \beta)]$$

$$+ \cos\psi\ \sin\alpha\ \cos(\phi - \beta)$$

In terms of the canonical momenta H is

$$H = \frac{p_R^2}{2\mu} + \frac{p_\alpha^2}{2\mu R^2} + \frac{p_\beta^2}{2\mu R^2\sin^2\alpha} + \frac{A}{2}\left[p_\phi\frac{\sin\psi}{\sin\theta} + p_\theta\cos\psi - \frac{p_\psi\cos\theta\ \sin\psi}{\sin\theta}\right]^2 \tag{2.3}$$

$$+ \frac{B}{2}\left[p_\phi\frac{\cos\psi}{\sin\theta} - p_\theta\sin\psi - p_\psi\frac{\cos\theta\ \cos\psi}{\sin\theta}\right]^2 + \frac{Cp_\psi^2}{2} + V(R,\gamma,\zeta)$$

where p_θ, p_ϕ, p_ψ are as in Appendix 1 and

$$p_R = \mu\dot{R} \tag{2.3a}$$

$$p_\alpha = \mu R^2\dot{\alpha}$$

$$p_\beta = \mu R^2\sin^2\alpha\dot{\beta}$$

(note that μ is the reduced mass of the "two-body" system where one body is the atom and the other is the rotor). Since ϕ and β only occur in the combination $(\phi - \beta)$, ϕ can be replaced by the new variable $\varepsilon = (\phi - \beta)$. This is done by the F_3 generator

$$F_2(\phi,\beta;\varepsilon,\beta) = -\beta p_\beta - \varepsilon p_\phi \tag{2.4}$$

which gives the new momenta $p_\varepsilon = p_\phi = m$ and $M = p_\varepsilon + p_\beta$, the projection of the total angular momentum on the space-fixed z axis. The orbital angular momentum ℓ is now introduced by an F_2 type generator using

$$\ell^2 = \frac{p\alpha^2}{2\mu R^2} + \frac{(M - m)^2}{2\mu R^2 \sin^2\alpha}$$

$$F_2(\varepsilon,\beta,\alpha;\ell,\ m,M) = m\varepsilon + \beta M + \ell\cos^{-1}\left[\frac{\ell\cos\alpha}{\sqrt{\ell^2 - (M - m)^2}}\right] \tag{2.5}$$

$$- (M - m)\ \cos^{-1}\left[\frac{(M - m)\ \cos\alpha}{\sin\alpha\sqrt{\ell^2 - (M - m)^2}}\right]$$

The new coordinates are

$$q'_\ell = \cos^{-1}\left[\frac{\ell\cos\alpha}{\sqrt{\ell^2 - (M - m)^2}}\right] \tag{2.6}$$

$$Q_2 = \beta - \cos^{-1}\left[\frac{(M - m)\ \cos\alpha}{\sin\alpha\sqrt{\ell^2 - (M - m)^2}}\right]$$

$$Q_3 = \varepsilon + \cos^{-1}\left[\frac{(M - m)\ \cos\alpha}{\sin\alpha\sqrt{\ell^2 - (M - m)^2}}\right]$$

The F_2 generator in Eq. (1.6) is now used (with ϕ replaced by Q_3) and the new coordinates are

$$q_j' = \cos^{-1}\left[\frac{j^2\cos\theta - mk}{\sqrt{j^2 - k^2}\,\sqrt{j^2 - m^2}}\right] \tag{2.7}$$

$$q_k = \psi - \cos^{-1}\left[\frac{k\cos\theta - m}{\sin\theta\sqrt{j^2 - k^2}}\right].$$

$$q_m = Q_3 - \cos^{-1}\left[\frac{m\cos\theta - k}{\sin\theta\sqrt{j^2 - m^2}}\right]$$

The space fixed components of $\vec{j}$ and $\vec{\ell}$ are now given by

$$j_x = -\sin(Q_2 + q_m)\sqrt{j^2 - m^2} \tag{2.8}$$

$$j_y = \cos(Q_2 + q_m)\sqrt{j^2 - m^2}$$

$$j_z = m$$

$$\ell_x = -\cos Q_2\sqrt{\ell^2 - (M - m)^2}$$

$$\ell_y = -\sin Q_2\sqrt{\ell^2 - (M - m)^2}$$

$$\ell_z = (M - m)$$

so that the magnitude of the total angular momentum J is given by

$$J^2 = j^2 + \ell^2 + 2m(M - m) + 2\sqrt{j^2 - m^2}\sqrt{\ell^2 - (M - m)^2}\,\sin q_m \tag{2.9}$$

It is now desired to replace m by J, and to express γ and ζ in terms of the final angle variables. The first is done with the generator

$$F_4(j,\ell,M,m;J,j,\ell,M) = J\sin^{-1}\left[\frac{M(J^2 + J^2 - \ell^2) - 2mJ^2}{\xi\sqrt{J^2 - M^2}}\right] \tag{2.10}$$

$$+ \ell\sin^{-1}\left[\frac{m(J^2 + \ell^2 - j^2) - M(J^2 - \ell^2 - j^2)}{\xi\sqrt{\ell^2 - (M - m)^2}}\right]$$

$$+ j\sin^{-1}\left[\frac{m(J^2 + j^2 - \ell^2) - 2Mj^2}{\xi\sqrt{j^2 - m^2}}\right] + M\sin^{-1}\left[\frac{(J^2 + j^2 - \ell^2) - 2M(M - m)}{2\sqrt{J^2 - M^2}\sqrt{\ell^2 - (M - m)^2}}\right]$$

$$- m\sin^{-1}\left[\frac{(J^2 - j^2 - \ell^2) - 2m(M - m)}{2\sqrt{j^2 - m^2}\sqrt{\ell^2 - (M - m)^2}}\right]$$

where $\xi^2 = -J^4 - j^4 - \ell^4 + 2J^2j^2 + 2J^2\ell^2 + 2j^2\ell^2$. The new coordinates are

$$q_j = q_j' + \sin^{-1}\left[\frac{m(J^2 + j^2 - \ell^2) - 2Mj^2}{\xi\sqrt{j^2 - m^2}}\right] \tag{2.11}$$

$$q_\ell = q_\ell' + \sin^{-1}\left[\frac{m(J^2 + \ell^2 - j^2) - M(J^2 - \ell^2 - j^2)}{\xi\sqrt{\ell^2 - (M - m)^2}}\right]$$

$$q_M = Q_2 + \sin^{-1}\left[\frac{(J^2 + \ell^2 - j^2) - 2M(M - m)}{2\sqrt{J^2 - M^2}\sqrt{\ell^2 - (M - m)^2}}\right]$$

$$q_J - \sin^{-1}\left[\frac{M(J^2 + j^2 - \ell^2) - 2mJ^2}{\xi\sqrt{J^2 - M^2}}\right]$$

because of the overall rotational symmetry of the system, M can be set equal to zero without loss of generality. The two potential parameters are given in this set of coordinates and momenta by

$$\cos\gamma = \frac{\sqrt{j^2 - k^2}}{j}\left[\cos q_\ell \cos q_j + \frac{(J^2 - j^2 - \ell^2)}{2\ell_j}\sin q_\ell \sin q_j\right] + \frac{k\xi \sin q_\ell}{2\ell j^2}$$

$$\cos\zeta = \frac{\sin q_k}{2\ell\sqrt{j^2 - k^2}}\,[2\ell k\cos\gamma - \xi\sin q_\ell] + \cos q_k\left[\cos q_\ell \sin q_j - \frac{(J^2 - j^2 - \ell^2)}{2\ell j}\sin q_\ell \cos q_j\right] \tag{2.12}$$

The Hamiltonian is now given by

$$H = \frac{p_R^2}{2\mu} + \frac{\ell^2}{2\mu R^2} + j^2[A\sin^2 q_k + B\cos^2 q_k] + k^2[C - A\sin^2 q_k - B\cos^2 q_k] + V(R,\gamma,\zeta) \tag{2.13}$$

APPENDIX 3. MONTE-CARLO TECHNIQUE FOR ASYMMETRIC ROTOR TRANSITIONS

Principally because the second "quantum number", ν, for defining the state of the asymmetric rotor is not an integer, and may be imaginary, several modifications must be made in the standard Monte-Carlo classical trajectory technique for evaluating the cross sections. The classical S-matrix result for the total cross section (see Eqs. (3.1) and (3.2)) is given by

$$\sigma_{j_2\nu_2 \leftarrow j_1\nu_1}(E) = \frac{\pi\hbar^2}{(2\mu E)(2j_1 + 1)} \sum_{J=0}^{\infty} (2J + 1) \sum_{\ell_1,\ell_2} |S^J_{\ell_2 j_2 \nu_2, \ell_1 j_1 \nu_1}|^2 \qquad (3.1)$$

where

$$S^J_{\ell_2,j_2,\nu_2;\ell_1,j_1,\nu_1} = \left[(-2\pi i\hbar)^3 \frac{\partial(\ell_2,j_2,\nu_2)}{\partial(q_{\ell_1},q_j,q_{\nu_1})}\right]^{-1/2} e^{i\phi(\ell_2,j_2,\nu_2;\ell_1,j_1,\nu_1)/\hbar} \qquad (3.2)$$

Equation (3.1) is transformed to a form suitable for Monte-Carlo evaluation by ignoring the phase in Eq. (3.2) and averaging over final quantum numbers so that the Jacobian factor in Eq. (3.2) cancels out.

We first approximate the infinite sum over ℓ_2 by an integral over ℓ_2. If this integral is then transformed into an integral over dq_ℓ, the factor

$$\left(\frac{\partial \ell_2}{\partial q_{\ell_1}}\right)$$

which arises cancels with the Jacobian in the square of the S-matrix element. We now have

$$\sigma^{(E)}_{j_2,\nu_2\leftarrow j_1,\nu_1} = \frac{\pi\hbar^2}{2\mu E(2j_1+1)} \sum_{J=0}^{\infty} (2J+1) \sum_{\ell_1} \int_0^1 d\left(\frac{q_{\ell_1}}{2\pi}\right) \frac{1}{(2\pi\hbar)^2} \times \left[\frac{\partial(j_2,\nu_2)}{\partial(q_{j_1},q_{\nu_1})}\right]^{-1} \tag{3.3}$$

To completely remove the Jacobian we want to average j_2 and ν_2 over "quantum number" intervals. This is straightforward for j_2 but not for ν_2 since this is non-integer for the desired final state and may be imaginary. Because of this last difficulty we average over a ν_2^2 interval rather than a ν_2 interval and take the averages of the ν^2 values for the various states as the endpoints. We now have

$$\sigma^{(E)}_{j_2,\nu_2\leftarrow j_1,\nu_1} = \frac{\pi\hbar^2}{2\mu E(2j_1+1)} \sum_{J=0}^{\infty} (2J+1) \sum_{\ell_1=|J-j_1|}^{J+j_1} \int_{j2-\frac{1}{2}}^{j2+\frac{1}{2}} \int_{\nu^2_{low}}^{\nu^2_{top}} d(\nu_2^2) \int_0^1 d\left(\frac{q_{\ell_1}}{2}\right) \times \frac{1}{\left(\nu^2_{top}-\nu^2_{low}\right)} \frac{1}{(2\pi\hbar)^2} \left[\frac{\partial(j_2,\nu_2)}{\partial(q_{j_1},q_{\nu_1})}\right]^{-1} \tag{3.4}$$

where ν^2_{top} and ν^2_{low} are the endpoints of the ν^2 interval. It is now desired to cancel out the Jacobian entirely by changing the integrals over j_2 and ν_2^2 to integrals over q_{j_1} and q_{ν_1}.

Since it is more convenient to compute the trajecotires in the k,q_k set of canonical variables rather than the ν,q_ν set, we would like the

expression to involve only the former set. From the results in Appendix 1 we have that

$$\frac{\partial q_{\nu_1}}{\partial q_{k_1}} = \frac{\nu_1}{\sqrt{(1+\kappa) + (1-\kappa)\sin^2 q_k}\sqrt{\nu_1^2 + j_1(j_1+1)(1-\kappa)\sin^2 q_{k_1}}} \tag{3.5}$$

so that

$$\int d\left(\nu_2^2\right) = 2\nu_2 \int d\nu_2 = 2\nu_2 \int \frac{\partial \nu_2}{\partial q_{\nu_1}} dq_{\nu_1}$$

$$= 2\nu_2 \int \left(\frac{\partial \nu_2}{\partial q_{\nu_1}}\right)\left(\frac{\partial q_{\nu_1}}{\partial q_{k_1}}\right) dq_{k_1}$$

If we insert a function χ that is one if a trajectory falls in the appropriate j_2, ν_2^2 "box" and zero otherwise we get finally

$$\sigma^{(E)}_{j_2,\nu_2 \leftarrow j_1,\nu_1} = \frac{\pi\hbar^2\nu_1}{2\mu E(2j_1+1)\,\Delta} \sum_{J=0}^{\infty} (2J+1) \sum_{\ell_1=|J-j_1|}^{J+j_1} \tag{3.6}$$

$$\int_0^1 d\left(\frac{q_{\ell_1}}{2\pi}\right) \int_0^1 \left(\frac{q_{j_1}}{2\pi}\right) \int_0^1 d\left(\frac{d_{k_1}}{2\pi}\right)$$

$$\times \frac{\chi\nu_2}{\sqrt{(1+\kappa) + (1-\kappa)\sin^2 q_{k_1}}\sqrt{\nu_1^2 + j_1(j_1+1)(1-\kappa)\sin^2 q_{k_1}}}$$

where Δ is the length of the ν_2^2 "box". Equation (3.6) is now in a form amenable to Monte-Carlo evaluation and is the desired result.

IV. SEMICLASSICAL THEORY OF NON-REACTIVE DIATOM-DIATOM COLLISIONS

In the previous section, the necessary formalism was developed for the semi-classical treatment of an atom colliding with an asymmetric rotor. Vibrational motion of the rotor was not included, but its only effect on the transformations of rotational coordinates is to make the moments of inertia varying with time. Despite the complexity of asymmetric rotor motion, this is still a one-center problem; only one of the collision partners is allowed to have internal degrees of freedom. This section considers the simplest case of a two-center problem, the collision of two rigid diatomic rotors.

Let one of the diatoms be molecule A made up of atoms labelled 1 and 2. Similarly, let the other be molecule B made up of atoms 3 and 4. The classical kinetic energy is

$$T = \frac{m_1}{2}\dot{\vec{r}}_1^{\,2} + \frac{m_2}{2}\dot{\vec{r}}_2^{\,2} + \frac{m_3}{2}\dot{\vec{r}}_3^{\,2} + \frac{m_4}{2}\dot{\vec{r}}_4^{\,2} \tag{1}$$

Now define the following new coordinates:

$$R_{cm} = \frac{1}{M}\sum_{i=1}^{4} m_i \vec{r}_i \tag{2a}$$

$$\vec{R} = \frac{1}{M_A}(m_1\vec{r}_1 + m_2\vec{r}_2) - \frac{1}{M_B}(m_3\vec{r}_3 + m_4\vec{r}_4) \tag{2b}$$

$$\vec{r}_A = \vec{r}_1 - \vec{r}_2 \tag{2c}$$

$$\vec{r}_B = \vec{r}_3 - \vec{r}_4 \tag{2d}$$

where $M_A = m_1 + m_2$, $M_B = m_3 + m_4$, $M = M_A + M_B$. Clearly $\vec{R}_{cm}$ is the location of the overall center of mass; $\vec{R}$ is the relative vector between the center of mass of A and that of B; $\vec{r}_A$ is the relative vector in A; and $\vec{r}_B$ is the

is the relative vector in B. The inverse transformation to Eqs. (2a-d) is given by

$$\vec{r}_1 = \vec{R}_{cm} + \frac{M_B}{M}\vec{R} + \frac{m_2}{M_A}\vec{r}_A \tag{3a}$$

$$\vec{r}_2 = \vec{R}_{cm} + \frac{M_B}{M}\vec{R} - \frac{m_1}{M_A}\vec{r}_A \tag{3b}$$

$$\vec{r}_3 = \vec{R}_{cm} - \frac{M_A}{M}\vec{R} + \frac{m_4}{M_B}\vec{r}_B \tag{3c}$$

$$\vec{r}_4 = \vec{R}_{cm} - \frac{M_A}{M}\vec{R} - \frac{m_3}{M_B}\vec{r}_B \quad . \tag{3d}$$

The kinetic energy in terms of the new coordinates thus becomes

$$T = \frac{M}{2}\dot{\vec{R}}_{cm}^2 + \frac{\mu_{AB}}{2}\dot{\vec{R}}^2 + \frac{\mu_A}{2}\dot{\vec{r}}_A^2 + \frac{\mu_B}{2}\dot{\vec{r}}_B^2 \tag{4}$$

where $\frac{1}{\mu_A} = \frac{1}{m_1} + \frac{1}{m_2}$, $\frac{1}{\mu_B} = \frac{1}{m_3} + \frac{1}{m_4}$, $\frac{1}{\mu_{AB}} = \frac{1}{M_A} + \frac{1}{M_B}$. The first term is the motion of the overall center of mass and can, therefore, be dropped.

We are now free to fix a point in the center of mass system as the origin of coordinates; the center of mass of molecule A is taken to be that point here. Let the spherical polar coordinates of $\vec{r}_A$ be (r_A,θ,ϕ) and of $\vec{R}$ be (R,α,β) where ϕ and β are azimuthal angles and θ, α are polar angles. In terms of the spherical coordinates

$$\frac{\mu_A}{2}\dot{\vec{r}}_A^2 = \frac{\mu_A}{2}\dot{r}_A^2 + \frac{I_A}{2}(\dot{\theta}^2 + \dot{\phi}^2\sin^2\theta) \tag{5a}$$

$$\frac{\mu_{AB}}{2}\dot{\vec{R}}^2 = \frac{\mu_{AB}}{2}\dot{R}^2 + \frac{\mu_{AB}R^2}{2}(\dot{\alpha}^2 + \dot{\beta}^2\sin^2\alpha) \tag{5b}$$

where $I_A = \mu_A r_A^2$.

It is much more difficult to set up an appropriate coordinate system for molecule B. To this end, let r_B be $|\vec{r}_B|$; let δ be the angle between $\vec{R}$ and $\vec{r}_B$; and let ε be the azimuthal angle in the plane perpendicular to $\vec{R}$ at its end with $\varepsilon = 0$ corresponding to the line of intersection of this plane with the plane containing $\vec{R}$ and the x-axis. This coordinate system is represented in Fig. 15. In terms of the spherical unit vectors of $\vec{R}$ $(\hat{R},\hat{\alpha},\hat{\beta})$, the following relations are obtained

$$\begin{aligned} \hat{R}\cdot\vec{r}_B &= r_B\cos\delta \\ \hat{\alpha}\cdot\vec{r}_B &= r_B\sin\delta\ \sin\varepsilon \\ \hat{\beta}\cdot\vec{r}_B &= r_B\sin\delta\ \cos\varepsilon \end{aligned} \tag{6}$$

It can thus be seen that δ,ε are the spherical angles of $\vec{r}_B$ with respect to the moving center of coordinates fixed at the center of mass of molecule B (with the "x axis" in this system defined by the intersection of two moving planes).

The space-fixed cartesian components of $\vec{r}_B$ in the coordinate system are

$$\vec{r}_B = r_B \begin{pmatrix} \sin\alpha\ \cos\beta\ \cos\delta + \cos\alpha\ \sin\beta\ \sin\delta\ \sin\varepsilon - \sin\beta\ \sin\delta\ \cos\varepsilon \\ \sin\alpha\ \sin\beta\ \cos\delta + \cos\alpha\ \sin\beta\ \sin\delta\ \sin\varepsilon + \cos\beta\ \sin\delta\ \cos\varepsilon \\ \cos\alpha\ \cos\delta - \sin\alpha\ \sin\delta\ \sin\varepsilon \end{pmatrix} \tag{7}$$

where the top element of the column matrix is the x component, etc. Now $\mu_B\dot{\vec{r}}_B^{\,2}$ is given by

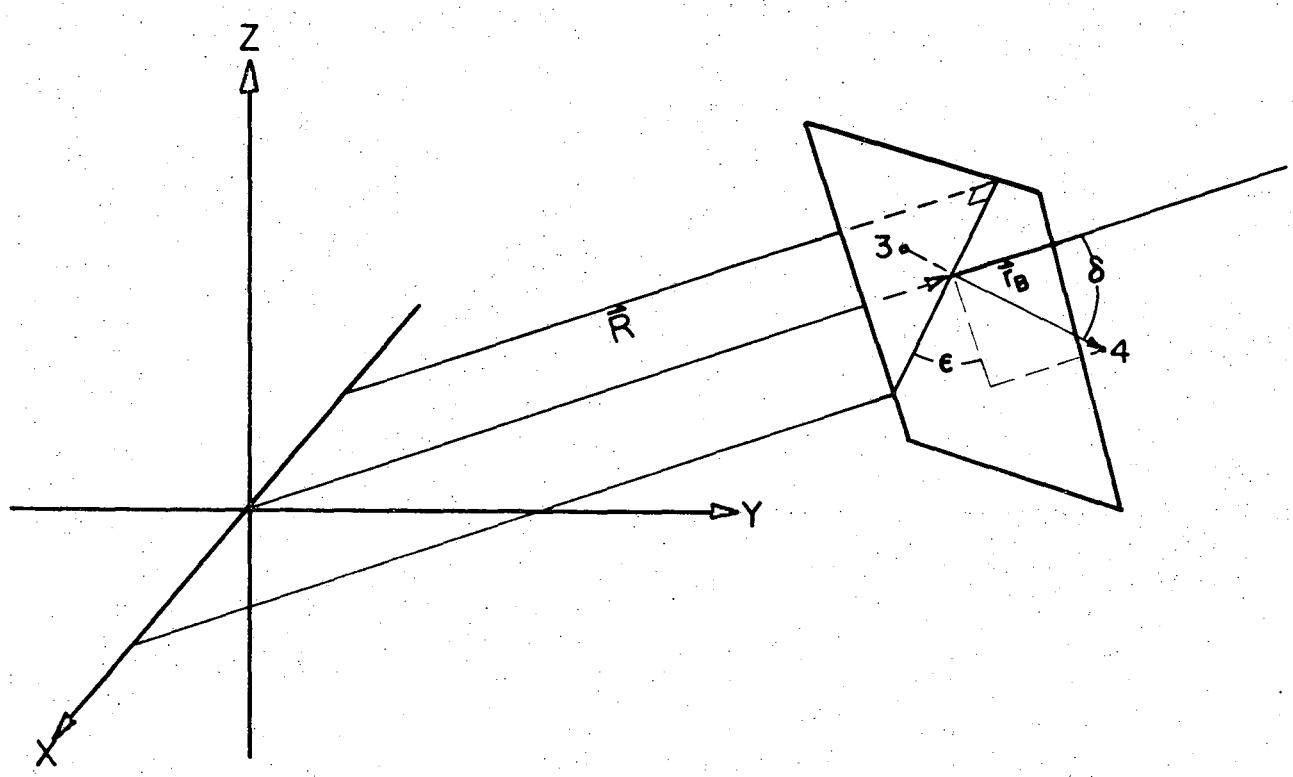

XBL 749-7137

Fig. 15. Coordinate system for the classical dynamics of the diatom-diatom system.

$$\mu_B \dot{\vec{r}}_B^{\,2} = \frac{\mu_B}{2}\dot{r}_B^2 + \frac{\mu_B r_B^2}{2}\,[c_1\dot{\alpha}^2 + c_3\dot{\beta}^2 + \dot{\delta}^2 + \dot{\varepsilon}^2\sin^2\delta + 2c_2\dot{\alpha}\dot{\beta} \tag{8a}$$

$$+ 2\dot{\alpha}\dot{\varepsilon}\sin\delta\,\cos\delta\,\cos\varepsilon + 2\dot{\alpha}\dot{\delta}\sin\varepsilon + 2\dot{\beta}\dot{\delta}\sin\alpha\,\cos\varepsilon - 2\dot{\beta}\dot{\varepsilon}c_4]$$

where

$$c_1 = \cos^2\delta + \sin^2\delta\,\sin^2\varepsilon \tag{8b}$$

$$c_2 = \sin\delta\,\cos\varepsilon(\sin\alpha\,\sin\delta\,\sin\varepsilon - \cos\alpha\,\cos\delta)$$

$$c_3 = \sin^2\alpha\,\cos^2\delta + \cos^2\alpha\,\sin^2\delta\,\sin^2\varepsilon + \sin^2\delta\,\cos^2\varepsilon$$
$$+ 2\sin\alpha\,\cos\alpha\,\sin\delta\,\cos\delta\,\sin\varepsilon$$

$$c_4 = \sin\delta(\cos\alpha\,\sin\delta + \sin\alpha\,\cos\delta\,\sin\varepsilon)$$

The momenta conjugate to the coordinates are now given by

$$p_\theta = I_A\dot{\theta} \tag{9}$$

$$p_\phi = I_A\dot{\phi}\sin^2\theta$$

$$p_{r_A} = \mu_A\dot{r}_A$$

$$p_R = \mu_{AB}\dot{R}$$

$$p_{r_B} = \mu_B\dot{r}_B$$

$$p_\alpha = \mu_{AB}R^2\dot{\alpha}^2 + \mu_B r_B^2(c_1\dot{\alpha} + c_2\dot{\beta} + \dot{\delta}\sin\varepsilon + \dot{\varepsilon}\sin\delta\,\cos\delta\,\cos\varepsilon)$$

$$p_\beta = \mu_{AB}R^2\dot{\beta}\sin^2\alpha + \mu_B r_B^2(c_3\dot{\beta} + c_2\dot{\alpha} + \dot{\delta}\sin\alpha\,\cos\varepsilon - c_4\dot{\varepsilon})$$

$$p_\delta = \mu_B r_B^2(\dot{\delta} + \dot{\alpha}\sin\varepsilon + \dot{\beta}\sin\alpha\,\cos\varepsilon)$$

$$p_\varepsilon = \mu_B r_B^2(\dot{\varepsilon}^2\sin^2\delta + \dot{\alpha}\sin\delta\,\cos\delta\,\cos\varepsilon - \dot{\beta}c_4) \quad .$$

Writing the kinetic energy in terms of p_θ, p_ϕ, $\dot{R}$, $\dot{r}_A$, $\dot{r}_B$, $\dot{\alpha}$, $\dot{\beta}$, $\dot{\delta}$, $\dot{\varepsilon}$ and the coordinates gives

$$T = \frac{p_\theta^2}{2I_A} + \frac{p_\phi^2}{2I_A \sin^2\theta} + \frac{\mu_{AB}}{2}(\dot{R}^2 + R^2\dot{\alpha}^2 + R^2\dot{\beta}^2\sin^2\alpha) + \frac{\mu_B}{2}\dot{r}_B^2 \tag{10}$$

$$+ \frac{\mu_A}{2}\dot{r}_A^2 + \frac{\mu_B r_B^2}{2}(c_1\dot{\alpha}^2 + c_3\dot{\beta}^2 + \dot{\delta}^2 + \dot{\varepsilon}^2\sin^2\delta + 2c_2\dot{\alpha}\dot{\beta}$$

$$+ 2\dot{\alpha}\dot{\varepsilon}\sin\delta\cos\delta\cos\varepsilon + 2\dot{\alpha}\dot{\delta}\sin\varepsilon + 2\dot{\beta}\dot{\delta}\sin\alpha\cos\varepsilon - 2c_4\dot{\beta}\dot{\varepsilon})$$

The terms in Eq. (10) can now be given some physical meaning. The first two terms are the rotational motion of molecule A. The second is the radial and orbital motion of the center of mass of B. The third and fourth terms are the vibrational motion of molecules A and B, respectively. The last term appears quite formidable but it contains some recognizeable parts. The part

$$\frac{\mu_B r_B^2}{2}(\dot{\delta}^2 + \dot{\varepsilon}^2\sin^2\delta)$$

is just the rotational motion of molecule B if its center of mass were fixed, and the rest represents coupling between the motion of $\vec{R}$ and the motion or $\vec{r}_B$.

In order to make further progress with Eq. (10) it is necessary to eliminate all the time derivatives of angles in favor of their canonical momenta. To this end we note that the transformation between the set $(\dot{\alpha},\dot{\beta},\dot{\delta},\dot{\varepsilon})$ and the set $(p_\alpha, p_\beta, p_\delta, p_\varepsilon)$ can be given by the matrix equation

$$\begin{pmatrix} p_\alpha \\ p_\beta \\ p_\delta \\ p_\varepsilon \end{pmatrix} = \left(\begin{array}{c|c|c|c} a + bc_1 & bc_2 & b\sin\varepsilon & b\sin\delta\cos\delta\cos\varepsilon \\ bc_2 & a\sin^2\alpha + bc_3 & b\sin\alpha\cos\varepsilon & -bc_4 \\ b\sin\varepsilon & b\sin\alpha\cos\varepsilon & b & 0 \\ b\sin\delta\cos\delta\cos\varepsilon & -bc_4 & 0 & b\sin^2\delta \end{array}\right) \begin{pmatrix} \dot\alpha \\ \dot\beta \\ \dot\delta \\ \dot\varepsilon \end{pmatrix} \tag{11}$$

where $a = \mu_{AB}R^2$ and $b = \mu_B r_B^{\,2}$. Inverting the 4×4 matrix gives the inverse transformation

$$\begin{pmatrix} \dot\alpha \\ \dot\beta \\ \dot\delta \\ \dot\varepsilon \end{pmatrix} = \left(\begin{array}{c|c|c|c} ab^2\sin^2\alpha\,\sin^2\delta & 0 & -ab^2\sin^2\alpha\,\sin^2\delta\,\sin\varepsilon & -ab^2\sin^2\alpha\,\sin\delta\cos\delta\cos\varepsilon \\ 0 & ab^2\sin^2\delta & -ab^2\sin\alpha\,\sin^2\delta\cos\varepsilon & ab^2c_4 \\ -ab^2\sin^2\alpha\,\sin^2\delta\,\sin\varepsilon & -ab^2\sin\alpha\,\sin^2\delta\cos\varepsilon & \sin^2\alpha\,\sin^2\delta(a^2b + ab^2) & -ab^2\sin\alpha\cos\alpha\,\sin^2\delta\cos\varepsilon \\ -ab^2\sin^2\alpha\,\sin\delta\cos\delta\cos\varepsilon & ab^2c_4 & -ab^2\sin\alpha\cos\alpha\,\sin^2\delta\cos\varepsilon & a^2b\sin^2\alpha + ab^2c_6 \end{array}\right) \begin{pmatrix} p_\alpha \\ p_\beta \\ p_\delta \\ p_\varepsilon \end{pmatrix} \tag{12}$$

where $c_6 = \sin^2\alpha\cos^2\delta + \cos^2\alpha\sin^2\delta + 2\sin\alpha\cos\alpha\sin\delta\cos\delta\sin\varepsilon$.

It should now be possible to introduce the orbital angular momentum $\vec{\ell}$ and the rotational angular momenta of A and B ($\vec{j}_A$ and $\vec{j}_B$). The cartesian components of $\vec{j}_A$ are given by

$$\vec{j}_A = I_A \begin{pmatrix} -\dot\theta\sin\phi - \dot\phi\sin\theta\cos\theta\cos\phi \\ \dot\theta\cos\phi - \dot\phi\sin\theta\cos\theta\sin\phi \\ \dot\phi\sin^2\theta \end{pmatrix} \tag{13}$$

so that $j_A^2 = I_A^2(\dot{\theta}^2 + \dot{\phi}^2 \sin^2\theta)$. Replacing $\dot{\theta}, \dot{\phi}$ by p_θ, p_ϕ

$$\vec{j}_A = \begin{pmatrix} -p_\theta \sin\phi - p_\phi \cot\theta \cos\phi \\ p_\theta \cos\phi - p_\phi \cot\theta \sin\phi \\ p_\phi \end{pmatrix} , \tag{14a}$$

$$j_A^2 = p_\theta^2 + \frac{p_\phi^2}{\sin^2\theta} . \tag{14b}$$

Also

$$\vec{\ell} = a \begin{pmatrix} -\dot{\alpha}\sin\beta - \dot{\beta}\sin\alpha \cos\alpha \cos\beta \\ \dot{\alpha}\cos\beta - \dot{\beta}\sin\alpha \cos\alpha \sin\beta \\ \dot{\beta}\sin^2\alpha \end{pmatrix} \tag{15a}$$

or

$$\vec{\ell} = \begin{pmatrix} -\sin\beta p_\alpha - \cot\alpha \cos\beta p_\beta + c_{11} p_\delta - \dfrac{p_\varepsilon}{\sin\alpha \sin\delta} \\ \cos\beta p_\alpha - \cot\alpha \sin\beta p_\beta - c_{12} p_\delta - \dfrac{-p_\varepsilon}{\sin\alpha \sin\delta} \\ p_\beta - \sin\alpha \cos\varepsilon p_\delta + c_5 p_\varepsilon / \sin\delta \end{pmatrix} \tag{15b}$$

$$\begin{pmatrix} (\cos\alpha \cos\beta c_5 - \sin\alpha \sin\beta \cos\delta \cos\varepsilon) \\ (\cos\alpha \sin\beta c_5 + \sin\alpha \cos\beta \cos\delta \cos\varepsilon) \end{pmatrix}$$

and

$$\ell^2 = p_\alpha^2 + \frac{p_\beta^2}{\sin^2\alpha} + p_\delta^2 + \frac{c_6}{\sin^2\alpha\,\sin^2\delta}\,p_\varepsilon^2 - 2\sin\varepsilon\,p_\alpha p_\delta - \frac{2\cos\delta\,\cos\varepsilon\,p_\alpha p_\varepsilon}{\sin\delta}$$

$$- \frac{2\cos\varepsilon}{\sin\alpha}\,p_\beta p_\delta + \frac{2c_4 p_\beta p_\varepsilon}{\sin^2\alpha\,\sin^2\delta} - \frac{2\cos\alpha\,\cos\varepsilon}{\sin\alpha}\,p_\delta p_\varepsilon \tag{15c}$$

where

$$c_5 = c_4/\sin\delta \tag{15d}$$

$$c_7 = \sin\delta\,\cos\varepsilon(\sin\alpha\,\cos\delta + \cos\alpha\,\sin\delta\,\sin\varepsilon)$$

$$c_8 = \sin\alpha\,\cos\alpha\,\sin^2\delta\,\sin^2\varepsilon - \sin\alpha\,\cos\alpha\,\cos^2\delta + \sin^2\alpha\,\sin\delta\,\cos\delta\,\sin\varepsilon - \cos^2\alpha\,\sin\delta\,\cos\delta\,\sin\varepsilon$$

$$c_9 = c_{10}/\sin\delta$$

$$c_{10} = \sin\delta(\cos\alpha\,\cos\delta\,\sin\varepsilon - \sin\alpha\,\sin\delta)$$

$$c_{11} = \cos\alpha\,\cos\beta\,\cos\varepsilon + \sin\beta\,\sin\varepsilon$$

$$c_{12} = \cos\beta\,\sin\varepsilon - \cos\alpha\,\sin\beta\,\cos\varepsilon$$

The components of $\vec{j}_B$ are

$$\vec{j}_B = b\begin{pmatrix} -\dot\alpha(\sin\beta c_1 + \cos\beta c_7) + \dot\beta(\cos\beta c_8 - \sin\beta c_2) - \dot\delta c_{11} \\ \dot\alpha(\cos\beta c_1 - \sin\beta c_7) + \dot\beta(\cos\beta c_2 + \sin\beta c_8) + \dot\delta c_{12} \\ \dot\alpha c_2 + \dot\beta c_3 + \dot\delta\sin\alpha\,\cos\varepsilon - \dot\varepsilon c_4 \end{pmatrix} \tag{16a}$$

$$\begin{pmatrix} + \dot\varepsilon(\cos\beta c_{10} - \sin\beta\,\sin\delta\,\cos\delta\,\cos\varepsilon) \\ + \dot\varepsilon(\cos\beta\,\sin\delta\,\cos\delta\,\cos\varepsilon + \sin\beta c_{10} \end{pmatrix}$$

or

$$\vec{j}_B = \begin{pmatrix} -c_{11}p_\delta + (\cos\beta c_{10} - \sin\beta \sin\delta \cos\delta \cos\varepsilon)\, p_\varepsilon/\sin^2\delta \\ c_{12}p_\delta + (\sin\beta c_{10} + \cos\beta \sin\delta \cos\delta \cos\varepsilon)\, p_\varepsilon/\sin^2\delta \\ p_\delta \sin\alpha \cos\varepsilon - p_\varepsilon c_5/\sin\delta \end{pmatrix} \tag{16b}$$

and

$$j_B^2 = p_\delta^2 + \frac{p_\varepsilon^2}{\sin^2\delta} \tag{16c}$$

It is now instructive to examine the results given in Eqs. (14), (15) and (16). The expressions for $\vec{j}_A$, j_A^2 are the usual results for a rigid diatomic rotor since $\vec{j}_A$ is so far uncoupled to the other angular momenta, $\vec{\ell}$ and ℓ^2 contain the terms to be expected if particle B had no internal motion plus terms proportional to p_δ and p_ε. Although the expression for $\vec{j}_B$ is quite formidable, it is remarkable that j_B^2 is given by the same expression that would be obtained if the center of mass of B were held fixed. The difference here is that p_δ and p_ε contain terms relating to the orbital motion of B as well as to its rotational motion.

Now expressing the kinetic energy in terms of the angular momenta

$$T = \frac{j_A^2}{2I_A} + \frac{p_{rA}^2}{2\mu_A} + \frac{p_R^2}{2\mu_{AB}} + \frac{\ell^2}{2\mu_{AB}R^2} + \frac{j_B^2}{2I_B} + \frac{p_{rB}^2}{2\mu_B} \tag{17}$$

where $I_B = \mu_B r_B^2$. It is again worth noting that exactly the same result is obtained as one would naively predict. This is also quite comforting since the choice of keeping the center of mass of A fixed was completely arbitrary so that the final result should be reasonably symmetric with respect to the two molecules.

It is now necessary to undertake the canonical transformations to formally replace p_θ, p_ϕ, p_α, p_β, p_δ and p_ε by the appropriate angular momentum expressions so that the potential energy can be put in terms of their canonical coordinates. To this end we first introduce the angular momentum $\vec{j}_1$ which is the vector sum of $\vec{j}_B$ and $\vec{\ell}$.

$$\vec{j}_1 = \begin{pmatrix} -\sin\beta p_\alpha - \cot\alpha \cos\beta p_\beta - \cos\beta p_\varepsilon/\sin\alpha \\ \cos\beta p_\alpha - \cot\alpha \sin\beta p_\beta - \sin\beta p_\varepsilon/\sin\alpha \\ p_\beta \end{pmatrix} \tag{18a}$$

and

$$j_1^2 = p_\alpha^2 + \frac{p_\beta^2 + p_\varepsilon^2 + 2p_\beta p_\varepsilon \cos\alpha}{\sin^2\alpha} \tag{18b}$$

It may be recalled from the previous section that the square of the angular momentum of an asymmetric rotor is given by

$$j^2 = p_\theta^2 + \frac{p_\phi^2 + p_\psi^2 - 2p_\phi p_\psi \cos\theta}{\sin^2\theta} \tag{19}$$

where p_ϕ is the component of $\vec{j}$ along the space fixed z axis and p_ψ is the component on the body-fixed z axis. In Eq. (18b), p_β is the component of $\vec{j}_1$ on the space-fixed z axis while $(-p_\varepsilon)$ is the component of $[\vec{j}_B$ and hence $j_1]$ on the axis coincident with the $\vec{R}$ vector. The resemblance between Eqs. (18b) and (19) is thus quite striking. It would, therefore, seem that the rotational motion of molecule B has a similar mathematical effect on the orbital motion of B as the body-fixed component of the angular momentum has on the rotational motion of an asymmetric motor.

Let us first now eliminate p_θ in favor of $|\vec{j}_A|$. This is accomplished by the canonical transformation

$$q_1 = \theta \qquad p_1 = p_\theta \qquad P_1 = j_A \qquad Q_1 = q_{j_A}'$$

$$q_2 = \phi \qquad p_2 = p_\phi \qquad P_2 = p_\phi = m_A \qquad Q_2 = q_{m_A}$$

using the generator

$$F_2(\theta,\phi;j_A,m_A) = \phi m_A + \int^{\theta} \frac{\sqrt{j_A^2\sin^2\theta' - m_A^2}}{\sin\theta'}\, d\theta' \tag{20a}$$

$$= \phi m_A + j_A\cos^{-1}\left[\frac{j_A\cos\theta}{\sqrt{j_A^2 - m_A^2}}\right] \quad m_A\cos^{-1}\left[\frac{m_A\cos\theta}{\sin\theta\sqrt{j_A^2 - m_A^2}}\right]$$

so that

$$q'_{j_A} = \cos^{-1}\left[\frac{j_A\cos\theta}{\sqrt{j_A^2 - m_A^2}}\right]$$

$$q_{m_A} = \phi - \cos^{-1}\left[\frac{m_A\cos\theta}{\sin\theta\sqrt{j_A^2 - m_A^2}}\right] \tag{20b}$$

Now to eliminate p_δ in favor of $|\vec{j}_B|$

$$q_1 = \delta \qquad p_1 = p_\delta \qquad P_1 = j_B \qquad Q_1 = q'_{j_B}$$

$$q_2 = \varepsilon \qquad p_2 = p_\varepsilon \qquad P_2 = p_\varepsilon \qquad Q_2 = Q_2$$

$$F_2(\delta,\varepsilon;j_B,p_\varepsilon) = \varepsilon p_\varepsilon + \int^{\delta} \frac{\sqrt{j_B^2\sin^2\delta' - p_\varepsilon^2}}{\sin\delta'}\, d\delta' \tag{21a}$$

$$= \varepsilon p_\varepsilon + j_B\cos^{-1}\left[\frac{j_B\cos\delta}{\sqrt{j_B^2 - p_\varepsilon^2}}\right] - p_\varepsilon\cos^{-1}\left[\frac{p_\varepsilon\cos\delta}{\sin\delta\sqrt{j_B^2 - p_\varepsilon^2}}\right]$$

and

$$q'_{j_B} = \cos^{-1}\left[\frac{j_B\cos\delta}{\sqrt{j_B^2 - p_\varepsilon^2}}\right]$$

$$Q_2 = \varepsilon - \cos^{-1}\left[\frac{p_\varepsilon\cos\delta}{\sin\delta\sqrt{j_B^2 - p_\varepsilon^2}}\right] \tag{21b}$$

Finally, to eliminate p_α in favor of $|\vec{j}_1|$

$$q_1 = \alpha \qquad p_1 = p_\alpha \qquad P_1 = j_1 \qquad Q_1 = q'_{j_1}$$

$$q_2 = \beta \qquad p_2 = p_\beta \qquad P_2 = m_1 = p_\beta \qquad Q_2 = q_{m_1}$$

$$q_3 = Q_2 \qquad p_3 = p_\varepsilon \qquad P_3 = p_\varepsilon \qquad Q_3 = Q_\varepsilon$$

$$F_2(\alpha,\beta,Q_2;j_1,m_1,p_\varepsilon) = Q_2 p_\varepsilon + m_1\beta + \int^{\alpha} \frac{\sqrt{j_1^2\sin^2\alpha' - m_1^2 - p_\varepsilon^2 - 2m_1 p_\varepsilon\cos\alpha'}}{\sin\alpha'}\, d\alpha'$$

$$= Q_2 p_\varepsilon + m_1\beta + j_1\cos^{-1}\left[\frac{j_1^2\cos\alpha + m_1 p_\varepsilon}{\sqrt{j_1^2 - m_1^2}\,\sqrt{j_1^2 - p_\varepsilon^2}}\right] \tag{22a}$$

$$- m_1\cos^{-1}\left[\frac{m_1\cos\alpha + p_\varepsilon}{\sin\alpha\sqrt{j_1^2 - m_1^2}}\right] + p_\varepsilon\cos^{-1}\left[\frac{-p_\varepsilon\cos\alpha - m_1}{\sin\alpha\sqrt{j_1^2 - m_1^2}}\right]$$

and

$$q'_{j_1} = \cos^{-1}\left[\frac{j_1^2\cos\alpha + m_1 p_\varepsilon}{\sqrt{j_1^2 - m_1^2}\,\sqrt{j_1^2 - p_\varepsilon^2}}\right] \tag{22b}$$

$$q_{m_1} = \beta - \cos^{-1}\left[\frac{m_1\cos\alpha + p_\varepsilon}{\sin\alpha\sqrt{j_1^2 - m_1^2}}\right]$$

$$Q_\varepsilon = Q_2 + \cos^{-1}\left[\frac{-m_1 - p_\varepsilon\cos\alpha}{\sin\alpha\sqrt{j_1^2 - p_\varepsilon^2}}\right]$$

The momenta which have quantum mechanical analogues are j_A, j_B and ℓ so that it is necessary to replace p_ε by ℓ. Since $\vec{j}_1 = \vec{\ell} + \vec{j}_B$ or $\ell = \vec{j}_1 - \vec{j}_B$ and $\vec{\ell}^2 = \vec{j}_1^2 + \vec{j}_B^2 - 2\vec{j}_1 \cdot \vec{j}_B$, we get

$$\ell^2 = j_1^2 + j_B^2 - 2p_\varepsilon^2 - 2\sqrt{j_B^2 - p_\varepsilon^2}\,\sqrt{j_1^2 - p_\varepsilon^2}\,\sin Q_\varepsilon \quad . \tag{23}$$

Now the canonical transformation

$$\begin{array}{llll}
q_1 = q'_{j_1} & p_1 = j_1 & P_1 = j_1 & Q_1 = q''_{j_1} \\
q_2 = q'_{j_B} & p_2 = j_B & P_2 = j_B & Q_2 = q_{j_B} \\
q_3 = Q_\varepsilon & p_3 = p_\varepsilon & P_3 = \ell & Q_3 = q_\ell
\end{array}$$

with the generator

$$F_2(q'_{j_1}, q'_{j_B}, Q_\varepsilon; j_1, j_B, \ell) = j_1 q'_{j_1} + j_B q'_{j_B} + \int^{Q_\varepsilon} p_\varepsilon(Q'_\varepsilon)\, dQ'_\varepsilon \tag{24}$$

$$= j_1 q'_{j_1} + j_B q'_{j_B} + Q_\varepsilon p_\varepsilon - \int^{Q_\varepsilon} Q'_\varepsilon \frac{\partial p_\varepsilon(Q'_\varepsilon)}{\partial Q'_\varepsilon}\, dQ'_\varepsilon$$

$$= j_1 q'_{j_1} + j_B q'_{j_B} + Q_\varepsilon p_\varepsilon - \int^{p_\varepsilon} Q_\varepsilon(p'_\varepsilon)\, dp'_\varepsilon$$

$$= j_1' q'_{j_1} + j_B q'_{j_B} + Q_\varepsilon p_\varepsilon - \int^{p_\varepsilon} \sin^{-1}\left[\frac{j_1^2 + j_B^2 - \ell^2 - 2p_\varepsilon'^2}{2\sqrt{j_B^2 - p_\varepsilon'^2}\,\sqrt{j_1^2 - p_\varepsilon'^2}}\right] dp'_\varepsilon$$

The integral in Eq. (24) may be integrated by parts to remove the inverse sin and the expression for the generator is then obtained

$$F_2(q'_{j_1}, q'_{j_B}, Q_\varepsilon; j_1, j_B, \ell) = j_1 q'_{j_1} + j_B q'_{j_B} - j_B \sin^{-1}\left[\frac{p_\varepsilon(\ell^2 + j_B^2 - j_1^2)}{\xi\sqrt{j_B^2 - p_\varepsilon^2}}\right] \tag{25}$$

$$- j_1 \sin^{-1}\left[\frac{p_\varepsilon(\ell^2 + j_1^2 - j_B^2)}{\xi\sqrt{j_1^2 - p_\varepsilon^2}}\right] + \ell \sin^{-1}\left(\frac{2\ell p_\varepsilon}{\xi}\right)$$

where $\xi^2 = -j_1^4 - \ell^4 - j_B^4 + 2^2_{j_1} j_B^2 + 2\ell^2 j_1^2 + 2\ell^2 j_B^2$. The canonical coordinates are

$$q''_{j_1} = q'_{j_1} - \sin^{-1}\left[\frac{p_\varepsilon(\ell^2 + j_1^2 - j_B^2)}{\xi\sqrt{j_1^2 - p_\varepsilon^2}}\right] \tag{26}$$

$$q_{j_B} = q'_{j_B} - \sin^{-1}\left[\frac{p_\varepsilon(\ell^2 + j_B^2 - j_1^2)}{\xi\sqrt{j_B^2 - p_\varepsilon^2}}\right]$$

$$q_\ell = \sin^{-1}\left(\frac{2\ell p_\varepsilon}{\xi}\right)$$

The final canonical transformation introduces the total angular momentum $\vec{J} = \vec{j}_1 + \vec{j}_A$. From Eqs. (14a), (18a), (20b) and (22b) it is obtained that the cartesian components of $\vec{j}_A$ and $\vec{j}_1$ are

$$\vec{j}_A = \begin{pmatrix} -\cos q_{m_A} \sqrt{j_A^2 - m_A^2} \\ -\sin q_{m_A} \sqrt{j_A^2 - m_A^2} \\ m_A \end{pmatrix} \tag{27a}$$

$$\vec{j}_1 = \begin{pmatrix} -\cos q_{m_1} \sqrt{j_1^2 - m_1^2} \\ -\sin q_{m_1} \sqrt{j_1^2 - m_1^2} \\ m_1 \end{pmatrix} \tag{27b}$$

so that

$$J^2 = j_A^2 + j_1^2 + 2m_1 m_A + 2\sqrt{j_A^2 - m_A^2}\,\sqrt{j_1^2 - m_1^2}\,\cos(q_{m_1} - q_{m_A}) \tag{28}$$

The final canonical transformation is now

$$\begin{array}{llll} q_1 = q''_{j_1} & p_1 = j_1 & P_1 = j_1 & Q_1 = q_{j_1} \\ q_2 = q'_{j_A} & p_2 = j_A & P_2 = j_A & Q_2 = q_{j_A} \\ q_3 = q_{m_1} & p_3 = m_1 & P_3 = J & Q_3 = q_J \\ q_4 = q_{m_A} & p_4 = m_A & P_4 = M & Q_4 = q_M \end{array}$$

with the generator (M having been set equal to zero)

$$F_4(j_1,j_A,m_1,m_A;j_1,j_A,J,M) = J\cos^{-1}\left(-\frac{2m_A J}{\eta}\right) \tag{29}$$

$$+ j_1\cos^{-1}\left[\frac{m_A(J^2 + j_1^2 - j_A^2)}{\eta\sqrt{j_1^2 - m_A^2}}\right] + j_A\cos^{-1}\left[\frac{m_A(J^2 + j_A^2 - j_1^2)}{\eta\sqrt{j_A^2 - m_A^2}}\right]$$

where $\eta^2 = -J^4 - j_1^4 - j_A^4 + 2J^2 j_1^2 + 2J^2 j_A^2 + 2j_1^2 j_A^2$. As was noted in the previous section M can be set equal to zero without any loss of generality because of the overall rotational symmetry of the system. The new canonical coordinates are now given by

$$q_J = \cos^{-1}\left(-\frac{2m_A J}{\eta}\right) \tag{30}$$

$$q_{j_1} = q''_{j_1} + \cos^{-1}\left[\frac{m_A(J^2 + j_1^2 - j_A^2)}{\eta\sqrt{j_1^2 - m_A^2}}\right]$$

$$q_{j_A} = q'_{j_A} + \cos^{-1}\left[\frac{m_A(J^2 + j_A^2 - j_1^2)}{\eta\sqrt{j_A^2 - m_A^2}}\right]$$

To complete the description of the diatom-diatom system, it is now necessary to consider the potential energy. The potential energy should depend only on the six distances between the four atoms. The position vectors of the four atoms in the center of mass system are given by Eqs. (3a-d) if $\vec{R}_{cm}$ is removed. Letting r_{ij} be the distance between atom i and atom j, it is obtained that

$$r_{12} = r_A \tag{31a}$$

$$r_{34} = r_B \tag{31b}$$

$$r_{13}^2 = R^2 + r_1^2 + r_3^2 + 2Rr_3\cos\delta - 2Rr_1\cos\gamma - 2r_1 r_3\cos\zeta \tag{31c}$$

$$r_{24}^2 = R^2 + r_2^2 + r_4^2 - 2Rr_4\cos\delta + 2Rr_2\cos\gamma - 2r_2 r_4\cos\zeta \tag{31d}$$

$$r_{14}^2 = R^2 + r_1^2 + r_4^2 - 2Rr_4\cos\delta - 2Rr_1\cos\gamma + 2r_1r_4\cos\zeta \tag{31e}$$

$$r_{23}^2 = R^2 + r_2^2 + r_3^2 + 2Rr_3\cos\delta + 2Rr_2\cos\gamma + 2r_2r_3\cos\zeta \tag{31f}$$

where

$$r_1 = \frac{m_2}{M_4} r_A \tag{32}$$

$$r_2 = \frac{m_1}{M_A} r_A$$

$$r_3 = \frac{m_4}{M_B} r_B$$

$$r_4 = \frac{m_3}{M_B} r_B$$

are the distances of the atoms from the center of mass of the appropriate diatoms. The angles δ, γ, ζ in Eqs. (31c-f) are defined by the relations

$$\vec{R}\cdot\vec{r}_A = Rr_A\cos\gamma$$

$$\vec{R}\cdot\vec{r}_B = Rr_B\cos\delta \tag{33}$$

$$\vec{r}_A\cdot\vec{r}_B = r_Ar_B\cos\zeta$$

so that

$$\cos\gamma = \cos\theta\,\cos\alpha + \sin\theta\,\sin\alpha\,\cos(\phi - \beta) \tag{34}$$

$$\cos\zeta = \cos\delta\,\cos\gamma + \sin\delta\,\sin\varepsilon[\sin\theta\,\cos\alpha\,\cos(\phi - \beta) - \sin\alpha\,\cos\theta] + \sin\delta\,\cos\varepsilon\,\sin\theta\,\sin(\phi - \beta) \quad .$$

(Since δ is one of the angles of our coordinate system for $\vec{r}_B$ (Eq. (6)) it needs no further elaboration.) The expression for $\cos\zeta$ is quite cumbersome so that it may be advantageous to introduce the angle ω defined by

$$\cos\zeta = \cos\gamma \cos\delta + \sin\gamma \sin\delta \cos\omega \tag{35}$$

The six distances, and hence the potential energy, has now been parameterized in terms of the six quantities r_A, r_B, R, $\cos\delta$, $\cos\gamma$, $\cos\omega$.

The physical interpretations of the six potential parameters can now be considered. The distances r_A and r_B are the interatomic separations of the two diatoms, and R is the distance between the centers of mass of the two diatoms. The angles γ and δ are the angles between the $\vec{R}$ vector and the internuclear axes of diatoms A and B, respectively. The angle ω is the dihedral angle between the plane containing $\vec{R}$ and $\vec{r}_A$ and the plane containing $\vec{R}$ and $\vec{r}_B$.

To complete the semiclassical theory, it is necessary that all of the Hamiltonian be expressed in terms of the classical momenta which correspond to quantum numbers and their canonical coordinates. Of the six terms in the kinetic energy, Eq. (17), the terms in j_A^2, ℓ^2, j_B^2 and p_R^2 have direct quantum analogies. The terms containing $p_{r_A}^2$ and $p_{r_B}^2$ can now be replaced by the classical equivalent of the vibrational quantum number. This transformation is identical to that for a single diatom and will, therefore, not be considered here. Similarly, the potential parameters r_A and r_B will be replaced with the coordinates conjugate to the vibrational quantum numbers. The parameter R of the potential needs no further work because p_R is a continuous variable quantum mechanically.

It now remains to express the remaining potential parameters $\cos\delta$, $\cos\gamma$, and $\cos\omega$ in terms of the appropriate momenta and their canonical coordinates. The expressions obtained are

$$\cos\delta = \cos q_{j_B} \cos q_\ell + \frac{(j_1^2 - \ell^2 - j_B^2)}{2\ell j_B} \sin q_{j_B} \sin q_\ell \tag{36}$$

$$\cos\gamma = \sin q_{j_A}\left[\sin q_{j_1} \cos q_\ell + \frac{(\ell^2 + j_1^2 - j_B^2)}{2\ell j_1} \sin q_\ell \cos q_{j_1}\right] \tag{37}$$

$$+ \frac{\cos q_{j_A}}{2 j_1 j_A}\left\{\frac{\xi\eta \sin q_\ell}{2\ell_{j_1}} + (J^2 - j_1^2 - j_A^2)\right.$$

$$\left.\left[\cos q_\ell \cos q_{j_1} + \frac{(j_B^2 - j_1^2 - \ell^2)}{2\ell j_1} \sin q_\ell \sin q_{j_1}\right]\right\}$$

$$\sin\gamma \sin\delta \cos\omega = \sin q_{j_A}\left\{\frac{(j_B^2 - j_1^2 - \ell^2)}{2\ell j_1} \sin q_\ell \cos q_\ell \cos q_{j_1} \cos q_{j_B}\right. \tag{38}$$

$$+ \sin^2 q_\ell \sin q_{j_1} \cos q_{j_B} - \frac{(j_1^2 - j_B^2 - \ell^2)}{2\ell j_B} \sin q_\ell \cos q_\ell \sin q_{j_1} \sin q_{j_B}$$

$$\left. + \cos q_{j_1} \sin q_{j_B}\left[\frac{\xi^2 \sin^2 q_\ell}{4\ell^2 j_1 j_B} - \frac{(\ell^2 - j_1^2 - j_B^2)}{2 j_1 j_B} \cos^2 q_\ell\right]\right\}$$

$$- \cos q_{j_A} \left\{ \frac{(J^2 - j_1^2 - j_A^2)}{2 j_1 j_A} \left[-\sin^2 q_\ell \cos q_{j_1} \cos q_{j_B} \right. \right.$$

$$+ \frac{(j_B^2 - j_1^2 - \ell^2)}{2\ell j_1} \sin q_\ell \cos q_\ell \sin q_{j_1} \cos q_{j_B}$$

$$+ \frac{(j_1^2 - j_B^2 - \ell^2)}{2\ell j_B} \sin q_\ell \cos q_\ell \cos q_{j_1} \sin q_{j_B}$$

$$\left. + \sin q_{j_1} \sin q_{j_B} \left(\frac{\xi^2 \sin^2 q_\ell}{4\ell^2 j_1 j_B} - \frac{(\ell^2 - j_1^2 - j_B^2)}{2 j_1 j_B} \cos^2 q_\ell \right) \right]$$

$$+ \frac{\xi\eta}{4\ell j_A j_1^2} \left[\sin q_\ell \cos q_\ell \cos q_{j_B} + \frac{\sin q_{j_B}}{2\ell j_B} \right.$$

$$\left. \left. \left((\ell^2 + j_1^2 - j_B^2) + (\ell^2 + j_B^2 - j_1^2) \cos^2 q_\ell \right) \right] \right\} .$$

It is quite probable that this last expression is in error or can be simplified considerably. Even if that is not true, it may be possible to find a new potential parameter to replace $\cos\omega$ whose expression is not so formidable.

The question may now be raised of what changes must be made to allow molecules A and B to be polyatomic. As has been seen the vibrational degrees of freedom are not coupled between the two molecules so that they may be treated in the same fashion as for a single isolated molecule. It may be seen from Eqs. (10), (14), (17) and (20)

that the kinetic energy terms for the rotation of molecule A are the same as for an isolated molecule. Thus it is straightforward to permit molecule A to be an asymmetric rotor since this can be handled in the same way as an isolated rotor. Of course, it this case more potential parameters will have to be added and the expressions for $\cos\gamma$ and $\cos\omega$ will be altered by the additional rotational degree of freedom. The generalization of the molecule B would seem to be considerably more complicated. But because the choice of keeping the center of mass of A fixed was completely arbitrary, it is expected that a great deal of symmetry in A and B should appear in the final expressions, as was indeed the case for the diatom-diatom system. Thus it is reasonable to envision the possibility of applying classical S-matrix theory to generalized binary collisions.

V. THE USE OF ACTION ANGLE VARIABLES FOR COLLISION DYNAMICS

The application of classical S-matrix theory requires that in the asymptotic regions the classical Hamiltonian be expressed in terms of quantities which are analagous to the quantum numbers of quantum mechanics. These classical quantities are the classical momenta ("action variables") which are conserved in the asymptotic regions. The canonical coordinates to the action variables ("angle variables") are then changing linearly with time.

For the purpose of applying classical S-matrix theory, it is immaterial in what set of classical variables the classical trajectories are computed as long as the proper transformations to the action-angle variables are made at the endpoints of the trajectory. It would seem that the action-angle variables may be a quite advantageous set in which to compute the trajectories since through much of the trajectory the action variables are conserved or nearly conserved. No definitive study has been made of the relative labor of computing classical trajectories in action-angle variables as opposed to cartesian coordinates, but indications are that the trajectories require two to five times the computer time for a typical system when run in cartesian coordinates.

There are, however, two important problems to be considered with the computation of classical trajectories in action-angle variables. One problem is that the time derivatives of the angle variables appear to have singularities in some cases; no singularities are possible in cartesian coordinates. Another problem arises with the computation of the complex valued trajectories that are necessary for the description of classically forbidden processes. The trajectories are independent of

the contour in the complex t plane as long as the endpoints are fixed, but along certain contours the computation of the trajectories may be numerically unstable. The angle variables are given by trigonometric functions of the momenta; so that when the momenta become complex, the angle variables may become exponentially increasing along certain time paths.

Therefore, two questions must be answered before action-angle variables can be stated to be categorically superior over cartesian coordinates for the computation of classical trajectories. Are there any singularities in the action-angle variable expressions; and, if there are, can they be handled in a physically meaningful manner? How may the complex-time path for a complex-valued trajectory be chosen so that the integration is stable in action-angle variables?

To shed some light on these questions let us consider a model problem. Assume a diatom-atom system where the diatom is a harmonic oscillator whose vibration is uncoupled to its rotation. The classical Hamiltonian may be written as

$$H = \frac{p_R^2}{2\mu} + \frac{p_\alpha^2}{2\mu R^2} + \frac{p_\beta^2}{2\mu R^2 \sin^2\alpha} + \frac{p_\theta^2}{2I} + \frac{p_\phi^2}{2I\sin^2\theta} + \frac{p_r^2}{2\mu_D} + \frac{\mu_D\omega^2}{2}(r - r_o)^2 \qquad (1)$$

$$+ V(R,r,\cos\gamma)$$

where θ,ϕ are the orientation angles for the diatom; R,α,β are the spherical polar coordinates of the atom; r is the internal coordinate; μ is the reduced mass of the system and μ_D is the reduced mass of the diatom; ω is the classical vibrational frequency; r_o is the equilibrium separation of the diatom and I is its moment of inertia = $\mu_D r_o^2$; and finally

$\cos\gamma$ is given by

$$\cos\gamma = \cos\theta \cos\alpha + \sin\theta \sin\alpha \cos(\phi - \beta) \quad . \tag{2}$$

Now introduce the action variables j, the rotational angular momentum of the diatom, and ℓ, the orbital angular momentum. These are given in terms of the old variables by

$$j^2 = p_\theta^2 + \frac{p_\phi^2}{\sin^2\theta} \tag{3a}$$

$$\ell^2 = p_\alpha^2 + \frac{p_\beta^2}{\sin^2\alpha} \tag{3b}$$

so that the relevant canonical transformation is

$$\begin{array}{llll}
q_1 = \theta & p_1 = p_\theta & P_1 = j & Q_1 = q_j' \\
q_2 = \phi & p_2 = p_\phi & P_2 = p_\phi = m_j & Q_2 = q_{m_j} \\
q_3 = \alpha & p_3 = p_\alpha & P_3 = \ell & Q_3 = q_\ell' \\
q_4 = \beta & p_4 = p_\beta & P_4 = p_\beta = m_\ell & Q_4 = q_{m_\ell}
\end{array}$$

with the generator

$$F_2(\theta,\phi,\alpha,\beta;j,m_j,\ell,\ m_\ell) = \phi m_j + \beta m_\ell + j\cos^{-1}\left[\frac{j\cos\theta}{\sqrt{j^2 - m_j^2}}\right] \tag{4}$$

$$- m_j\cos^{-1}\left[\frac{m_j\cos\theta}{\sin\theta\sqrt{j^2 - m_j^2}}\right] + \ell\cos^{-1}\left[\frac{\ell\cos\alpha}{\sqrt{\ell^2 - m_\ell^2}}\right]$$

$$- m_\ell\cos^{-1}\left[\frac{m_\ell\cos\alpha}{\sin\alpha\sqrt{\ell^2 - m_\ell^2}}\right]$$

The canonical coordinates are thus given by

$$q_j' = \cos^{-1}\left[\frac{j\cos\theta}{\sqrt{j^2 - m_j^2}}\right] \tag{5a}$$

$$q_{m_j} = \phi - \cos^{-1}\left[\frac{m_j\cos\theta}{\sin\theta\sqrt{j^2 - m_j^2}}\right] \tag{5b}$$

$$q_\ell' = \cos^{-1}\left[\frac{\ell\cos\alpha}{\sqrt{\ell^2 - m_\ell^2}}\right] \tag{5c}$$

$$q_{m_\ell} = \beta - \cos^{-1}\left[\frac{m_\ell\cos\alpha}{\sin\alpha\sqrt{\ell^2 - m_\ell^2}}\right] \tag{5d}$$

where m_j is the component of $\vec{j}$ along the space fixed z axis and m_ℓ is the component of $\vec{\ell}$ on the same axis.

The projection of the total angular momentum on the space-fixed z axis, $M = m_\ell + m_j$, can be set equal to zero because of the overall rotational symmetry of the system. The total angular momentum J is thus given by the expression

$$J^2 = j^2 + \ell^2 - 2m^2 + 2\sqrt{j^2 - m^2}\sqrt{\ell^2 - m^2}\cos(q_{m_j} - q_{m_\ell}) \tag{6}$$

where $m = m_j = -m_\ell$, and is introduced by the canonical transformation

$q_1 = q_j'$	$p_1 = j$	$P_1 = j$	$Q_1 = q_j$
$q_2 = q_\ell'$	$p_2 = \ell$	$P_2 = \ell$	$Q_2 = q_\ell$
$q_3 = q_{m_j}$	$p_3 = m_j$	$P_3 = J$	$Q_3 = q_J$
$q_4 = q_{m_\ell}$	$p_4 = m_\ell$	$P_4 = M$	$Q_4 = q_M$

with the generator

$$F_4(j,\ell,m;j,\ell,J) = J\cos^{-1}\left(-\frac{2mJ}{\xi}\right) + \ell\cos^{-1}\left[\frac{m(J^2+\ell^2-j^2)}{\xi\sqrt{\ell^2-m^2}}\right] \tag{7}$$

$$+ j\cos^{-1}\left[\frac{m(J^2+j^2-\ell^2)}{\xi\sqrt{j^2-m^2}}\right]$$

where $\xi^2 = -J^2 - j^4 - \ell^4 + 2\ell^2j^2 + 2J^2j^2 + 2J^2\ell^2$. The new coordinates of interest, q_ℓ and q_j, are given by

$$q_\ell = q'_\ell + \cos^{-1}\left[\frac{m(J^2+\ell^2-j^2)}{\xi\sqrt{\ell^2-m^2}}\right] \tag{8a}$$

$$q_j = q'_j + \cos^{-1}\left[\frac{m(J^2+j^2-\ell^2)}{\xi\sqrt{j^2-m^2}}\right] \tag{8b}$$

The action variable n which is proportional to the vibrational energy is now introduced by the canonical transformation

$$q_1 = r \qquad p_1 = p_r \qquad P_1 = n \qquad Q_1 = q_n$$

with the generator

$$F_2(r,n) = \int^{r-r_o} dx\sqrt{2\mu_D\omega(n+1/2) - \mu_D\omega^2x^2} \tag{9}$$

$$= (n+1/2)\sin^{-1}\left[(r-r_o)\sqrt{\frac{\omega\mu_D}{(2n+1)}}\right]$$

$$+ \frac{r}{2}\sqrt{2\mu_D(n+1/2)\omega - \mu_D^2\omega^2(r-r_o^2)}$$

so that the angle variable is

$$q_n = \sin^{-1}\left[(r - r_o)\sqrt{\frac{\omega\mu_D}{(2n+1)}}\right] \quad . \tag{10}$$

The potential parameters may now be expressed in terms of the action angle variables,

$$\cos\gamma = \cos q_\ell \cos q_j + \frac{(J^2 - j^2 - \ell^2)}{2\ell j} \sin q_\ell \sin q_j \tag{11a}$$

$$r = r_o + \sqrt{\frac{2n+1}{\omega\mu_D}} \sin q_n \tag{11b}$$

It may be noted that the harmonic oscillator portion of the potential, i.e.,

$$\frac{\mu_o^2\omega^2}{2}(r - r_o)^2$$

has been incorporated into n so that the Hamiltonian is now given by

$$H = \frac{P_R^2}{2\mu} + \frac{\ell^2}{2\mu R^2} + \frac{j^2}{2I} + (n + 1/2)\,\omega + V(R,n,q_n,\cos\gamma) \tag{12}$$

The second of the questions propounded above, concerning the stability of complex-valued trajectories, will be considered first. Let the complex time be expressed in polar form, i.e., $z = te^{i\tau}$ where z is the complex time. In the numerical computation of classical trajectories, t must be changed in small steps governed by the criterion that the truncation error of the integration be acceptably low. However, it would seem that the changes in τ from one step to the next are completely arbitrary since the endpoints of the trajectory should

be independent of the path in the complex t plane. Some paths in the complex t plane though can be numerically unstable or require excessively long contours.

If q_n is complex, Eq. (11b) becomes

$$r = r_o + \sqrt{\frac{2n+1}{\omega\mu_D}}\ \frac{1}{2i}\ \{\exp[iRe(q_n)]\ \exp[-Im(q_n)] - \exp[-iRe(q_n)]\ \exp[+Im(q_n)]\}\ . \tag{13}$$

Now, if τ is such that $Im(q_n)$ is increasing along the contour, the real part of r will be exponentially increasing. This may move r outside of the range of validity of the potential surface or indeed force it to go to infinity during the trajectory. Therefore, in order to compute complex-valued classical trajectories in action-angle variables, it is necessary that it be known how τ should be changed to keep the trajectory under control.

Let D be an arbitrary dynamical variable with real part u and imaginary part v. In polar form the operator for the derivative with respect to time is given by

$$\frac{d}{dz} = \frac{e^{i\tau}}{2}\left(\frac{\partial}{\partial t} - \frac{i}{t}\ \frac{\partial}{\partial \tau}\right) \tag{14}$$

Since the dynamical variables are analytic functions of the time, the Cauchy-Riemann equations are applicable, i.e.,

$$\frac{\partial u}{\partial t} = \frac{1}{t}\ \frac{\partial v}{\partial \tau} \tag{15a}$$

$$\frac{\partial v}{\partial t} = -\frac{1}{t}\ \frac{\partial u}{\partial \tau} \tag{15b}$$

The quantity $\dot{D} = \frac{dD}{dz}$ is obtainable from the equations of motion. Now

$$\dot{D} = \frac{d}{dz}(u + iv) = \frac{e^{i\tau}}{2}\left(\frac{\partial}{\partial t} - \frac{i}{t}\frac{\partial}{\partial \tau}\right)(u + iv) \tag{16}$$

$$= \frac{e^{i\tau}}{2}\left(\frac{\partial u}{\partial t} + \frac{1}{t}\frac{\partial v}{\partial t} - \frac{i}{t}\frac{\partial u}{\partial} + \frac{i\partial v}{\partial t}\right)$$

If the Couchy-Riemann conditions, Eqs. (15a,b) are substituted in Eq. (16), the expression for $\dot{D}$ becomes

$$\dot{D} = \frac{e^{i\tau}}{t}\frac{\partial}{\partial \tau}(v - iu) \quad . \tag{17}$$

Separating the real and imaginary parts

$$\dot{D} = \left(\frac{\cos\tau}{t}\frac{\partial v}{\partial \tau} + \frac{\sin\tau}{t}\frac{\partial u}{\partial \tau}\right) + i\left(\frac{\sin\tau}{t}\frac{\partial v}{\partial \tau} - \frac{\cos\tau}{t}\frac{\partial u}{\partial \tau}\right) \tag{18}$$

The numerical values of the real and complex part of $\dot{D}$ are known at each step of the numerical integration from the equations of motion. From Eq. (18), therefore,

$$\mathrm{Re}(\dot{D}) = \frac{\cos\tau}{t}\frac{\partial v}{\partial \tau} + \frac{\sin\tau}{t}\frac{\partial u}{\partial \tau} \tag{19a}$$

$$\mathrm{Im}(\dot{D}) = \frac{\sin\tau}{t}\frac{\partial v}{\partial \tau} - \frac{\cos\tau}{t}\frac{\partial u}{\partial \tau} \tag{19b}$$

so that $\frac{\partial v}{\partial \tau}$ and $\frac{\partial u}{\partial \tau}$ may be solved for to give

$$\frac{\partial v}{\partial \tau} = t[\sin\tau\ \mathrm{Im}(\dot{D}) + \cos\tau\ \mathrm{Re}(\dot{D})] \tag{20a}$$

$$\frac{\partial u}{\partial \tau} = t[\sin\tau\ \mathrm{Re}(\dot{D}) - \cos\tau\ \mathrm{Im}(\dot{D})] \tag{20b}$$

Equations (20a,b) can now be used to determine the sign of the rates of change of u and v with respect to τ. Thus for each new time step, the change in τ can be chosen to produce the desired results. A particular example is that the change in τ may be chosen so that the absolute value of the imaginary part of q_n is decreasing along the trajectory. This will then prevent the exponential runaway of r as was previously mentioned. The only restriction here is that τ can not be allowed to go outside the range $+\pi/2, 0, -\pi/2$ since such a situation corresponds to going backward in time.

A review of the generators and other expressions for the model problem provides examples for the first question. The expressions in Eqs. (4) and (5a-d) apparently become pathalogical when the projection of one of the angular momenta is equal to its magnitude (i.e., $j = m_j$ or $\ell = m_\ell$). In Eq. (11a) the term $(J^2 - j^2 - \ell^2)/2\ell j$ may be troublesome when ℓ or j is equal to zero. From Eqs. (11a) and (12), the time derivative of q_j is given by

$$\dot{q}_j = + \frac{\partial H}{\partial j} = + \frac{j}{I}\left[\frac{\partial V}{\partial \cos\gamma}\right] \frac{(J^2 + j^2 - \ell^2)}{2\ell j^2} \sin q_\ell \sin q_j \quad ; \qquad (21)$$

a similar expression being obtained for $\dot{q}_\ell$. Now when j or ℓ goes to zero, the second term in Eq. (21) is apparently singular.

In a semiclassical approach, quantum mechanical constraints are put on the action variables at the endpoints of the classical trajectories. At the beginning of the trajectory then

$$\ell^2 = \hbar^2(\ell + 1/2)^2$$
$$j^2 = \hbar^2(j + 1/2)^2$$

where the ℓ, j on the righthand side are the integer quantum numbers. It is also true that the quantum mechanical requirements make the quantity $(j^2 - m_j^2)$ greater than zero at the start. It is now to be investigated whether, given these initial conditions, the troublesome situations can arise during the trajectory.

In the limit that j or ℓ goes to zero, both the numerator and denominator of the factor $(J^2 - j^2 - \ell^2)/2\ell j$ in Eq. (11a) also go to zero. Define λ_1 to be the ratio m/j and λ_2 to be m/ℓ. Equation (4) can now be written

$$F_2(\theta,\phi,\alpha,\beta;\ j,m_j,\ell,m_\ell) = \phi m - \beta m + j\cos^{-1}\left[\frac{\cos\theta}{\sqrt{1 - \lambda_1^2}}\right] \tag{4'}$$

$$- m\cos^{-1}\left[\frac{\lambda_1\cos\theta}{\sin\theta\sqrt{1 - \lambda_1^2}}\right] + \ell\cos^{-1}\left[\frac{\cos\alpha}{\sqrt{1 - \lambda_2^2}}\right] + m\cos^{-1}\left[\frac{-\lambda_2\cos\alpha}{\sin\alpha\sqrt{1 - \lambda_2^2}}\right]$$

so that

$$q_j' = \cos^{-1}\left[\frac{\cos\theta}{\sqrt{1 - \lambda_1^2}}\right] \tag{5a'}$$

$$q_\ell' = \cos^{-1}\left[\frac{\cos\alpha}{\sqrt{1 - \lambda_2^2}}\right] \tag{5b'}$$

$$q_m = \phi - \beta - \cos^{-1}\left[\frac{\lambda_1\cos\theta}{\sin\theta\sqrt{1 - \lambda_1^2}}\right] + \cos^{-1}\left[\frac{-\lambda_2\cos\alpha}{\sin\alpha\sqrt{1 - \lambda_2^2}}\right] \tag{5c'}$$

Now from Eq. (6)

$$J^2 = j^2 - m^2 + \ell^2 - m^2 + 2\sqrt{j^2 - m^2}\,\sqrt{\ell^2 - m^2}\,\cos q_m \tag{22}$$

$$= j^2(1 - \lambda_1^2) + \ell^2(1 - \lambda_2^2) + 2j\ell\sqrt{1 - \lambda_1^2}\,\sqrt{1 - \lambda_2^2}\,\cos q_m$$

and

$$\frac{(J^2 - j^2 - \ell^2)}{2\ell j} = -\lambda_1\lambda_2 + \sqrt{1 - \lambda_1}\,\sqrt{1 - \lambda_2}\,\cos q_m \tag{23}$$

The behavior of $\lambda_{1,2}$ as j or ℓ goes to zero must now be considered in order to elucidate the limiting value of Eq. (23). Quantum mechanically the ratio λ_1 is

$$\lambda_1^2 = \frac{m^2}{j(j+1)} \leqslant \frac{j^2}{j(j+1)}$$

so that if j is allowed to go to zero as a continuous variable, the limit will be zero. Since m and j both go to zero in the limit j goes to zero, L'Hospital's rule gives that the limit of m/j is the same as the limit of $\dot{m}/\dot{j}$. To evaluate this limit classically, $\cos\gamma$ can be expressed in the set of variables j, ℓ, m, q_j', q', q_m as

$$\cos\gamma = \sqrt{j^2 - m^2}\,\sqrt{\ell^2 - m^2}\left\{\frac{\cos q_j'\,\cos q_\ell'}{\ell j} + \cos q_m\left[\sin q_\ell'\,\sin q_j' - \frac{m^2}{\ell j}\cos q_\ell'\,\cos q_j'\right] + \sin q_m\left[\frac{m}{\ell}\sin q_j'\,\cos q_\ell' + \frac{m}{j}\cos q_j'\,\sin q_\ell'\right]\right\} \tag{24}$$

Since $\dot{m} = -\frac{\partial H}{\partial q_m}$ and $\dot{j} = -\frac{\partial H}{\partial q_j'}$, the ratio $\dot{m}/\dot{j}$ is given by the expression

$$\begin{aligned}\dot{m}/\dot{j} = \{&m\cos q_m[j\sin q_j' \cos q_\ell' + \ell\cos q_j' \sin q_\ell'] \\ &- \sin q_m[\ell j\sin q_j' \sin q_\ell' - m^2\cos q_\ell' \cos q_j'\} \\ \{&-\sin q_j' \cos q_\ell' + \cos q_m[m^2\sin q_j' \cos q_j' + \ell j\cos q_j' \sin q_\ell'] \\ &+ m\sin q_m[j\cos q_j' \cos q_\ell' - \ell\sin q_j' \sin q_\ell']\}^{-1}\end{aligned} \tag{25}$$

Although the behavior of Eq. (25) may not be obvious for certain special cases, the limit of the expression for j and m going to zero is zero. Since the equations are symmetric in j and ℓ, it must also be true that λ_2 goes to zero as ℓ goes to zero.

Inspection of Eq. (4') now reveals that the generator has no singularities as j or ℓ go to zero. The conjugate coordinates in this limit become

$$\begin{aligned} q_j'(j = 0) &= \theta \\ q_\ell'(\ell = 0) &= \alpha \\ q_m(j \text{ or } \ell = 0) &= \phi - \beta \end{aligned} \tag{26}$$

Thus the limit of Eq. (23) is

$$\lim_{\substack{j\to 0\\ \ell\to 0}} \frac{(J^2 - j^2 - \ell^2)}{2\ell_j} = \cos(\phi - \beta) \tag{27}$$

The expression for $\cos\gamma$ in Eq. (24) may also be used to shed light on whether the situation j = m is classically accessible. The formulas for the time derivatives of j and m are

$$\dot{j} = -\frac{\partial V}{\partial \cos\gamma}\sqrt{j^2 - m^2}\sqrt{\ell^2 - m^2}\left\{-\frac{\sin q_j' \cos q_\ell'}{\ell j}\right. \tag{28a}$$

$$+ \cos q_m\left[\frac{m^2}{\ell j}\sin q_j' \cos q_\ell' + \cos q_j' \sin q_\ell'\right]$$

$$\left. + m\sin q_m\left[\frac{\cos q_j' \cos q_\ell'}{\ell} - \frac{\sin q_j' \sin q_\ell'}{j}\right]\right\}$$

$$\dot{m} = -\frac{\partial V}{\partial \cos\gamma}\sqrt{j^2 - m^2}\sqrt{\ell^2 - m^2}\left\{\cos q_m\left[\frac{m}{\ell}\sin q_j' \cos q_\ell' + \frac{m}{j}\cos q_j' \sin q_\ell'\right]\right. \tag{28b}$$

$$\left. - \sin q_m\left[-\frac{m^2}{\ell j}\cos q_\ell' \cos q_j' + \sin q_j' \sin q_\ell'\right]\right\}$$

As m approaches j, both $\dot{j}$ and $\dot{m}$ go to zero. However, this is not sufficient in itself to insure that an infinite amount of time will be required for the limit j = m to be reached. No easy argument can, therefore, be found at present to prove that j = m is classically inaccessible.

The most serious difficulty with the representation of the dynamics in terms of the action-angle variables is the apparent singularity of the time derivatives of the angle variables. Thus Eq. (21)

$$\dot{q}_j = \frac{j}{I} - \frac{\partial V}{\partial \cos\gamma}\,\frac{(J^2 + j^2 - \ell^2)}{2\ell j^2}\sin q_\ell \sin q_j$$

would appear to be suspect when j or ℓ is equal to zero. Near j = 0, it may be possible to show that the limit is finite since both the numerator and denominator vanish. However, when ℓ = 0 in the expression for $\dot{q}_j$, only the denominator vanishes and it would seem then that $\dot{q}_j$ is hopelessly singular.

Examination of Eq. (28a) reveals that $\frac{dj}{dt}$ vanishes in the limit that j goes to zero. It may be possible to show that the situation, j or ℓ going to zero, is classically inaccessible given the starting conditions j, ℓ unequal to zero. If not, it may still be possible to find a limiting procedure to proceed safely through the trouble region. No definitive answer is presently available.

VI. CLASSICAL TRAJECTORY STUDY OF ROTATIONAL EXCITATION IN LOW ENERGY He-CO COLLISIONS

Green and Thaddeus[51] have recently carried out accurate quantum mechanical coupled channel calculations for rotational excitation of CO by He. Classical mechanical trajectory calculations were carried out for the purpose of comparing dynamically exact classical mechanics with dynamically exact quantum mechanics.[52]

The He-CO system was treated as a rigid rotor-atom system, the potential being the same as that used for the quantum calculation.[51] The classical calculations were carried out in a way which is equivalent to the now-standard quasi-classical trajectory procedure.[53]

The rotational qunatum number j is defined by

$$E_{rot} = B(j + 1/2)^2 \tag{1}$$

where E_{rot} is the classical rotational energy of the rotor and B the rotational constant ($B_{CO} = 1.9226\ cm^{-1}$). Trajectories were all begun with j = 0, and after collision the final rotational quantum number was determined by first solving for the final non-integral value of j from Eq. (1) and then assigning the closest integer. The cross section for the 0 → j transition is then given by

$$\sigma_{j\leftarrow 0} = \pi b^2_{max}(N_j/N_{tot}) \tag{2}$$

where b_{max} is the maximum impact parameter which defines the usual impact parameter sampling[53] (i.e., $b = b_{max}\sqrt{\xi}$, where ξ is a random number), N_{tot} is the total number of trajectories run, and N_j is the number of these for which the final rotational quantum number is j. For this work,

b_{max} was chosen to be 6.5 a_o and N_{tot} was about 1000 (the number varied because some trajectories were discarded).

The classical trajectories were computed in the action-angle variables relevant to the atom-rigid rotor collision system.[54] In this representation it is necessary to specify the values of the initial orbital angular momentum and the total angular momentum. The orbital angular momentum is given in the usual manner by

$$\ell = (\sqrt{2\mu E_1})\ b + 1/2 \tag{3}$$

where b is determined in a random way as described above. The square of the total angular momentum was determined by

$$J^2 = \ell_1^2 + j_1^2 + 2\ell_1 j_1 (2\xi_2 - 1) \tag{4}$$

where ℓ_1, j_1 are the initial orbital and rotational angular momenta and ξ_2 is a random number between zero and one. The other two Monte-Carlo variables, q_j and q_ℓ, were selected randomly in the interval $[0,2\pi]$.

The equations of motion in the action-angle variables are

$$\dot{R} = p_R/\mu \tag{5a}$$

$$\dot{q}_j = 2Bj + \frac{\partial V}{\partial \cos\gamma}\ \frac{\partial \cos\gamma}{\partial j} \tag{5b}$$

$$\dot{q}_\ell = \ell/(\mu R^2) + \frac{\partial V}{\partial \cos\gamma}\ \frac{\partial \cos\gamma}{\partial \ell} \tag{5c}$$

$$\dot{p}_R = \ell^2/(\mu R^3) - \frac{\partial V}{\partial R} \tag{5d}$$

$$\dot{j} = -\frac{\partial V}{\partial \cos\gamma}\ \frac{\partial \cos\gamma}{\partial q_j} \tag{5e}$$

$$\dot{\ell} = -\frac{\partial V}{\partial \cos\gamma}\ \frac{\partial \cos\gamma}{\partial q_\ell} \tag{5f}$$

where μ is the reduced mass, V the potential energy and R, p_R the translational coordinate and its conjugate momentum, respectively. The potential parameter $\cos\gamma$ and its partial derivatives are given by

$$\cos\gamma = \cos q_j \cos q_\ell + \frac{(J^2 - j^2 - \ell^2)}{2\ell j} \sin q_j \sin q_\ell \tag{6}$$

$$\frac{\partial\cos\gamma}{\partial j} = - \frac{(J^2 + j^2 - \ell^2)}{2\ell j^2} \sin q_j \sin q_\ell \tag{7a}$$

$$\frac{\partial\cos\gamma}{\partial \ell} = - \frac{(J^2 + \ell^2 - j^2)}{2\ell j^2} \sin q_j \sin q_\ell \tag{7b}$$

$$\frac{\partial\cos\gamma}{\partial q_j} = - \sin q_j \cos q_\ell + \frac{(J^2 - j^2 - \ell^2)}{2\ell j} \cos q_j \sin q_\ell \tag{7c}$$

$$\frac{\partial\cos\gamma}{\partial q_\ell} = - \cos q_j \sin q_\ell + \frac{(J^2 - j^2 - \ell^2)}{2\ell j} \sin q_j \cos q_\ell \tag{7d}$$

The trajectories were started with the initial conditions

$$\begin{aligned} R &= R_{max} \\ q_j &= q_{j_1} \\ q_\ell &= q_{\ell_1} \\ p_R &= -\sqrt{(2\mu E_1 - \ell_1^2/R_{max}^2)} \\ j &= \hbar(j_1 + 1/2) \\ \ell &= \hbar(\ell_1 + 1/2) \end{aligned} \tag{8}$$

where R_{max} is a value of R where $\frac{\partial V}{\partial \cos\gamma}$ is negligible (R_{max} = 20.0 a_o for this case), and were terminated when $R = R_2$ was greater than or equal to R_{max} and p_R was positive. The trajectories were rejected unless the quantity

$$j_2 - \left\{ j_1^2 + \left[2\mu E_1 - p_{R_2}^2 - \ell_2^2/R_2^2 \right] / (2\mu B) \right\}^{1/2} \tag{9}$$

was less than 0.04. (Note that if energy is exactly conserved, this quantity will be zero.)

In the initial stages of the project, the trajectories were computed in cartesian coordinates. This provided to be unsatisfactory because the nature of the potential surface. The attractive well present in the potential gave considerable complex formation at these low energies (10 cm^{-1} to 150 cm^{-1}). When this occurred, as was verified by detailed examination of selected individual trajectories, enough time steps were required to make the numerical integration inaccurate.

When the trajectories were computed in action-angle variables, the trajectories required about half the computer time on the average as the trajectories in cartesian coordinates. Even so, complex formation remained a considerable problem, necessitating the discarding of numerically inaccurate trajectories. This problem was quite energy dependent; about 5% of the trajectories at an energy of 150 cm^{-1} were too much in error to be used while this figure was close to 20% at 10 cm^{-1}. The computer time required per trajectory was also strongly influenced by the translational energy. On the CDC 7600 used, a typical trajectory required 1.0 and 0.4 secs at an energy of 10 and 150 cm^{-1}, respectively.

The results of the calculation are represented in Fig. 16 as a function of initial translational energy, along with the quantum mechanical results of Green and Thaddeus.[51] The overall agreement is quite reasonable, probably typical of what one should expect of a quasi-classical trajectory calculation.

A more interesting comparison is shown in Fig. 17; here the cross section for the $0 \rightarrow j$ excitation is plotted as a function of j for a fixed initial translational energy of 100 cm^{-1}. (The comparison is similar for other values of E.) The quantum mechanical results[51] show an oscillatory structure which the classical values do not reproduce; this is the reason that the classical cross sections of the $0 \rightarrow 2$ and $0 \rightarrow 3$ transitions in Fig. 16 are consistently too small and too large, respectively. Miller[52] describes the oscillations in the quantum results in Fig. 17 as a remnant of the $\Delta j = 2$ selection rule and discusses the implications.

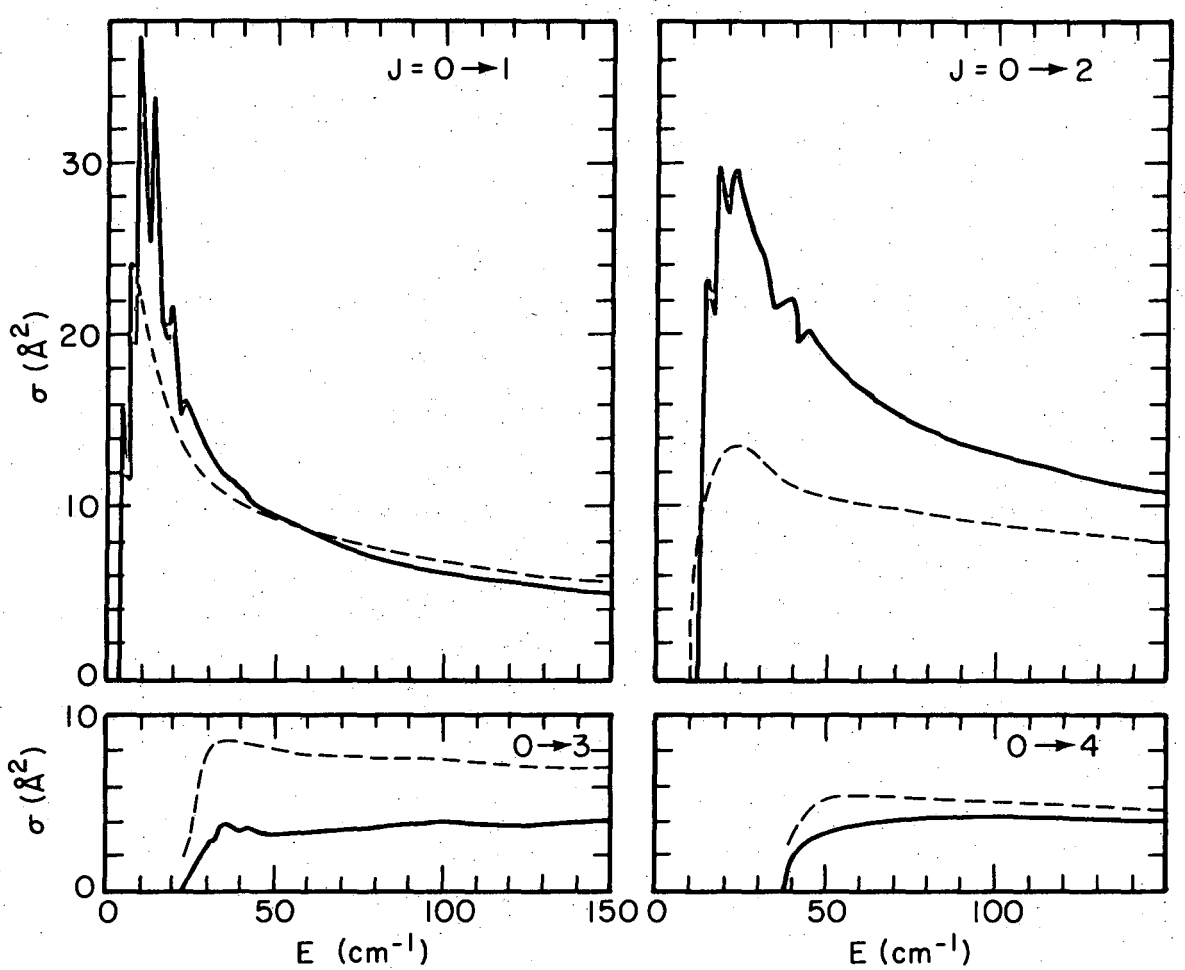

Fig. 16. The cross section for the 0→j, j=1-4, rotational excitation of CO by He, as a function of the initial translational energy. The solid curve is the accurate quantum mechanical result of Green and Thaddeus,[51] and the dashed curve the results of the classical trajectory calculation.

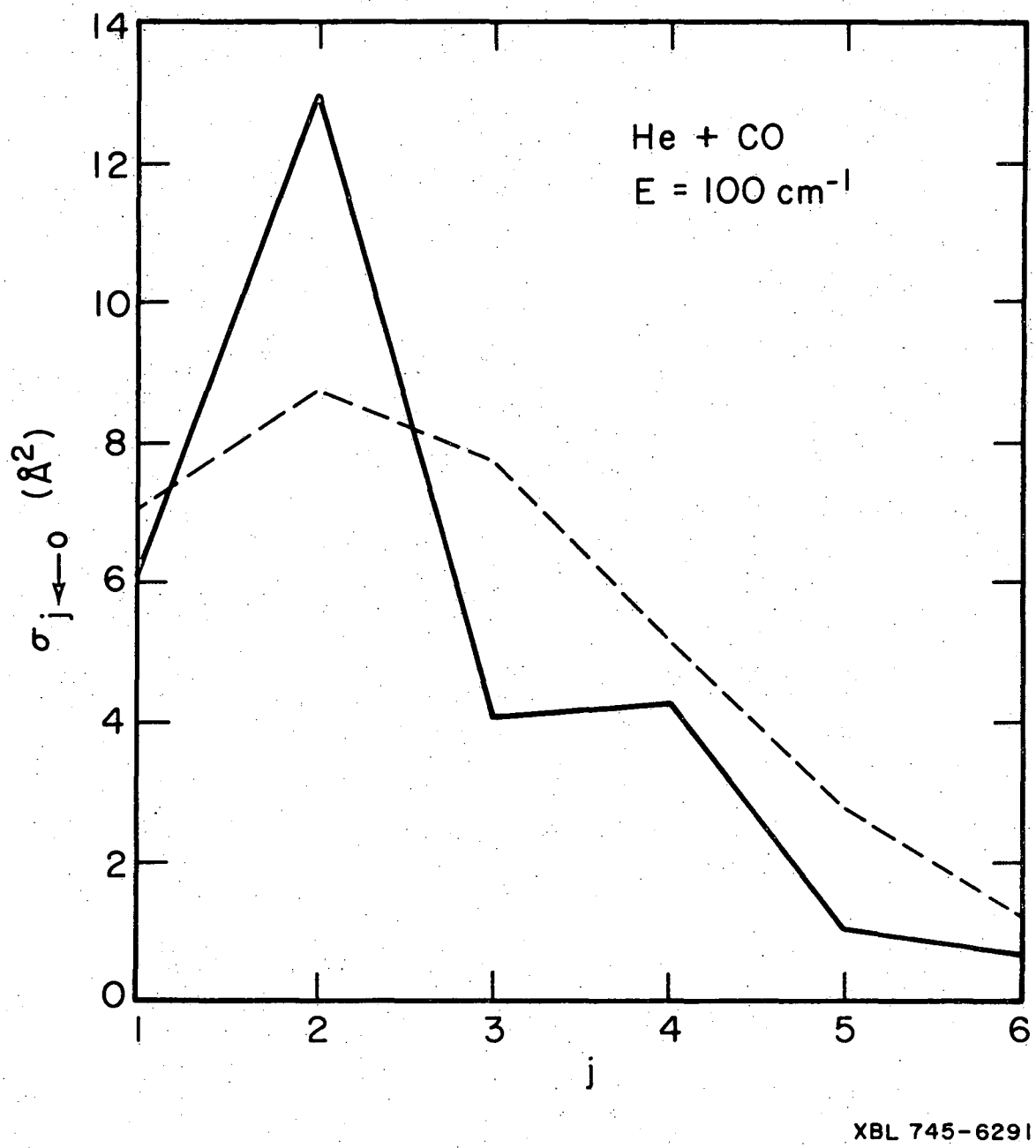

Fig. 17. The same quantity as in Fig. 16 (solid line = quantum, dashed line = classical) but shown as a function of final rotational quantum number; for a given initial translational energy E = 100 cm^{-1}.

VII. ADDITIONAL TOPICS

A. Alternate Calculation of Jacobians

In order to apply classical S-matrix methods to compute the cross section for a transition, it is necessary to calculate the classical action along the trajectories connecting the initial and final quantum states. It is also necessary to compute the Jacobian of the final quantum numbers with respect to their initial conjugate coordinates. One way to calculate the derivatives needed for the Jacobian is to compute classical trajectories close to the desired one and then compute the derivatives by standard means of numerical analysis.

There is another means of claculating the derivatives which uses the properties of classical mechanics. Consider a one-dimensional system with a Hamiltonian

$$H = \frac{p^2}{2m} + V(q) \quad . \tag{1}$$

The classical trajectory is now determined by the initial values p_1, q_1 and the equation of motion

$$m\ddot{q}(t) = - \left.\frac{\partial V}{\partial q}\right|_{q(t)} = F[q(t)] \tag{2}$$

If a small perturbation is applied to the initial momentum, $p_1 \to p_1 + dp_1$, the new trajectory $q'(t)$ may be written as

$$q'(t) = q(t) + \lambda(t) \tag{3}$$

where $\lambda(t)$ is presumably small. The equation of motion is now

$$m(\ddot{\lambda} + \ddot{q}) = F(q + \lambda) \quad . \tag{4}$$

If the force is expanded in a power series in λ and only the first order term retained

$$m\ddot{\lambda} \cong F(q) + \lambda \left.\frac{\partial F}{\partial q}\right|_{q(t)} - m\ddot{q} \tag{5}$$

$$= \lambda \left.\frac{\partial F}{\partial q}\right|_{q(t)}$$

$$= -\lambda \frac{\partial^2 V}{\partial q^2}[q(t)]$$

The derivative $\frac{\partial q_2}{\partial p_1}$ is defined as

$$\frac{\partial q_2}{\partial p_1} = \lim_{dp_1 \to 0} \frac{q(t_2, p_1 + dp_1) - q(t_2, p_1)}{dp_1} \tag{6}$$

where q_2 is the value of the coordinate at the end of the trajectory ($t = t_2$). But

$$q(t_2, p_1 + dp_1) = q'(t_2) = q(t_2, p_1) + \lambda(t_2)$$

so that

$$\frac{\partial q_2}{\partial p_1} = \lim_{dp_1 \to 0} \frac{\lambda(t_2)}{dp_1} \tag{7}$$

where $\lambda(t)$ is computed with the equation of motion, Eq. (5), with the initial conditions

$$\lambda(t_1) = 0 \tag{8}$$

$$\dot{\lambda}(t_1) = \frac{dp_1}{m}$$

The actual partial derivative required in classical S-matrix theory is

$$\frac{\partial^2 \phi}{\partial p_1 \partial p_2}$$

where ϕ is the classical action along the trajectory. But since

$$\frac{\partial \phi(p_2,p_1)}{\partial p_2} = -q_2 \tag{9a}$$

and

$$\frac{\partial \phi(p_2,p_1)}{p_1} = q_1 \quad , \tag{9b}$$

$$\frac{\partial \phi(p_2,p_1)}{\partial p_1 \partial p_2} = -\frac{\partial q_2}{\partial p_1} = \frac{\partial p_2}{\partial q_1} \tag{10}$$

so that the partial derivatives necessary in the computation of the Jacobian can be calculated from Eq. (7).

The above method can be easily generalized to a multi-dimensional system. In that case the new trajectory $q_i'(t)$ for the perturbation $p_j(t_1) \to p_j(t_1) + dp_j$ is given by

$$q_i'(t) = q_i(t) + \lambda_i(t) \tag{11}$$

for all i, so that $\lambda_i(t)$ is determined by

$$m_i \ddot{\lambda}_i(t) = -\sum_i \left\{ \frac{\partial V}{\partial q_j \partial q_i} \right\} \qquad \text{all } i \tag{12}$$

with the initial conditions

$$\dot{\lambda}_i(t_1) = 0 \qquad \text{all } i \tag{13}$$

$$\dot{\lambda}_i(t_1) = 0 \qquad i \neq j$$

$$\dot{\lambda}_j(t_1) = \frac{dp_j}{m_j}$$

The apparent difficulty of computing the λ's from Eqs. (12) and (13) would seem to make this an impractical method for computing the partial derivatives. It remains, however, an interesting curiosity which may be of value for some systems.

B. Three-Dimensional Generalization of the Wall-Porter Potential

The two dimensional Wall-Porter potential surface for collinear reactions[55] permits the independent adjustment of the position and curvatures of the sadde-point, the activation energy and the shape of the diatomic potential curves. Thus it is a most useful functional form with which to fit or approximate the collinear reactive potential surface for an atom-diatom system.

The Wall-Porter form for the potential surface essentially is a Morse-curve of varying well depth and curvature that pivots between the two dissociation limits. The expression for the potential in the symmetric case is

$$V(x,y) = \gamma\{[1 - \exp(-\alpha\xi)]^2 - 1\} \tag{14}$$

where

$$\gamma = D(1 - a\sin^{\ell}2\theta) \tag{15}$$

$$\alpha = \alpha_o + (\alpha^{\ddagger} - \alpha_o) \sin^4 2\theta \tag{16}$$

$$\xi = [\sqrt{2}(R_o - S_o) - (R_o - x_o)] \sin^4 2\theta + (R_o - x_o) - (R_o - x) \sec\theta \tag{17}$$

$$\theta = \tan^{-1}[(R_o - y)/(R_o - x)] \tag{18}$$

In the above expressions the coordinates x and y are the two distances in the collinear arrangement. The rotation is about the point $x = R_o$, $y = R_o$ and the assumption is made that for x or y greater than R_o the potential is the pure diatomic Morse function. The saddle point is located at $x = y = S_o$, and the values of q, ℓ and $\alpha^{\ddagger}$ can be adjusted to give specificed values of the activation energy and the symmetric and unsymmetric curvatures at the saddle point.

Formidable extra requirements are presented if this approach is to be generalized to a three-dimensional surface. There are now three dissociation limits and the surface must flow smoothly into all three. The collinear orientations, of which there are now three, must be lower in energy than the surrounding parts of the surface. The potential should have adjustable saddle-point locations and curvatures in all three collinear planes and should be roughly of the two-dimensional Wall-Porter type on these planes.

By analogy with the two-dimensional surface for the symmetric case (all three atoms identical), choose the rotation to be about the point (R_o, R_o, R_o) where the three coordinates are the three distances r_1, r_2 and r_3. Let the potential be expressed as

$$V(r_1, r_2, r_3) = \gamma\{[1 - \exp(-\alpha\xi)]^2 - 1\} \tag{19}$$

where $\alpha(r_1,r_2,r_3)$, $\gamma(r_1,r_2,r_3)$ and $\xi(r_1,r_2,r_3)$ are adjusted to meet the various conditions. By analogy, it is also postulated that the surface is the appropriate pure diatomic Morse potential for any of the nearest-neighbor distances greater than R_o.

Define the auxilliary coordinates x, y and z by $x = (R_o - r_1)$, $y = (R_o - r_2)$ and $z = (R_o - r_3)$. Choose $\gamma(x,y,z)$ to be given by

$$\gamma(x,y,z) = D(1 - a) + aD\left[\frac{\lambda - f(x,y,z)}{\lambda}\right]^{\ell} - Dbg^k(x,y,z) \tag{20}$$

where

$$f(x,y,z) = \frac{2(xy + xz + yz)}{x^2 + y^2 + z^2} \tag{21}$$

and

$$g(x,y,z) = \frac{3\sqrt{3}(z + R_o - x - y)(x + R_o - y - z)(y + R_o - x - z)}{(x^2 + y^2 + z^2)^{3/2}} \tag{22}$$

The function $g(x,y,z)$ is zero on each of the three planes of collinear orientation so that it can be assured that those orientations are lower in energy. Much of the role of $\sin 2\theta$ for the two-dimensional case is apparently occupied by $f(x,y,z)$ in this formulation. This function goes to zero whenever any two of the variables $(R_o - r_1)$, $(R_o - r_2)$, $(R_o - r_3)$ are zero and is equal to 2 along the main diagonal $(x = y = z)$. The other quantities in the potential expression are chosen as

$$\alpha(x,y,z) = \alpha^{\ddagger} + (\alpha_o - \alpha^{\ddagger})\left[\frac{\lambda - f(x,y,z)}{\lambda}\right]^{m} - cg^k(x,y,z) \tag{23}$$

$$\xi(x,y,z) = f^n(x,y,z)\, q + R_o - r_o - \sqrt{x^2 + y^2 + z^2} - dg^k(x,y,z) \quad . \tag{24}$$

It is now necessary to see what limitations are placed upon the heretofore unrestrained parameters ℓ, λ, a, b, c, d, q, $\alpha^{\ddagger}$. The saddle points in the collinear orientation are located at $r_i = r_j = S_o$, $r_k = 2S_o$. Again by analogy with the two-dimensional case, aD should be the activation energy and $\alpha^{\ddagger}$ the curvature of the Morse function at the saddle point. Then λ is chosen to be the value of f(x,y,z) at the saddle point or

$$\lambda = \frac{2[3R_o^2 + 5S_o^2 - 8R_oS_o]}{[3R_o^2 + 6S_o^2 - 8\,R_oS_o]} \quad . \tag{25}$$

$\xi(x,y,z)$ must vanish at the saddle point so that q must be given by

$$q = \lambda^{-n}\left[r_o - R_o + \sqrt{3R_o^2 - 8R_oS_o + 6S_o^2}\right] \quad . \tag{26}$$

The three exponents n, m, k are free to be chosen so that the potential is smooth, and the constant b, c, d should reflect the extent to which the collinear orientation is favored.

The interrelation of some of these constants can now hopefully be adjusted to specify the symmetric and unsymmetric curvatures at the saddle point. Unfortunately, it appears that this is not possible. Both of the first derivatives are zero at the saddle point and the second derivative in the unsymmetric direction is nonzero. However, the second derivative in the symmetric direction is equal to zero (the third derivative does not vanish) so that the point is not really

a true saddle point in the mathematical sense. Still the shape of the surface is approximately right in this region and it is not known how serious this deficiency is.

ACKNOWLEDGEMENTS

I would like to thank Professor William H. Miller and all the others who have contributed to my graduate education.

This work was done under the auspices of the U. S. Atomic Energy Commission.

REFERENCES

1. M. Born and J. R. Oppenheimer, Ann. Physik 84, 457 (1927).
2. Felix J. Smith, Phys. Rev. 179, 111 (1969), for detailed consideration of adiabatic and diabatic representations.
3. L. D. Landau and E. M. Lifshitz, Quantum Mechanics (Pergamon, Oxford, 1965), p. 279.
4. R. T. Pack and J. O. Hirschfelder, J. Chem. Phys. 49, 4009 (1968), gives the formalism for the exact separation of rotational coordinates for a diatomic system.
5. L. D. Landau, Physik. Z. Sowjetunion 2, 46 (1932).
6. C. Zener, Proc. Roy. Soc. (London) A137, 696 (1932).
7. E. C. G. Stueckelberg, Helv. Phys. Acta 5, 369 (1932).
8. W. R. Thorson, J. Chem. Phys. 50, 1702 (1968).
9. D. R. Bates, Proc. Royal Soc. A257, 22 (1960).
10. C. A. Coulson and K. Zalewski, Proc. Royal Soc. A268, 437 (1962).
11. See for example M. L. Goldberger and K. M. Watson, Collision Theory (John Wiley and Sons, N. Y., 1967), p. 326.
12. A. Zwaan, Dissertation, Utrecht, 1929.
13. E. C. Kemble, Phys. Rev. 48, 549 (1935).
14. O. K. Rice, J. Chem. Phys. 3, 386 (1935).
15. W. R. Thorson, J. B. Delos and S. A. Boorstein, Phys. Rev. A 4 1052 (1971).
16. W. H. Miller and T. F. George, J. Chem. Phys. 56, 5637 (1972), indicated that this term is the same as obtained by taking the first order term in the expansion of the integrand in powers of $\frac{1}{V(R_x)}$.

17. E. E. Nikitin, V. K. Bykhovskii and M. Ya Ovchinnikova, Sov. Phys. JETP 20, 500 (1965).

18. Rather than imposing regularity on the solutions to Eq. (22), Ref. 17 requires that the solutions be exponentially decreasing for $x \to -\infty$. Mathematical purity may, therefore, require an exponential substitution for R at this point. See R. E. Langer, Phys. Rev. 51, 669 (1937).

19. M. Abramowitz and I. A. Stegun, eds., Applied Mathmatics Series (National Bureau of Standards (U. S.), 1964), Vol. 55, p. 448.

20. See also Ref. 3, p. 331.

21. W. H. Miller, private communication.

22. R. E. Langer, Trans. Amer. Math. Soc. 67, 461 (1949).

23. See Ref. 11 or P. M. Morse and H. Feshbach, Methods of Theoretical Physics (McGraw-Hill, N. Y., 1953), p. 434.

24. S. D. Augustin, W. H. Miller, P. K. Pearson and H. F. Schaefer, III, J. Chem. Phys. 58, 2845 (1973).

25. P. H. Pritchard and C. W. Kern, J. Chem. Phys. 57, 2590 (1972).

26. See for example, (a) H. Lefebore-Brion and C. M. Moser, J. Chem. Phys. 44, 2951 (1966); and (b) R. L. Ellis, R. Squire and H. H. Jaffe, J. Chem. Phys. 55, 3499 (1971).

27. E. U. Condon and G. H. Shortley, The Theory of Atomic Spectra (Cambridge U. P., London, 1963), p. 266.

28. C. E. Moore, National Bureau of Standards (U. S.) Circular 467 (1949).

29. M. Abramowitz and I. A. Stegun, eds., Applied Mathematics Series (National Bureau of Standards (U. S.), 1964), Vol. 55, p. 888.

30. W. H. Miller, private communication.

31. Reference 29, p. 300.

32. See for example, W. H. Miller, J. Chem. Phys. 54, 4174 (1971).

33. P. Palmer, B. Zuckerman, D. Buhl and L. E. Snyder, Astrophys. J. 156, L147 (1969).

34. N. J. Evans. G. Morris, T. Sato and B. Zuckerman, in preparation.

35. C. H. Townes and A. C. Cheung, Astrophys. J. 157, L103 (1969).

36. For a review of Monte Carlo trajectory methods, see D. L. Bunker, Methods in Comp. Phys. 10, 287 (1971).

37. For a review of classical S-matrix theory, see W. H. Miller, Adv. Chem. Phys. 25, 69 (1974).

38. (a) W. H. Miller, J. Chem. Phys. 53, 3578 (1974); (b) Chem. Phys. Lett. 7, 525 (1970); (c) J. Chem. Phys. 54, 5386 (1971); (d) J. D. Doll and W. H. Miller, J. Chem. Phys. 57, 5019 (1972); and others cited in Ref. 5.

39. Some other applications of the semi-classical theory are (a) W. H. Wong and R. A. Marcus, J. Chem. Phys. 55, 5663 (1971); (b) J. R. Stine and R. A. Marcus, Chem. Phys. Lett. 15, 536 (1972); (c) J. R. Stine and R. A. Marcus, J. Chem. Phys. 59, 5145 (1973).

40. C. H. Townes and A. L. Schawlow, Microwave Spectroscopy (McGraw-Hill, N. Y., 1955), p. 83.

41. G. W. King, J. Chem. Phys. 15, 820 (1947).

42. W. H. Miller, J. Chem. Phys. 53, 1949 (1970).

43. The standard ordering of rotational constants as indicated at the beginning of Section B would make the C-O axis the x axis of the molecule. The component of $\vec{j}$ on this axis (k' of Eq. (3b)) is thus a nearly conserved quantity. For mathematical simplicity, the CO axis will be taken to be the body fixed z axis in the remainder of this section so that the prime on k' will be dropped.

44. In this set of coordinates and momenta a typical trajectory required 0.12 seconds of computer time on a CDC 7600.

45. For a more detailed discussion of the term "classically allowed", see Ref. 6a.

46. R. A. Marcus, J. Chem. Phys. 57, 4093 (1972).

47. For a comparison of classical Monte Carlo trajectory and quantum mechanical coupled channel calculations for rotational excitation of CO by He at collision energies similar to the present ones, see S. D. Augustin and W. H. Miller, Chem. Phys. Lett., in press.

48. N. J. Evans, private communication.

49. H. Goldstein, Classical Mechanics (Addison-Wesley, Massachusetts, 1950), p. 107.

50. H. Goldstein, Classical Machanics, (Addison-Wesley, Massachusetts, 1950), p. 241.

51. S. Green and P. Thaddeus, to be published.

52. A detailed discussion of the comparison for this system as well as that for He-H_2 rotational excitation is contained in S. D. Augustin and W. H. Miller, Chem. Phys. Lett.

53. See for example, M. Karplus, R. N. Porter and R. D. Sharma, J. Chem. Phys. 43, 3259 (1965). For a recent review, see D. L. Bunker, Methods in Comp. Phys. 10, 287 (1971).

54. William H. Miller, J. Chem. Phys. 54, 5386 (1971).

55. F. J. Wall and R. N. Porter, J. Chem. Phys. 36, 3256 (1962).

LEGAL NOTICE

This report was prepared as an account of work sponsored by the United States Government. Neither the United States nor the United States Atomic Energy Commission, nor any of their employees, nor any of their contractors, subcontractors, or their employees, makes any warranty, express or implied, or assumes any legal liability or responsibility for the accuracy, completeness or usefulness of any information, apparatus, product or process disclosed, or represents that its use would not infringe privately owned rights.

TECHNICAL INFORMATION DIVISION
LAWRENCE BERKELEY LABORATORY
UNIVERSITY OF CALIFORNIA
BERKELEY, CALIFORNIA 94720